



THESIS APPROVAL

GRADUATE SCHOOL, KASETSART UNIVERSITY

Master of Science (Chemistry)

DEGREE

Chemistry

Chemistry

FIELD

DEPARTMENT

TITLE: Molecular Dynamics Simulations of Vitamin E and Inulin
in the Lipid Bilayer

NAME: Miss Waraporn Boonyarat

THIS THESIS HAS BEEN ACCEPTED BY

THESIS ADVISOR

(Miss Patchreenart Saparpakorn, Ph.D.)

THESIS CO-ADVISOR

(Associate Professor Supa Hannongbua, Dr.rer.nat.)

THESIS CO-ADVISOR

(Assistant Professor Kiattawee Choowongkomon, Ph.D.)

DEPARTMENT HEAD

(Assistant Professor Noojaree Prasitpan, Ph.D.)

APPROVED BY THE GRADUATE SCHOOL ON _____

DEAN

(Associate Professor Gunjana Theeragool, D.Agr.)

THESIS

MOLECULAR DYNAMICS SIMULATIONS OF
VITAMIN E AND INULIN IN THE LIPID BILAYER

WARAPORN BOONYARAT

A Thesis Submitted in Partial Fulfillment of
the Requirements for the Degree of
Master of Science (Chemistry)
Graduate School, Kasetsart University
2010

Waraporn Boonyarat 2010: Molecular Dynamics Simulations of Vitamin E and Inulin in the Lipid Bilayer. Master of Science (Chemistry), Major Field: Chemistry, Department of Chemistry. Thesis Advisor: Miss Patchreenart Saparpakorn, Ph.D. 79 pages.

Currently, the uses of foods which may exert a positive functional effect on health are widely focused. Two of these functional foods are known as probiotics and prebiotics, which have a favourable effect on the good bacteria that reside in digestive systems, also known as gut micro flora. Probiotics actions are the synthesis of short-chain fatty acids (SCFAs) and vitamins. In addition, prebiotics are natural saccharides that locate the large intestine undigested. Difference between probiotics and prebiotics is absorbed into intestina. This absorption of probiotics and prebiotics is unclear and interesting to study the mechanism. In this study, the distribution of Vitamin E (probiotic) and inulin (prebiotic) at water/membrane interface has been investigated by molecular dynamics (MD) simulations. The MD simulations running on the time of 10 ns were carried out in the same conditions by using GROMACS software and the SPC (single-point charge) parameters were used. The dipalmitoylphosphatidylcholine (DPPC) bilayer was stabilized by the energy minimization at 323 K and 1 bar as constant. The MD study focused on favorable binding sites of Vitamin E and inulin embedded into DPPC bilayer. The simulations were shown that vitamin E was preferably accommodated at the head of the bilayer upper the glycerol moiety. In addition, it was found that the hydrophobic aromatic part of the vitamin E was located inside more ordered region of DPPC from the hydrophobic character of vitamin E. The snapshots revealed the depth of the vitamin E localization which was gradually shifted deeper inside the hydrocarbon core of the bilayer. The results showed that the vitamin E showed weak hydrogen bonding to DPPC bilayer and the distribution of vitamin E molecule simulations was presented at the opposite of the entrance. The depth of the inulin localization was shifted deeper inside between the phosphate and glycerol core of the bilayer. Moreover, the possibility of the penetration of the inulin through the bilayer was analyzed. During our MD analysis, we found that cannot cross the bilayer from one leaflet to the other. The strong hydrogen bond was found between hydroxyl group (OH) of inulin and oxygen atoms of phosphate and glycerol.

Student's signature

Thesis Advisor's signature

____ / ____ / ____

ACKNOWLEDGEMENTS

First, I would like to thank my advisor, Dr. Patchreenart Saparpakorn, for her excellent supervision, inspiring guidance and helpful criticism throughout the course of this study. I am also thankful to my co-advisor, Associate Professor Supa Hannongbua for her kindness, valuable suggestions, encouragement, continuous support and constant inspiration in the course of my degree. Moreover, I would sincerely like to thank Assistant Professor Kiattawee Choowongkomon for kindly providing valuable suggestions and helpful guidance. I also wish to express my appreciation to Dr. Witcha Treesuwan for valuable suggestions and comments to make my thesis complete.

Furthermore, I would like to thank my advisory committee Dr. Songwut Suramitr and Assistant Professor Mayuso Kuno for their helpful criticism and suggestion.

This work was supported in part by the Thailand Research Fund (RTA5080005), the National Center of Excellence on Petroleum, Petrochemicals Technology and Advanced Materials, (NCE-PPAM) and the Center of Nanotechnology, Kasetsart University were gratefully acknowledged.

Special thanks are due to the Laboratory for Computational and Applied Chemistry (LCAC) at Kasetsart University is also gratefully acknowledged for computational resource and software facilities.

I appreciate my colleagues at LCAC for their helpful assistance and supporting during my study. Finally, I would like to thank my parents and my sisters, who encouraged me to achieve success in my education.

Waraporn Boonyarat

April, 2010.

TABLE OF CONTENTS

	Page
TABLE OF CONTENTS	i
LIST OF TABLES	ii
LIST OF FIGURES	iii
LIST OF ABBREVIATIONS	vi
INTRODUCTION	1
OBJECTIVES	6
LITERATURE REVIEW	7
METHODS OF CALCULATIONS	15
RESULTS AND DISCUSSION	23
CONCLUSIONS	55
LITERATURE CITED	57
APPENDICES	63
Appendix A Parameter for simulated	64
Appendix B Poster and Oral Presentation to Conferences	68
CURRICULUM VITAE	79

LIST OF TABLES

Table		Page
1	Averaging properties between 64DPPC and 64DPPC/water lipid bilayer.	25
2	Averaging properties between 128DPPC and 128DPPC/water lipid bilayer.	28
3	Averaging properties between 64 and 128 DPPC/water lipid bilayer.	31
4	Optimized bond length, angle and torsion of vitamin E by B3LYP/6-31G (d,p) and molecular dynamics simulations in water at 2 ns.	37
5	Optimized bond length, angle and torsion of inulin by B3LYP/6-31G (d,p) and molecular dynamics simulations in water at 2 ns.	46

LIST OF FIGURES

Figure		Page
1	Structure of vitamin E (tocopherol).	2
2	Structure of inulin.	3
3	Model of membrane phospholipids.	4
4	Structure of dipalmitoylphosphatidylcholine (DPPC), with a number of atoms and atom group. GROMOS symbols are used for atoms: NL = Nitrogen, OS = Ester Oxygen, OM = Phosphate Oxygen and O = Carbonyl Oxygen.	5
5	Molecular structure of α -tocopherol with the assigned atom numbers.	12
6	Snapshots of α -tocopherol/DPPC configurations at three temperatures.	13
7	Schematic representation of the bond interaction contributions to a molecular mechanics force field.	17
8	Non-bonded interactions of molecular mechanics force field.	17
9	Structures of 64 DPPC (a) and 64 DPPC/water molecules.	23
10	Total energy plot vs. Time (ps) of 64DPPC and 64DPPC/water lipid bilayer.	24
11	RMSD of 64DPPC and 64DPPC/water lipid bilayer for 2 ns.	24
12	Mass density along z-dimension of 64DPPC and 64DPPC/water lipid bilayer.	25
13	Structures of 128DPPC (a) and 128DPPC/water (b) molecules at 2 ns.	26
14	RMSD of 128DPPC and 128DPPC/water lipid bilayer for 2 ns.	27
15	Total energy plot vs. Time (ps) of 128DPPC and 128DPPC/water lipid bilayer	27
16	Mass density along z-dimension of 128DPPC and 128DPPC/water lipid bilayer.	28

LIST OF FIGURES (Continued)

Figure		Page
17	Snapshots of 64 (a) and 128 (b) DPPC lipids bilayer in water at 2 ns.	29
18	Total energy plot vs. Time (ps) of 64 and 128 DPPC lipid bilayer in water for 2 ns.	29
19	RMSD of 64 and 128 DPPC lipid bilayer in water for 2 ns.	30
20	Mass density along z-dimension of 64 and 128 DPPC lipid bilayer in water.	31
21	Energy comparison of three 128DPPC/water simulations for 20 ns.	32
22	Temperature comparison of three 128DPPC/water simulations for 20 ns.	33
23	Pressure comparison of three 128DPPC/water simulations for 20 ns.	33
24	RMSD comparison of three 128DPPC/water simulations for 20 ns	34
25	Mass density of 128DPPC/water at 2, 10, 20 and 50 ns.	34
26	Mass density of 128DPPC/water lipid bilayer at 10 ns.	35
27	Starting structure of vitamin E (tocopherol).	36
28	Optimized structure of vitamin E using by B3LYP/6-31G (d, p) (a) and molecular dynamics simulations in water (b).	36
29	Snapshots of the MD boxes taken from the simulations of vitamin E molecules in the 128DPPC bilayer at 0 ns, 2 ns and 10 ns.	38
30	Surface area of 128DPPC bilayer (a) and vitamin E (b) for 10 ns.	39
31	Total energy of 128DPPC/vitamin E system (a) and RMSD of vitamin E (b) for 10 ns.	40

LIST OF FIGURES (Continued)

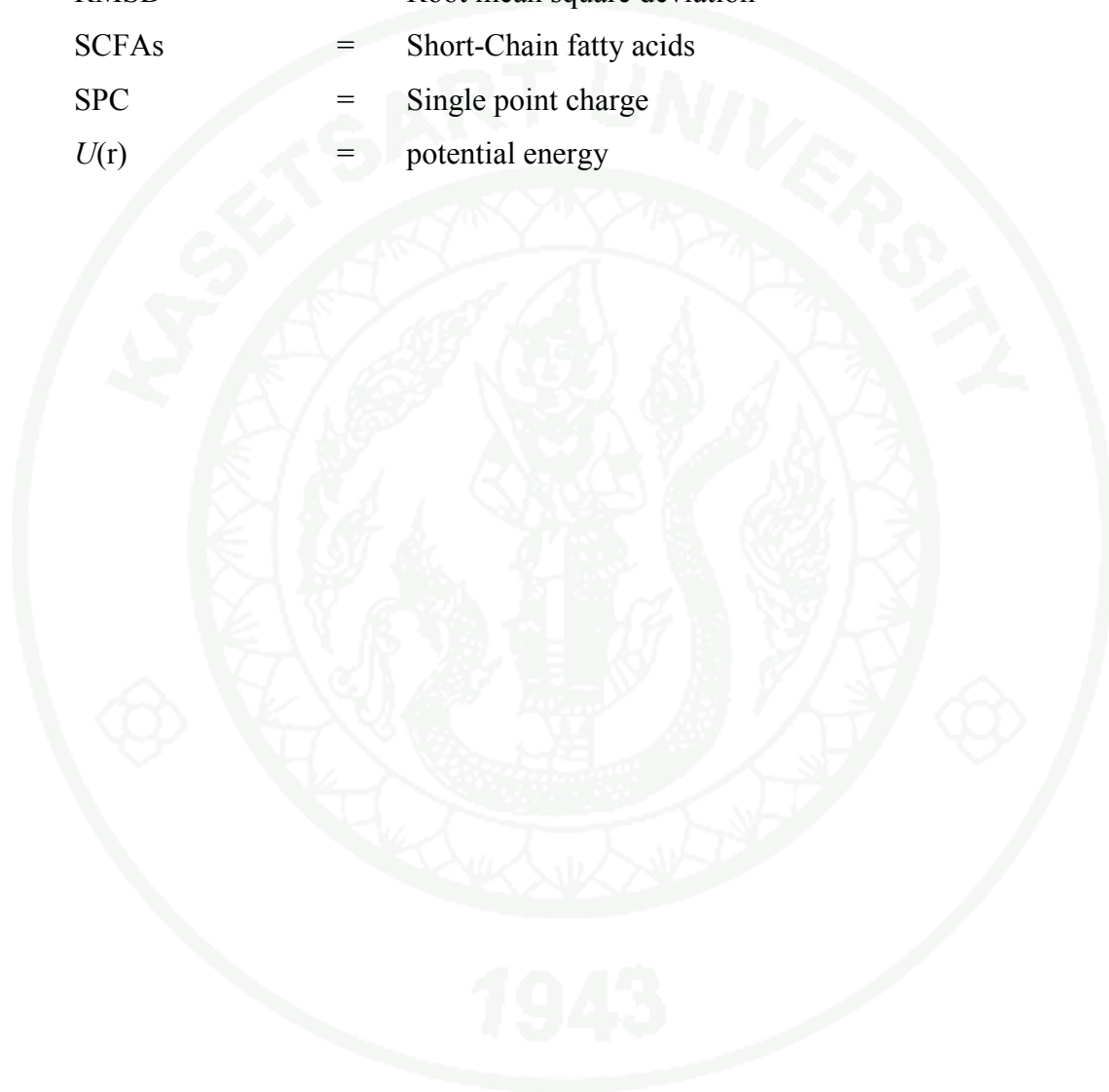
Figure		Page
32	Mass density distribution profiles for individual components of the 128DPPC bilayer and for the total density distribution of molecules of vitamin E.	41
33	Snapshots of vitamin E molecule in the 128DPPC bilayer at 10 ns.	42
34	Radial pair distribution functions $g(R)$ between the O–H hydrogen atom of vitamin E and the oxygen atoms of the phosphate (a) and glycerol (b) groups of the 128DPPC lipids.	44
35	Starting structure of inulin.	45
36	Optimized structure of inulin using by B3LYP/6-31G (d, p) (a) and molecular dynamics simulations in water (b).	45
37	Snapshots of inulin molecule in the DPPC bilayer at 1.5 ns.	47
38	Surface area of 128DPPC bilayer (a) and inulin (b) at 1.5 ns.	49
39	Total energy of inulin/DPPC system (a) and RMSD of inulin (b) at 1.5 ns.	50
40	Mass density distribution profiles for individual components of the DPPC bilayer and for the total density distribution of molecules of inulin.	51
41	Interaction between inulin and DPPC.	52
42	Radial pair distribution functions $g(R)$ between the O–H hydrogen atom of inulin and the oxygen atoms of the phosphate (a) and glycerol (b) groups of the DPPC lipids.	53

LIST OF ABBREVIATIONS

Å	=	Angstrom
atm	=	Atmosphere
B3LYP	=	Beck's three parameter hybrid functional using the LYP correlation functional
DFT	=	Density functional theory
DP	=	Degree of polymerisation
DPH	=	1,6-diphenyl-1.3.5-hexatriene
DPPC	=	Dipalmitoylphosphatidylcholine
DSE	=	Differential scanning calorimeter
g(R)	=	Radial distributions functions
K	=	Kelvin
kg	=	Kilogram
kJ	=	Kilojoule
MD	=	Molecular Dynamics
N	=	Nitrogen atom
NL	=	GROMOS symbol for Nitrogen atom
nm	=	Nanometer
ns	=	Nanosecond
P	=	Phosphate atom
PME	=	Particle mesh Ewald
ps	=	picosecond
PtdCho	=	Phosphatidylcholin
PtdEtn	=	Phosphatidylethanolamine
PtdIns	=	Phosphatidylinositol
PtdSer	=	Phosphatidylserine
O	=	Oxygen atom
OH	=	Hydroxyl group
OM	=	GROMOS symbol for Phosphate oxygen
OS	=	GROMOS symbol for Ester oxygen

LIST OF ABBREVIATIONS (Continued)

SPC/E	=	Extended single point charge
RDF	=	Radial distribution function
RMSD	=	Root mean square deviation
SCFAs	=	Short-Chain fatty acids
SPC	=	Single point charge
$U(r)$	=	potential energy



MOLECULAR DYNAMICS SIMULATIONS OF VITAMIN E AND INULIN IN THE LIPID BILAYER

INTRODUCTION

Currently, there is huge interest in the use of foods which may exert a positive functional effect on health. Two of these functional foods are known as probiotics and prebiotics, both of which have a favourable effect on the good bacteria that reside in digestive systems, also known as gut micro flora. These good bacteria live naturally in intestines and are essential to good health having a number of positive effects, primarily helping digestive systems work efficiently (Gibson, 2003).

Probiotics are live microorganisms that can reach the gut in viable form and exert effects beneficial to the host. Their actions are the synthesis of short-chain fatty acids (SCFAs) and vitamins. In addition, prebiotics are natural saccharides that locate the large intestine undigested and serve as nutrients for probiotic (saccharolytic) bacteria. Difference between probiotics and prebiotics is absorbed into intestinal. This absorption of probiotics and prebiotics is unclear and interesting to study the mechanism.

Vitamin E (tocopherol) is one of four fat-soluble vitamins. It is synthesized by plants and found in plant oils. Vitamin E is a probiotic that presented in high amounts within the chloroplast and leaves of most plants. Moreover it is hydrophobic and absorbed similarly to other dietary lipids. After solubilization by bile acid, it is absorbed into small intestinal epithelial cells, incorporated into chylomicrons and transported into blood via lymphatic. It is liberated from chylomicrons and taken up by liver, where it is repackaged into very low density lipoproteins. Vitamin E is stored with the fat droplets of adipose tissue cells. The general structure of vitamin E is shown in Figure 1.

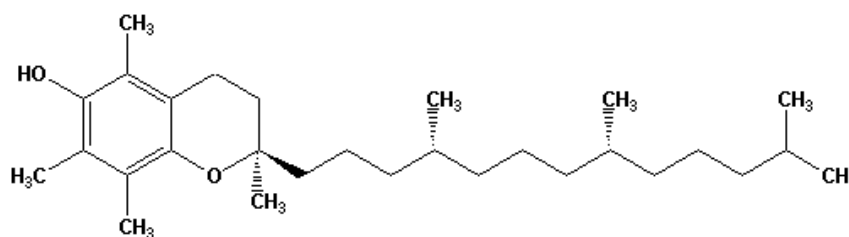


Figure 1 Structure of vitamin E (tocopherol).

Inulin is categorized into a group of naturally occurring polysaccharide produced by many types of plants. Inulin belongs to a class of dietary fiber known as fructan. Inulin is used by some plants as a means of storing energy and is typically found in root or rhizome. Most plants that synthesize and store inulin do not store other materials such as starch. Inulin is used increasingly in foods because it has unusual nutritional characteristics. It ranges from completely bland to subtly sweet and can be used to replace sugar, fat, and flour. This is particularly advantageous because inulin contains a third to a quarter of the food energy of sugar or other carbohydrates and sixth to ninth of the food energy of fat. It also increases calcium absorption (Abrams *et al.*, 2005) and possibly magnesium absorption (Coudray *et al.*, 2003), inulin while promoting the growth of intestinal bacteria. Nutritionally, it is considered as a form of dietary fiber and is sometimes seen as a prebiotic. When incorporated in the diet, the inulin acts as “prebiotic”, promoting selective development of beneficial microorganisms. This fact derives from the incapacity of the stomach and small intestine endogenous enzymes to hydrolyse the inulin and its derivatives, only occurring degradation by bacterial fermentation at the colon’s level. The general structure of inulin is shown in Figure 2.

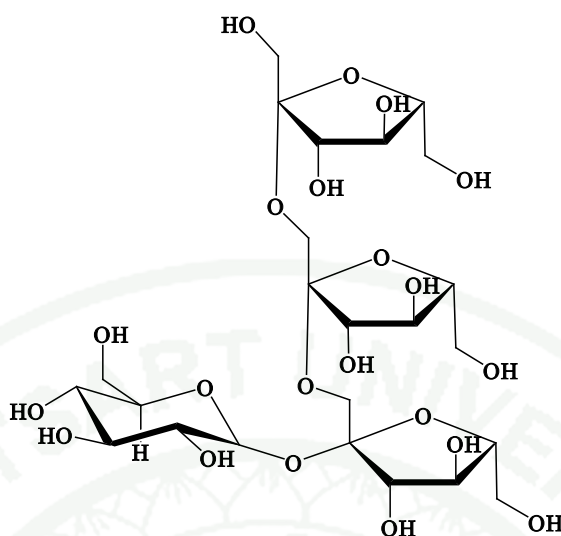


Figure 2 Structure of inulin.

Bilayer lipid membrane is a membrane composed of two lipid molecules and made of a bilayer. The lipid bilayer is a critical component of all biological membrane, including cell membrane, and so is absolutely essential for all known life on Earth. The structure of a bilayer explains its function as a barrier. Lipids are amphiphilic since they consist of chemical polarity head groups and chemical polarity fatty acid tails. The bilayer is composed of two layers of lipids arranged so that their hydrocarbon tails face one another to form an oily core held together by the hydrophobic effect, while their charged heads face the aqueous solutions on either side of the membrane. The hydrophilic interfacial regions are saturated with water, while the lipophilic core region contains essentially no water. Model of bilayer lipid membrane is shown in Figure 3. Examples of the major membrane phospholipids and glycolipids are phosphatidylcholine (PtdCho), Phosphatidylethanolamine (PtdEtn), Phosphatidylinositol (PtdIns) and Phosphatidylserine (PtdSer).

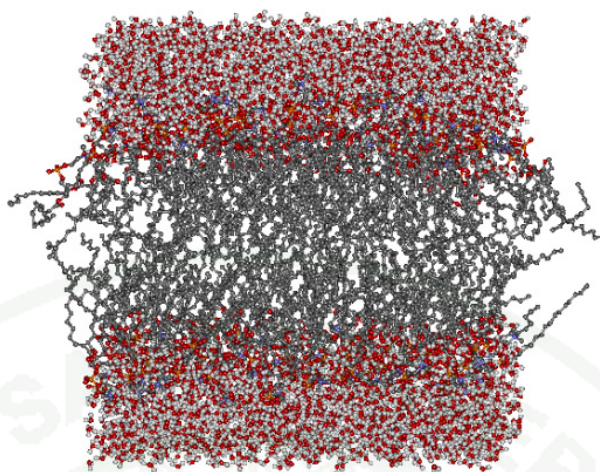


Figure 3 Model of membrane phospholipids.

Source: Tieleman *et al.* (1997)

We chose the binary system dipalmitoylphosphatidylcholine (DPPC)/water as a representative for biological membrane, which consists mainly of phospholipids. The structural formula is shown in Figure 4. The lecithin head group is zwitterions, overall neutral, with positive electron charge distributed over the choline group and a negative electron charge on the phosphate group. The paraffinic chains are fully saturated and of equal length (16 carbon atoms) (Egberts *et al.*, 1994).

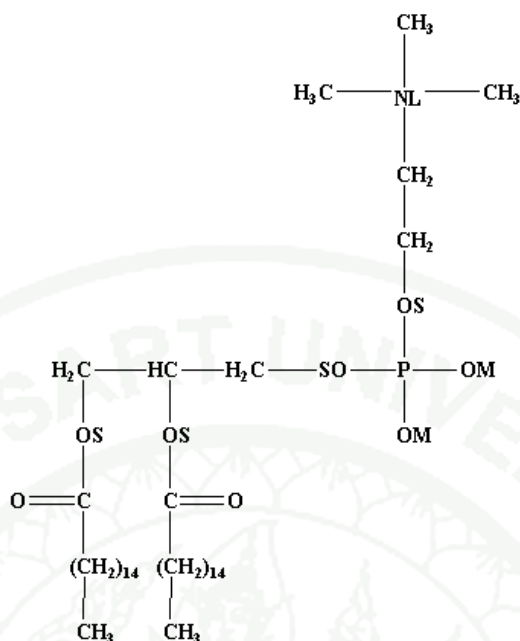
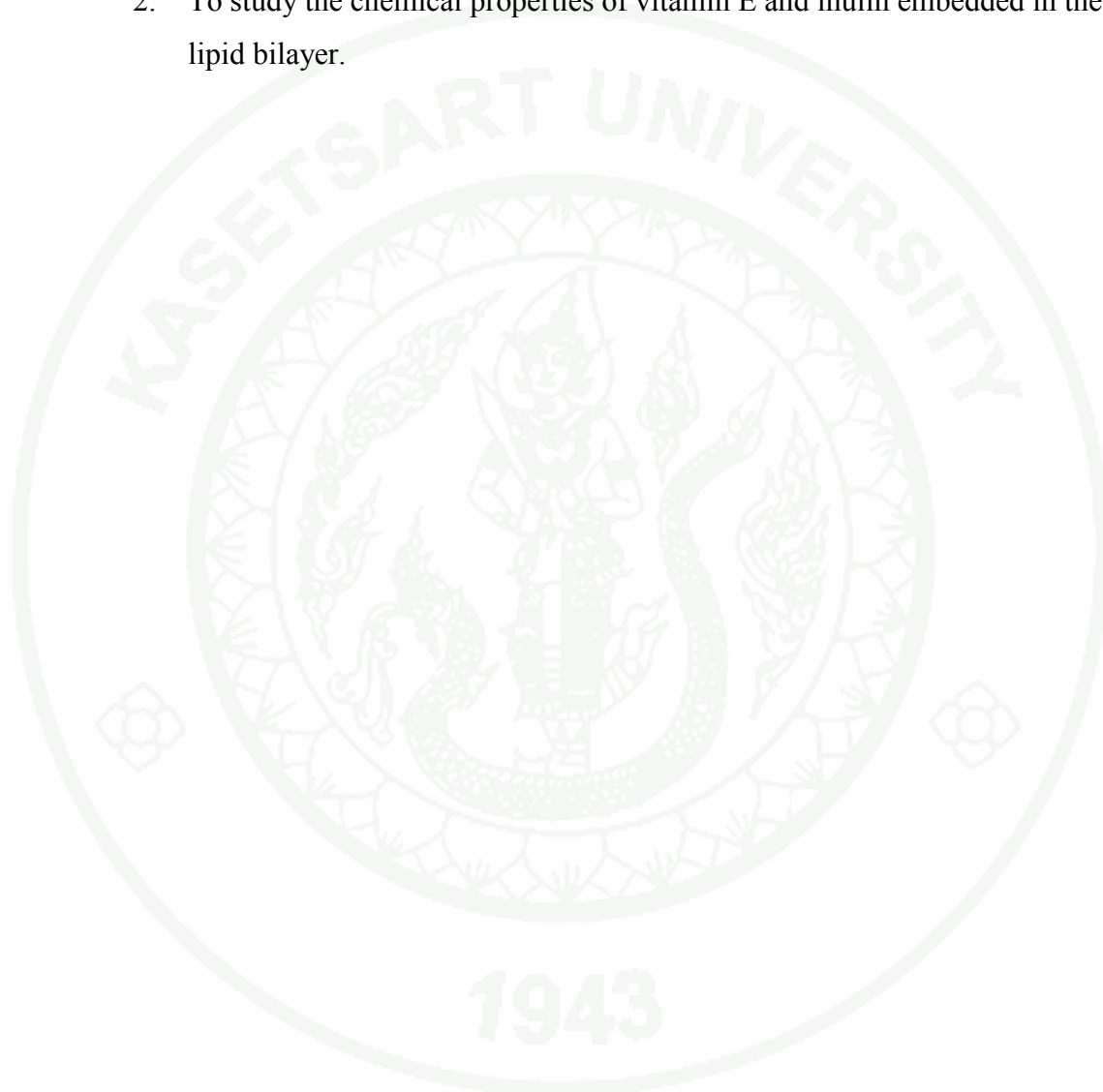


Figure 4 Structure of dipalmitoylphosphatidylcholine (DPPC), with a number of atoms and atom group. GROMOS symbols are used for atoms: NL = Nitrogen, OS = Ester Oxygen, OM = Phosphate Oxygen and O = Carbonyl Oxygen.

The binding of vitamin E and inulin in a biomembrane and its subsequent influence on membrane properties are an important problem. The vitamin E and inulin can severely influence various physiological processes in the body. A microscopic understanding of the location of vitamin E and inulin within the membrane is crucial as it will provide direct information regarding its interaction with membrane components. Such information will have an impact on the mechanism of the effect of vitamin E and inulin on regular membrane properties. However, despite significant efforts, understanding of the mechanism of action of vitamin E and inulin are not clear. This is primarily due to the existing regarding the possible binding sites for vitamin E and inulin within a membrane.

OBJECTIVES

1. To compare vitamin E and inulin toward interface of the lipid bilayer.
2. To study the chemical properties of vitamin E and inulin embedded in the lipid bilayer.



LITERATURE REVIEW

Fructans are a group of fructose-based oligo- and polysaccharides (Vereyken *et al.*, 2003). They are proposed to be involved in membrane protection of plants during dehydration. In accordance with this hypothesis, they show an interaction with hydrated lipid model systems. However, the structural requirements for this interaction are not known both with respect to the fructans as to the lipids. To get insight into this matter, the interaction of several inulins and levan with lipids was investigated using a monomolecular lipid system or the MC 540 probe in a bilayer system. MD was used to get conformational information concerning the polysaccharides. It was found that levan-type fructan interacted comparably with model membranes composed of glyco- or phospholipids but showed a preference for lipids with a small head group. Furthermore, it was found that there was an inulin chain-length-dependent interaction with lipids. The results also suggested that inulin-type fructan had a more profound interaction with the membrane than levan-type fructan. MD simulations indicated that the favorable conformation for levan is a helix, whereas inulin tends to form random coil structures. This suggests that flexibility is an important determinant for the fructan-lipid interaction.

Symbiosis between host and gut bacteria can be optimized by prebiotics. Inulin-type fructans have been shown to improve the microbial balance of the intestinal ecosystem by stimulating the growth of bifidobacteria and lactobacilli. Inulin-type fructans induce changes of the intestinal mucosa characterized by higher villi, deeper crypts, increased number of goblet cells, and a thicker mucus layer on the colonic epithelium (Guarner, 2007). In contrast, study with rats fed a low-calcium diet suggested a negative effect of prebiotics on intestinal barrier function. However, the adverse effect was clearly ascribed to the strong reduction of dietary calcium, it could be reversed by oral administration of calcium. The adverse effect of a low-calcium diet on intestinal permeability has not been observed in humans. Inulin and oligofructose are now being tested in human studies aimed at prevention of bacterial translocation in critical health conditions. Mixtures of probiotics and prebiotics including inulin or oligofructose significantly reduced the rate of postoperative

infections in liver transplant patients. Finally, inulin and oligofructose have been proven to be useful to prevent mucosal inflammatory disorders in animal models and in patients with inflammatory bowel disease.

Inulin is a generic term to cover all linear fructans. Chicory inulin is a linear fructan (degree of polymerisation (DP) 2 to 60; $DP_{av} = 12$), its partial enzymatic hydrolysis product is oligofructose (DP 2 to 8; $DP_{av}=4$), and by applying specific separation technologies a long-chain inulin known as inulin HP (DP 10 to 60; $DP_{av}=25$) can be produced. Finally, a specific product known as oligofructose-enriched inulin is obtained by combining chicory long-chain inulin and oligofructose (Roberfroid, 2007). A series of animal studies demonstrate that inulin-type fructans affect the metabolism of lipids primarily by decreasing triglyceridaemia. The human data largely confirm the animal experiments. A large number of animal data convincingly showed that inulin-type fructans reduce the risk of colon carcinogenesis and nutrition intervention trials are now performed to test that hypothesis in human subjects known to be at risk for polyps and cancer development in the large bowel.

Vitamin E is absorbed along with chylomicrons. However, they previously reported that human colon carcinoma Caco-2 cells use dual pathways, apolipoprotein B (apoB)-lipoproteins and HDLs, to transport vitamin E. Here, they used primary enterocytes and rodents to identify in vivo vitamin E absorption pathways. Uptake of [3H] α -tocopherol by primary rat and mouse enterocytes increased with time and reached a maximum at 1 h. In the absence of exogenous lipid supply, these cells secreted vitamin E with HDL. Lipids induced the secretion of vitamin E with intermediate density lipoproteins, and enterocytes supplemented with lipids and oleic acid secreted vitamin E with chylomicrons (Anwar *et al.*, 2007).

Comparison of molecular dynamics simulations of a bilayer of 128 phospholipid (DPPC) molecules was investigated using different parameters and macroscopic boundary conditions. The same system was studied under constant pressure, constant volume and constant surface tension boundary conditions, with two different sets of charges, the single point charge (SPC) and extended single point

charge (SPC/E) water model and two different sets of Lennard Jones parameters for the interaction between water and methyl/methylene (Tieleman and Berendsen, 1996). In relatively high water concentration, it is possible to use ab initio derived charges with constant pressure boundary conditions. The SPC water model showed a larger area per head group and a broader interface than the SPC/E model. There was a slight difference between simulations with constant pressure and constant surface tension. The use of constant volume, using a reasonable estimation for the initial box dimensions, easily introduces artifacts. In 1997, D. P. Tieleman *et al.* focused on the application of MD to biologically relevant lipid and lipid-protein system (Tieleman *et al.*, 1997). They reviewed the structure of a pure DPPC liquid crystalline bilayer, as it emerges from simulations when a number of current applications of MD, focusing on phenomena of biological importance: transport of small molecules across the bilayer, the connection between lipid structure.

Repakova *et al.*, (2004) employed 50 ns molecular dynamics simulations to study the distribution, orientation, and dynamics of 1,6-diphenyl-1,3,5-hexatriene (DPH) fluorescent probes in a dipalmitoylphosphatidylcholine (DPPC) bilayer. They found no evidence for clustering of DPH molecules, and their results showed that DPH does not prefer to be embedded in the membrane center where free volume was largest. Rather, DPH prefers to be accommodated in the hydrophobic acyl chain region of DPPC, oriented such that the long axis of DPH along its rodlike shape was approximately aligned in the direction of the normal bilayer, thus reflecting the ordering of lipid acyl chains. These conclusions were supported by further studies of radial distribution functions indicating DPH to be located beside the lipid acyl chains. Studies of DPH dynamics in DPPC bilayers reveal a number of rare events, including flip-flops of DPH molecules from one leaflet to another, their rotational diffusion whose time scale could be compared with that found through experiments, and the lateral diffusion of DPH in the plane of the bilayer. For lateral diffusion of DPH, they considered its diffusion mechanism and found that it took place through jumps from one void to another. Finally, their results were in favor of using DPH for probing lipid membranes.

In 2005, they studied through MD simulations that the perturbations induced by free DPH were very pronounced in its vicinity. For example, the ordering of DPPC hydrocarbon tails neighboring DPH was enhanced by 40% compared to lipids in a pure DPPC bilayer, and the lateral diffusion of lipids surrounding DPH was suppressed substantially. When the analysis was extended to all lipids in a system, providing a global average comparable to experiments, the effects due to DPH were found to be much smaller. DPH was found to influence a wide range of membrane properties, such as the packing and ordering of hydrocarbon tails and the lateral diffusion of lipid molecules.

Loura *et al.*, (2008) presented a combined theoretical (molecular dynamics, MD) and experimental studies of the effect of 7-nitrobenz-2-oxa-1,3-diazol-4-yl (NBD) acyl chain-labeled fluorescent phospholipid analogs on 1,2-dipalmitoyl-sn-glycero-3-phosphocholine (DPPC) bilayers. DSC measurements reveal that <1 mol% of NBD-PC causes elimination of the pretransition and a large loss of cooperativity of the main transition of DPPC. Labeling with C6-NBD-PC or C12-NBD-PC shifts the main transition temperature to lower or higher values, respectively. The following recent reported on the location and dynamics of these probes in fluid phase DPPC, they presented a detailed analysis of 100 ns MD simulations of systems containing either C6-NBD-PC or C12-NBD-PC, focused on their influence on several properties of the host bilayer. Whereas most monitored parameters were not severely affected for 1.6 mol % of probe, for the higher concentration studied (6.2 mol %) important differences are evident. In agreement with published reports, they observed that the average area per phospholipid molecule increases, whereas DPPC acyl chain order parameters decrease. Moreover, they predicted that incorporation of NBD-PC should increase the electrostatic potential across the bilayer and, especially for C12-NBD-PC, slow lateral diffusion of DPPC molecules and rotational mobility of DPPC acyl chains.

The distribution of 1H-pyrrolo[3,2-h]quinoline (PQ), 11H-dipyrido[2,3-a]carbazole (PC) and 7-azaindole (7AI) at a water/membrane interface has been investigated by molecular dynamics (MD) simulations. The MD study focused on favorable binding sites of the azaaromatic probes across a dipalmitoylphosphatidylcholine (DPPC) bilayer (Kyrychenko and Waluk, 2008). In contrast to PQ and PC, 7AI was characterized by a broad distribution between a DPPC interface and water, so that the three preferable binding sites were found across a water/membrane interface. It was found that in the sequence 7AI–PQ–PC, due to the increase of the number of aromatic rings, and hence, the hydrophobic character of the probes, the depth of the probe localization was gradually shifted deeper inside the hydrocarbon core of the bilayer. They found that the probe–lipid hydrogen-bonding contributed weakly to the favorable localizations of the azaaromatic probes inside the DPPC bilayer, so that the probe localization was mainly driven by electrostatic dipole–dipole and van der Waals interactions.

Devireddy (2009) studied statistical thermodynamics of biomembranes. An overview of the major issues involved in the statistical thermodynamic treatment of phospholipid membrane at the atomistic level was summarized thermodynamic ensembles, initial configuration, force field representation as well as the representation of long-range interactions. This was followed by a description of the various ways that the simulated ensembles can be analyzed area of the lipid, mass density profiles, radial distribution functions (RDFs), water orientation profile, deuterium order parameter, free energy profiles and void (pore) formation with particular focus on the results obtained from our recent molecular dynamic simulations of phospholipids interacting with dimethylsulfoxide (Me₂SO), a commonly used cryoprotective agent (CPA).

Structural and kinetic properties of vitamin E (Figure 5) in biomembranes provided the key to understand the biological functions of this lipophilic vitamin (Qin *et al.*, 2009). They reported a series of molecular dynamics simulations of two α -tocopherol/ phosphatidylcholine systems and two α -tocopherol/ phosphatidylethanolamine systems in water at 280, 310, and 350 K (Figure 6). The

preferential position, hydrogen bonding, orientation, and dynamic properties of α -tocopherol molecule in the bilayers had been examined. In all four systems simulated, the vitamin remained in one leaflet of lipid bilayer at 280 and 310 K but flips over from one side to the other at 350 K within 200 ns of the simulation. The hydroxyl oxygen in the head group of α -tocopherol preferred a location between the third and the fifth carbon atom in the *sn*-2 acyl chains of the lipids. Hydrogen bonding analysis was shown that the hydrogen bonds were mainly with the oxygens of the fatty acid esters rather than with the phosphate oxygens of the lipid molecule and those with the amino groups were trivial in the case of phosphatidylethanolamines, at all three temperatures. The hydrogen bonds with phosphatidylethanolamines were more stable than those with phosphatidylcholines at low temperatures. The orientation of α -tocopherol in the bilayers was relatively flexible: the chromanol ring takes various tilt angles with respect to the bilayer normal, and the isoprenyl chain was mobile and able to adopt many different conformers. Calculation of lateral diffusion coefficients of α -tocopherol and phospholipid molecules were shown that α -tocopherol had a comparable diffusion rate with phospholipid molecules at the gel phase but diffused more rapidly than lipid molecules at the liquid-crystal phase.

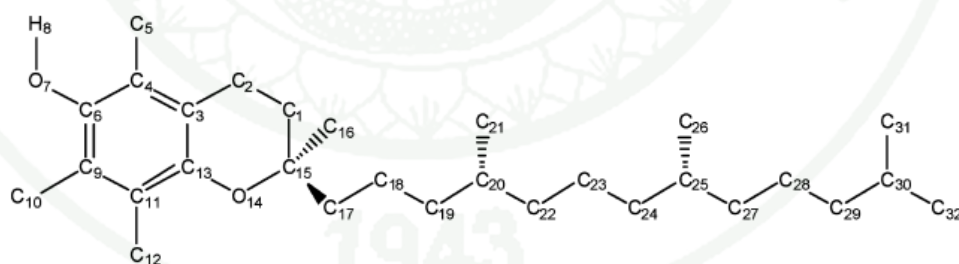


Figure 5 Molecular structure of α -tocopherol with the assigned atom numbers.

Source: Qin *et al.* (2009).

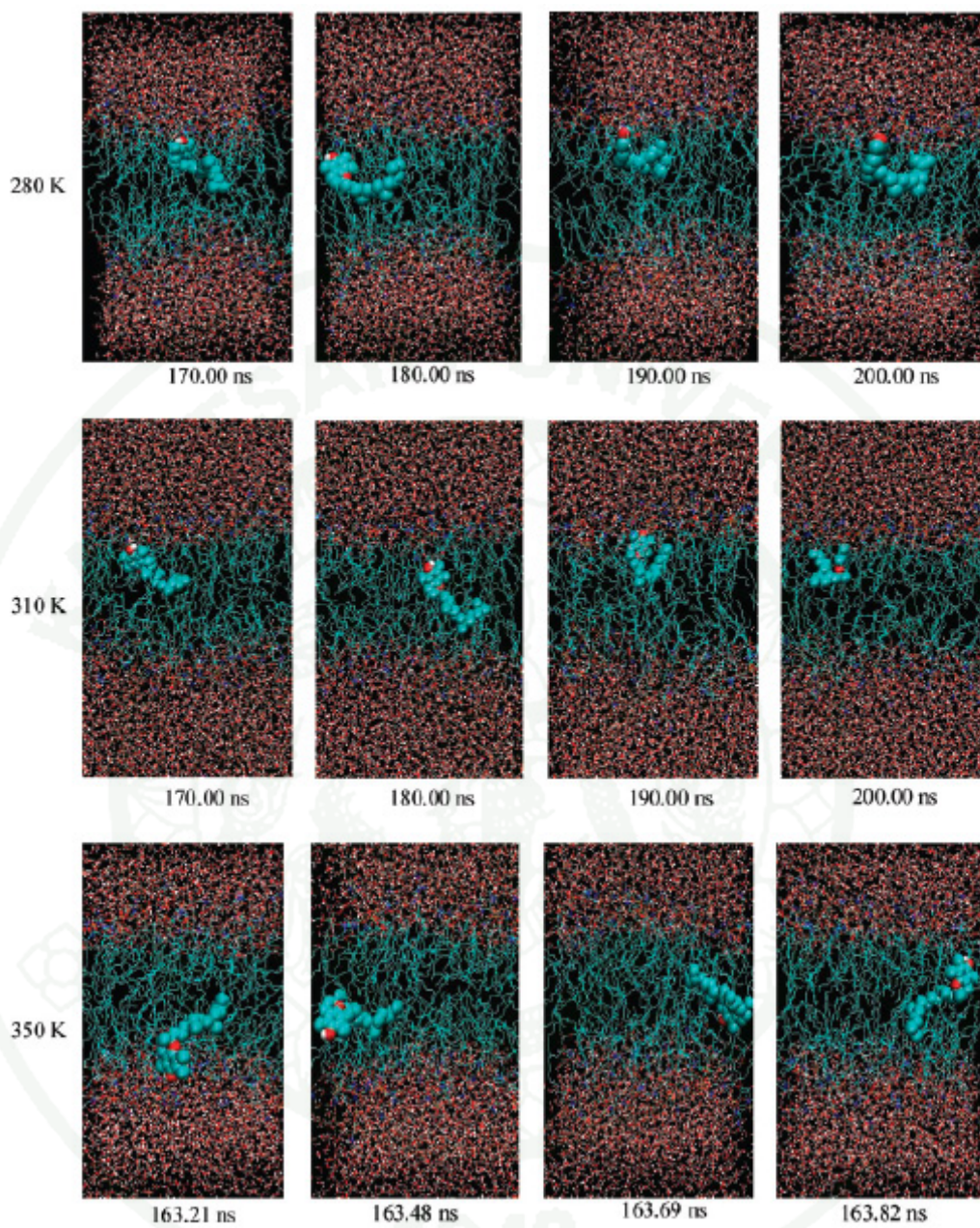


Figure 6 Snapshots of α -tocopherol/DPPC configurations at three temperatures.

Source: Qin *et al.* (2009).

Vitamins are essential nutrients, body needs in small amounts for various roles in the human body. Vitamins are divided into two groups: water soluble (B-complex and C) and fat-soluble (A, D, E and K). Unlike water-soluble vitamins that need regular replacement in the body, fat-soluble vitamins are stored in the liver and fatty tissues, and are eliminated slower than water-soluble vitamins. Because fat-soluble vitamins are stored for long periods, they generally pose a greater risk for toxicity than water-soluble vitamins when consumed in excess. Eating a normal, well-balanced diet will not lead to toxicity in otherwise healthy individuals. However, taking vitamin supplements that contain mega doses of vitamins A, D, E and K may lead to toxicity. Remember, the body only needs small amounts of any vitamin. While diseases caused by a lack of fat-soluble vitamins are rare in the United States, symptoms of mild deficiency can develop without adequate amounts of vitamins in the diet. Additionally, some health problems may decrease the absorption of fat, and in turn, decrease the absorption of vitamins A, D, E and K. (Anderson J. and Young L., Revised 8/08).

METHODS OF CALCULATIONS

Molecular Dynamics Simulations

Molecular simulations are a very powerful toolbox in modern molecular modeling and enable us to understand structure and dynamics with extreme detail literally on scales where motion of individual atoms can be tracked. The two most commonly used methods, energy minimization and molecular dynamics that, respectively, optimize structure and simulate the natural motion of biological macromolecules. The common theoretical framework based on statistical mechanics is covered briefly as well as limitations of the computational approach, for instance, the lack of quantum effects and limited timescales accessible. The chapter also describes how to analyze the simulation in terms of potential energies, structural fluctuations, coordinate stability, geometrical features, and, finally, how to create beautiful ray-traced movies that can be used in presentations.

In molecular dynamics simulations, this amount to choose the potential function $U(r_1, \dots, r_N)$ of the position of the nuclei which present the potential energy of the system when the atoms are arranged in specific configuration. The potential energy is usually constructed from the relative positions of the atom with respect to each other. Forces are derived as the gradients of the potential with respect to atomic displacement.

$$F_i = -\nabla_{r_i} U(r_1, \dots, r_N) \quad (1)$$

This form implies the presence of a conservation law of the total energy $E=K+V$ where K is the instantaneous kinetic energy.

The translational motion of spherical molecules is caused by a force F_i exerted by some external agent. The motion and the applied force are explicitly interpreted

by Newtonian. Newton's equation of motion of N particle system is written as a set of N coupled second order differential equation in time (Charles, *et al.*, 1995).

$$m_i \frac{d^2 \mathbf{r}_i}{dt^2} = -\nabla_i [U(\mathbf{r}_1, \mathbf{r}_2, \dots, \mathbf{r}_N)] \quad i=1, N \quad (2)$$

when m is the mass of the molecule, \mathbf{r}_i is a vector that locates the molecule with respect to a set of coordinate axes.

1. Force field

Force field ignores to calculate the energy and electronics motions of system as a function of the nuclear position. Molecular mechanic is based on a rather simple model of the interactions within the system with contributions from process such as the terms representing bonded interactions seek to account for the stretching of bonds, the bending of valence angles, and the rotation of dihedrals and non-bonded interactions aim to capture electrostatics, dispersion, and Pauli exclusion. (Guvench and MacKerell, 2008)

$$U(\mathbf{r}) = \sum_{\text{bonds}} K_b (b - b_0)^2 + \sum_{\text{angles}} K_\theta (\theta - \theta_0)^2 + \sum_{\text{dihedrals}} K_\chi [1 + \cos(n\chi - \sigma)] \\ + \sum_{\text{nonbonded pairs } ij} \left(\epsilon_{ij} \left[\left(\frac{R_{\text{min},ij}}{r_{ij}} \right)^{12} - 2 \left(\frac{R_{\text{min},ij}}{r_{ij}} \right)^6 \right] + \frac{q_i q_j}{r_{ij}} \right) \quad (3)$$

$U(\mathbf{r})$ denotes the potential energy which is a function of the position \mathbf{r} of N particles. The first term in equation 3 model the interaction between pairs of bonded atom by harmonic potential. The second term is angle which is a summation over all valence angles in molecule, modeled using harmonic potential. The third term is a dihedral potential that models how the energy change as bond rotates. The several of contributions of bond interactions are represented in Figure 7.

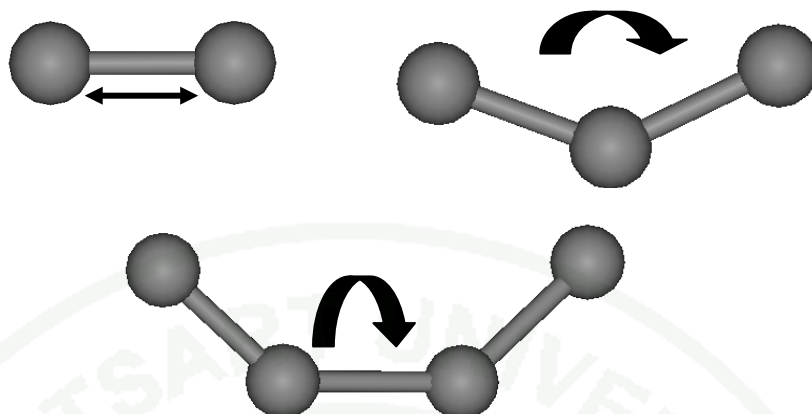


Figure 7 Schematic representation of the bond interaction contributions to a molecular mechanics force field.



Figure 8 Non-bonded interactions of molecular mechanics force field.

The fourth contribution is the non-bonded term as shown in Figure 8. This is calculated between all pairs of atoms (i and j) that are in different molecule or in the same molecule but separated by at least three bonds. In the simple force field this term is usually modeled using a Coulomb potential for electrostatic interactions and Lennard-Jones potential for van der Waals interactions.

2. Algorithms for molecular dynamics

In more realistic models of intermolecular interactions, the force on each particle will change whenever the particle changes its position. Under the influence of a continuous potential the motions of all the particles are coupled together, giving rise to a many body problem that cannot be solved analytically. Under such

circumstance the equations of motions are integrated using a finite difference method. Finite difference techniques are used to generate molecular dynamics trajectories. The general idea is the integration is broken down into many small stages, each separated in time by a fixed time δt . The total force on each particle in the configuration at a time t is calculated as the vector sum of its interactions with other particles. From the force we can determine the acceleration of particle which are then combined with the positions and velocities at a time t to calculate the positions and velocities a time $t+\delta t$. The force is assumed to be constant during the time step. The forces on the particles in their new positions are then determined, leading to new positions and velocities at a time $t+2\delta t$, and so on. There are many algorithms for integration the equations of motion using finite different methods. Verlet's algorithm which uses positions and velocities from previously calculated steps. The predictor-corrector algorithms are used to estimate positions and velocities for future steps.

2.1 Verlet's algorithm

Verlet's algorithm (Verlet, 1968), the basic is to write two third-order Taylor expansions for positions $\mathbf{r}(t)$, forward and backward in time.

$$\mathbf{r}(t+\Delta t) = \mathbf{r}(t) + \mathbf{v}(t)\Delta t + (1/2)\mathbf{a}(t)\Delta t^2 + (1/6)\mathbf{b}(t)\Delta t^3 + O(\Delta t^4) \quad (4)$$

$$\mathbf{r}(t-\Delta t) = \mathbf{r}(t) - \mathbf{v}(t)\Delta t + (1/2)\mathbf{a}(t)\Delta t^2 - (1/6)\mathbf{b}(t)\Delta t^3 + O(\Delta t^4) \quad (5)$$

This \mathbf{v} is the velocities, \mathbf{a} is the accelerations, and \mathbf{b} is the third derivatives of \mathbf{r} with respect to t . Adding the two expressions gives,

$$\mathbf{r}(t+\Delta t) = 2\mathbf{r}(t) - \mathbf{r}(t-\Delta t) + \mathbf{a}(t)\Delta t^2 + O(\Delta t^4) \quad (6)$$

This is the basic form of the Verlet algorithm. Since it is integrating Newton's equations, $\mathbf{a}(t)$ is just the force divided by the mass, and the force is in turn a function of the positions (Δt) :

$$\mathbf{a}(t) = -(1/m)\nabla V(\mathbf{r}(t)) \quad (7)$$

This is one of the most important tests to verify that molecular dynamics simulations are proceeding correctly. One could compute the velocities from the positions by using:

$$\mathbf{v}(t) = \frac{\mathbf{r}(t+\Delta t) - \mathbf{r}(t-\Delta t)}{2\Delta t} \quad (8)$$

An ever better implementation of the same basic algorithm is so-called velocity Verlet scheme, where positions, velocities and accelerations at time $t + \Delta t$ are obtained from the same quantities at time t in the following way.

$$\mathbf{r}(t+\Delta t) = \mathbf{r}(t) + \mathbf{v}(t)\Delta t + (1/2)\mathbf{a}(t)\Delta t^2 \quad (9)$$

$$\mathbf{v}(t+\Delta t/2) = \mathbf{v}(t) + (1/2)\mathbf{a}(t)\Delta t \quad (10)$$

$$\mathbf{a}(t+\Delta t) = -(1/m)\nabla V(\mathbf{r}(t+\Delta t)) \quad (11)$$

$$\mathbf{v}(t+\Delta t) = \mathbf{v}(t+\Delta t/2) + (1/2)\mathbf{a}(t+\Delta t)\Delta t \quad (12)$$

2.2 Predictor-corrector algorithm

Predictor-corrector algorithm constitutes another commonly used class of methods to integrate the equations of motion. Those more often used in molecular dynamics are consist of three steps:

1. Predict the positions and time derivatives $t+\Delta t$ by means of Taylor expansion.

$$\mathbf{r}(t+\Delta t) = \mathbf{r}(t) + \mathbf{v}(t)\Delta t \quad (13)$$

$$\mathbf{v}(t+\Delta t) = \mathbf{v}(t) + \mathbf{a}(t)\Delta t \quad (14)$$

2. Force evaluation is taking the gradient of the potential at the predicted positions at time $t+\Delta t$ and hence accelerations from the new position.

$$\frac{f(t+\Delta t)}{m} = \frac{dV}{dt} = -\omega^2 r(t+\Delta t) \quad (15)$$

3. Correct the predictions by new accelerations. The Euler's method performs again.

$$r(t+\Delta t) = r(t) + v(t)\Delta t \quad (16)$$

$$v(t+\Delta t) = v(t) - \omega^2 r(t+\Delta t)\Delta t \quad (17)$$

Predictor-corrector method is well flexibility in that many choices are possible for both the prediction and correction steps.

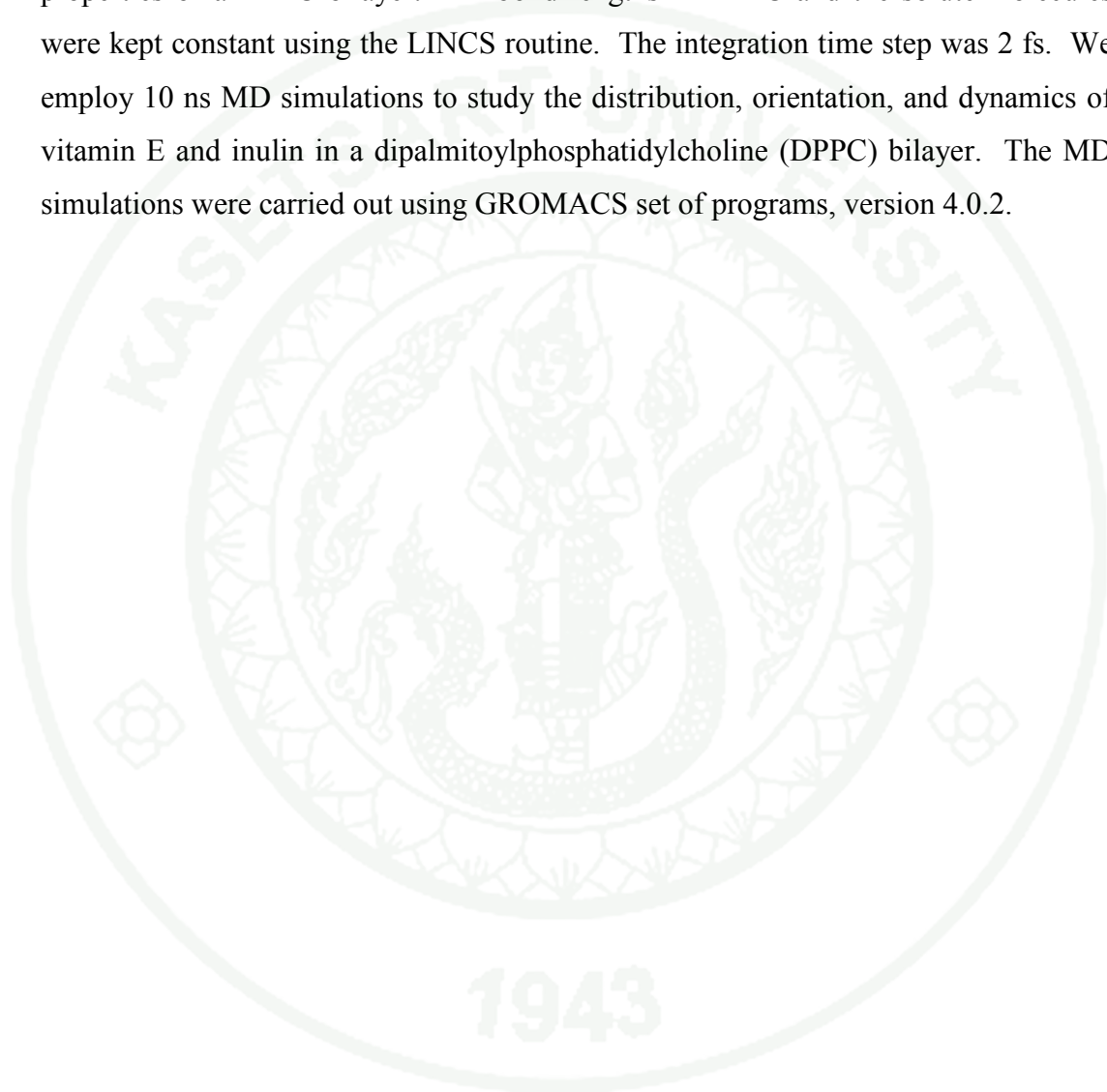
Methods of Calculations

The structure of phospholipid bilayer-water system with 64 DPPC and 3864 water molecules and 128 DPPC molecules and 3655 water molecules were taken from http://moose.bio.ucalgary.ca/index.php?page=Structures_and_Topologies. The lipid force field parameters (FFgmx) were used. The simulation is performed by using the GROMACS software. For water molecules, the SPC (single-point charge) parameters are used. The given bilayer is stabilized by an energy minimization. After that, the MD simulations were done for 2 ns in the NPT ensemble. In order to reach L_α state, the temperature was set to 323 K and the pressure was set to 1 bar. The temperature and pressure are controlled using the Berendsen method. In order to verify the appropriate simulation time, MD simulation with 128 DPPC/water molecules were performed for 50 ns.

The force-field used for the vitamin E and inulin molecules was parameterized according to the equilibrium B3LYP/6-31G (d,p) optimized structure and electronic charges. This force-field was previously adopted to the GROMOS96 force-field and it is tested to reproduce hydrogen bonding behavior of these compounds in bulk water as described in our previous study.

The distribution of vitamin E and inulin within a model membrane was modeled for a lipid bilayer, existing in the bio relevant liquid crystalline phase, so that the simulation temperature was chosen to be 323 K. At the beginning of MD simulations, the whole system was pre-equilibrated for 2 ns at the constant number of particles, constant pressure 1 atm, and the constant temperature 323 K (NPT ensemble). Three-dimensional periodic boundary conditions were applied with the z axis lying along a direction normal to the bilayer. The pressure was controlled semiisotropically, so that the x-y and z sizes of the simulation box were allowed to fluctuate independently from each other, keeping the total pressure constant. Thus, membrane area and thickness were therefore free to adjust under the NPT condition. The reference temperature and pressure were kept constant using a weak coupling scheme (Berendsen *et al.*, 1984) with coupling constant of $\tau_p=0.1$ ps for temperature

coupling and $\tau_t=1.0$ ps for pressure coupling. Electrostatic interactions were simulated with the particle mesh Ewald (PME) approach using the long-range cutoff of 1.8 nm. The cut-off distance of Lennard-Jones interactions was also equal to 1.8 nm. This MD setup has been demonstrated to be optimal for the simulations of the equilibrium properties of a DPPC bilayer. All bond lengths in DPPC and the solute molecules were kept constant using the LINCS routine. The integration time step was 2 fs. We employ 10 ns MD simulations to study the distribution, orientation, and dynamics of vitamin E and inulin in a dipalmitoylphosphatidylcholine (DPPC) bilayer. The MD simulations were carried out using GROMACS set of programs, version 4.0.2.



RESULTS AND DISCUSSION

1. 64DPPC and 64DPPC/water lipids bilayer

After the 2 ns of 64DPPC and 64DPPC/water simulation, configurationally energy (Figure 10) and volume of the simulation cell were converged. Total energy of 64DPPC and 64DPPC/water lipid bilayer was -4.45×10^5 and -1.14×10^5 kJ/mol, respectively. RMSD of 64DPPC and 64DPPC/water was 0.1 and 0.4 nm, respectively (Figure 11). The area per head group and lamellar spacing as a function of time during the entire run were calculated. The average values of the surface area per lipid of 64DPPC and 64DPPC/water were 36.2 and 34.5 \AA^2 , respectively. Although the average repeat distance did not change significantly of 64DPPC and 64DPPC/water systems, the average area per lipid became slightly lower. The change in the geometry of the membrane had little effect on the chain ordering.

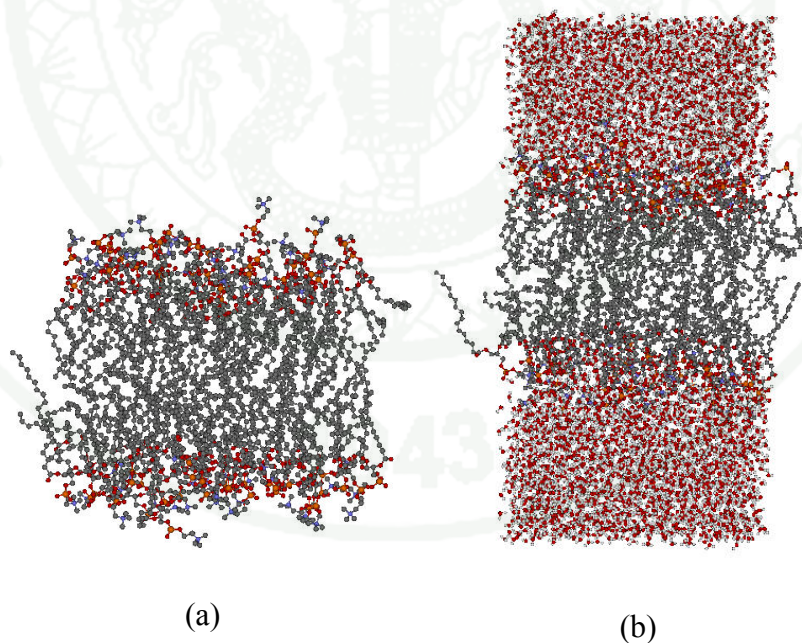


Figure 9 Structures of 64 DPPC (a) and 64 DPPC/water molecules.

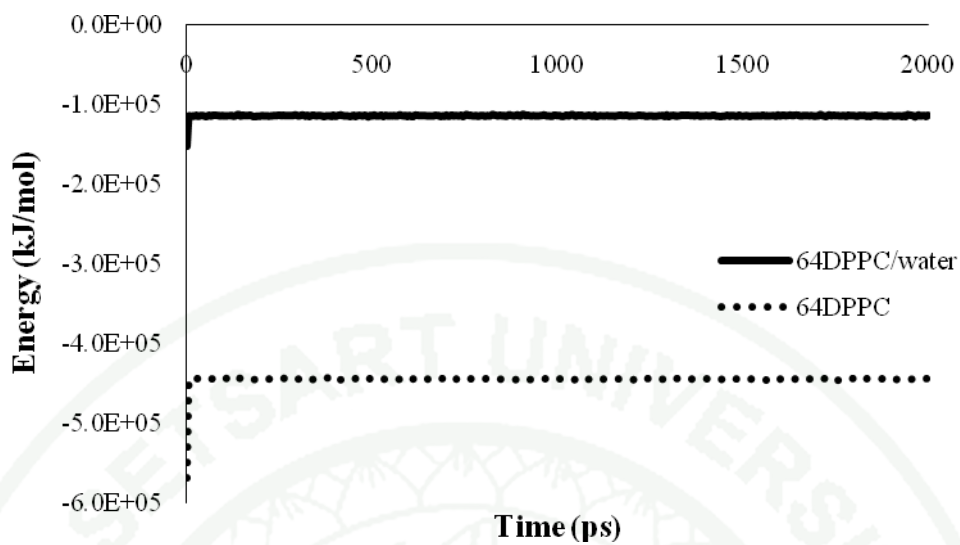


Figure 10 Total energy plot vs. Time (ps) 64DPPC and 64DPPC/water lipid bilayer.

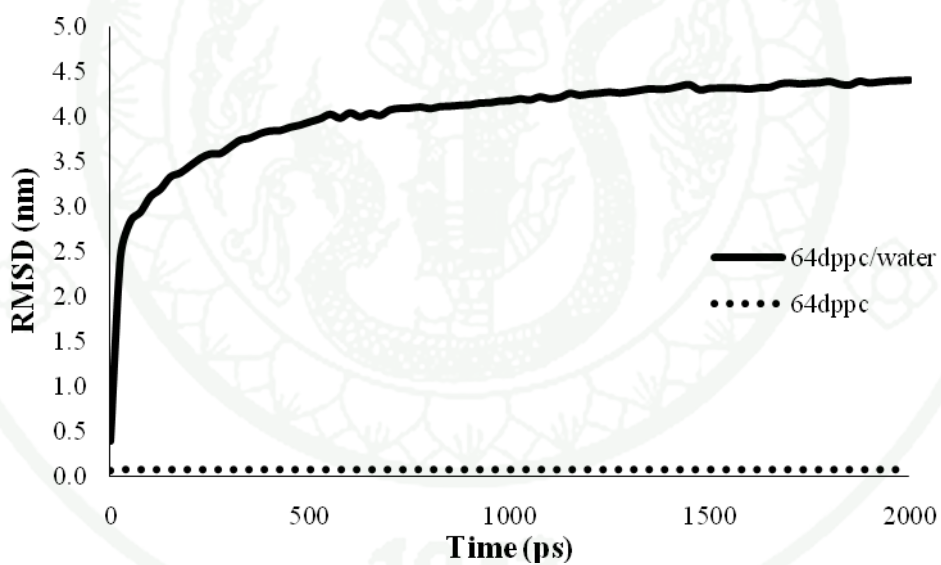


Figure 11 RMSD of 64DPPC and 64DPPC/water lipid bilayer for 2 ns.

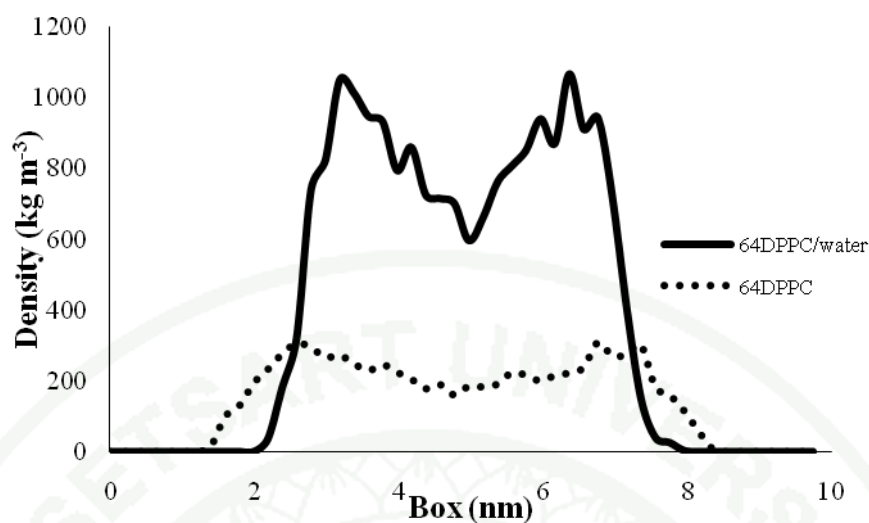


Figure 12 Mass density along z-dimension of 64DPPC and 64DPPC/water lipid bilayer.

The position of all atoms in the system were calculated and averaged with respect to the z axis, normal to the bilayer. Using the symmetry of the bilayer, the mass density profiles were also averaged over the two bilayer leaflets. The mass density profiles were obtained by averaging the MD trajectory for the last 2 ns of the simulation period. The results for the density distribution of the 64DPPC and 64DPPC/water (Figure 12) was similar to the one observed in bilayers with polar head groups located towards the water region and a hydrophobic interface with the triglyceride phase separating the aliphatic phospholipids' tails.

Table 1 Averaging properties between 64DPPC and 64DPPC/water lipid bilayer

Properties	64DPPC	64DPPC/water
Surface Area (\AA^2)	36.2	34.5
RMSD (nm)	0.1	4.0
Energy (kJ/mol)	-4.45×10^5	-1.14×10^5
Temperature (K)	326	327
Pressure (bar)	1.0	1.0

2. 128DPPC and 128DPPC/water lipids bilayer

128DPPC and 128DPPC/water simulation, configurationally energy (Figure 15) and volume of the simulation cell were converged after the 2 ns. The total energy of 128DPPC and 128DPPC/water lipid bilayer was -7.5×10^5 and -3.8×10^4 kJ/mol, respectively. RMSD was 0.07 and 3.22 nm, respectively (Figure 14). The area per head group and lamellar spacing as a function of time during the entire run were calculated. The average values of the surface area per lipid of 128DPPC and 128DPPC/water were 69.5 and 63.3 Å², respectively. The average area per lipid became slightly lower. The change in the geometry of the membrane had little effect on the chain ordering.

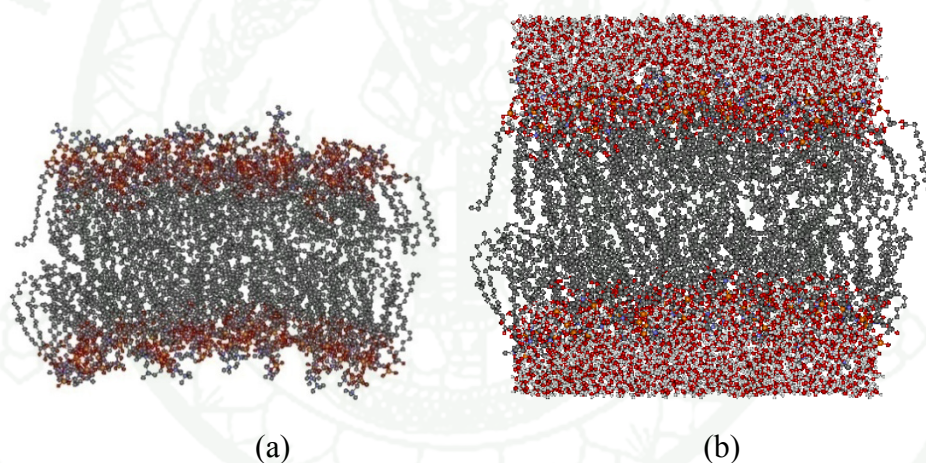


Figure 13 Structures of 128DPPC (a) and 128DPPC/water (b) molecules at 2 ns.

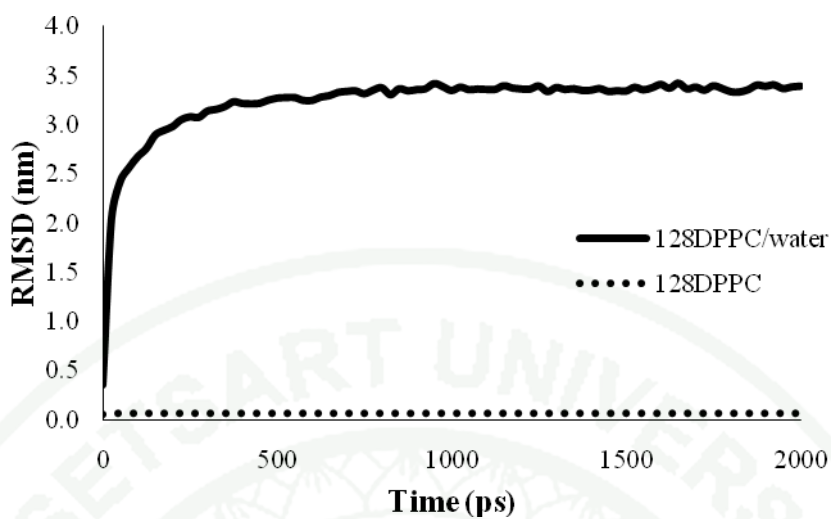


Figure 14 RMSD of 128DPPC and 128DPPC/water lipid bilayer for 2 ns.

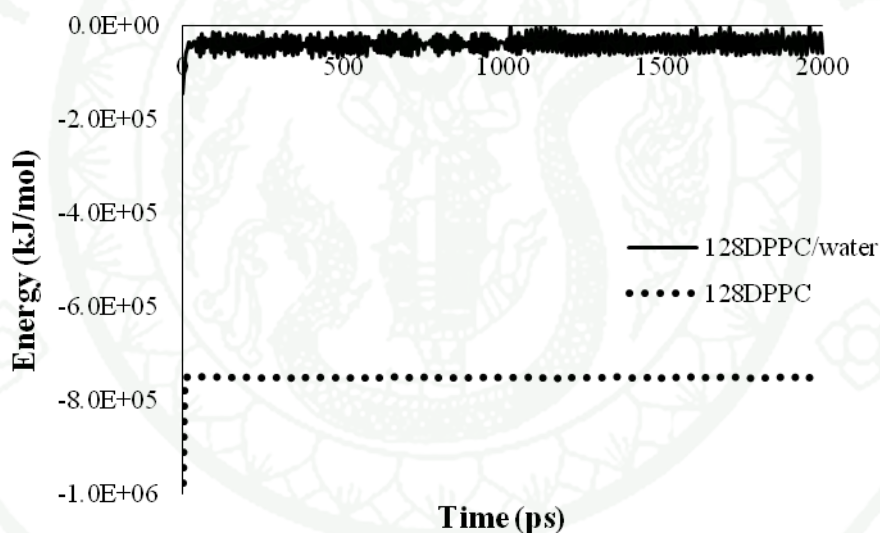


Figure 15 Total energy plot vs. Time (ps) 128DPPC and 128DPPC/water lipid bilayer.

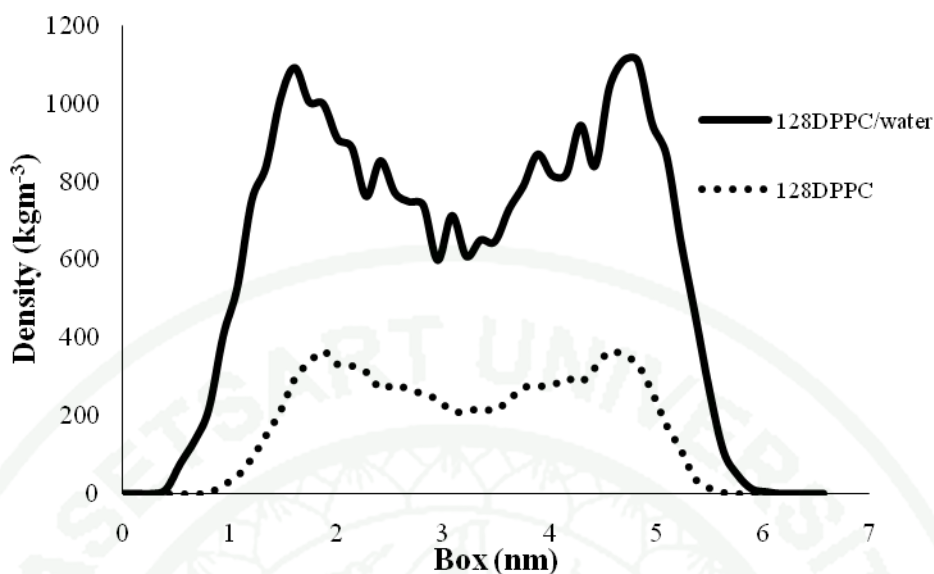


Figure 16 Mass density along z-dimension of 128DPPC and 128DPPC/water lipid bilayer.

Figure 16 displays the mass density across the phospholipid bilayers. In addition, these figures were compared between 128DPPC and 128DPPC/water lipid bilayer. Using the symmetry of the bilayer, the mass density profiles were also averaged over the two bilayer leaflets. The asymmetry in the bilayer induced a gradient in the total atomic density, so that the total density in the leaflet containing the 128DPPC/water was higher than that in the leaflet composed only of 128DPPC molecules.

Table 2 Averaging properties between 128DPPC and 128DPPC/water lipid bilayer

Properties	128DPPC	128DPPC/water
Surface Area (\AA^2)	69.5	63.3
RMSD (nm)	0.07	3.22
Energy (kJ/mol)	-7.5×10^5	-3.8×10^4
Temperature (K)	326	326
Pressure (bar)	1.0	1.0

3. 64 and 128 DPPC lipid bilayer in the water

Molecular dynamics simulations of 64 and 128 DPPC lipids bilayer in the water was run for 2 ns with constant temperature and pressure. In the simulations, parameters were investigated including energy components and phosphate density profiles. Snapshot structures of 64 and 128 DPPC lipid bilayer in the water from MD simulations at 2 ns were shown in Figure 17.

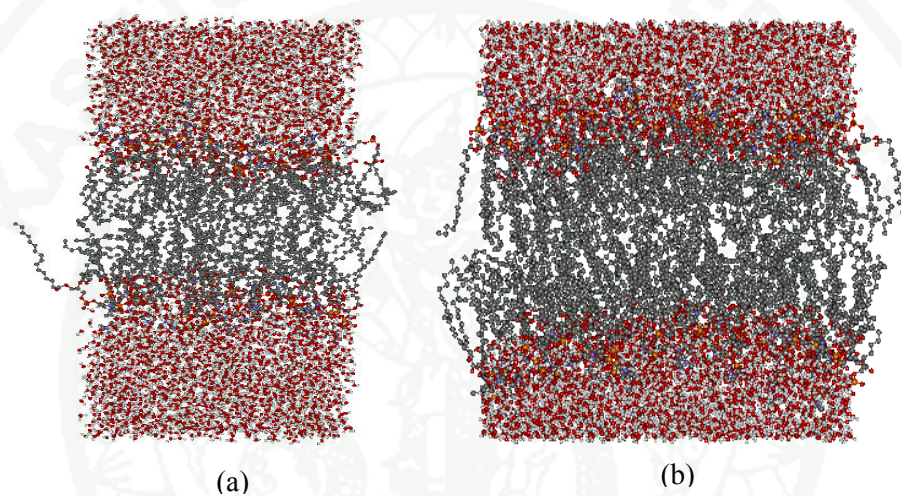


Figure 17 Snapshots of 64 (a) and 128 (b) DPPC lipids bilayer in the water at 2 ns.

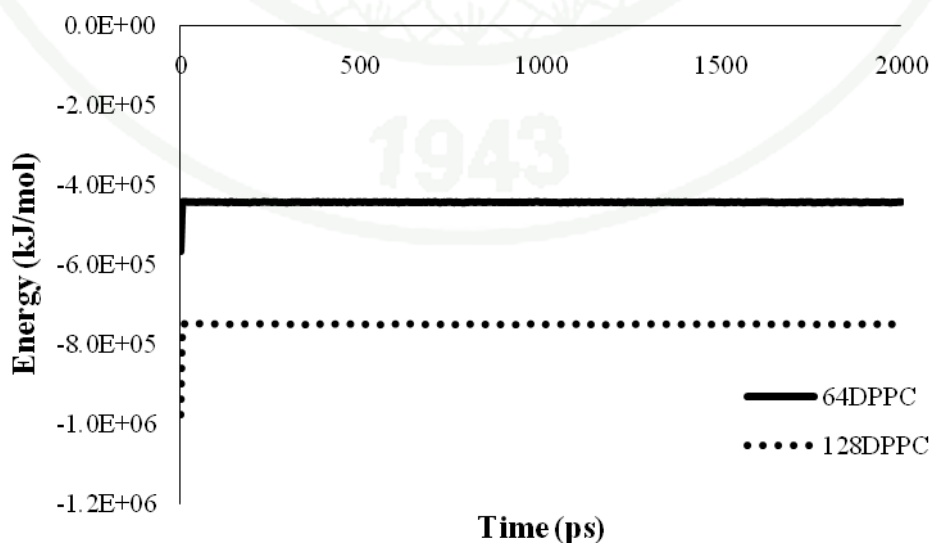


Figure 18 Total energy plot vs. Time (ps) of 64 and 128 DPPC lipid bilayer.

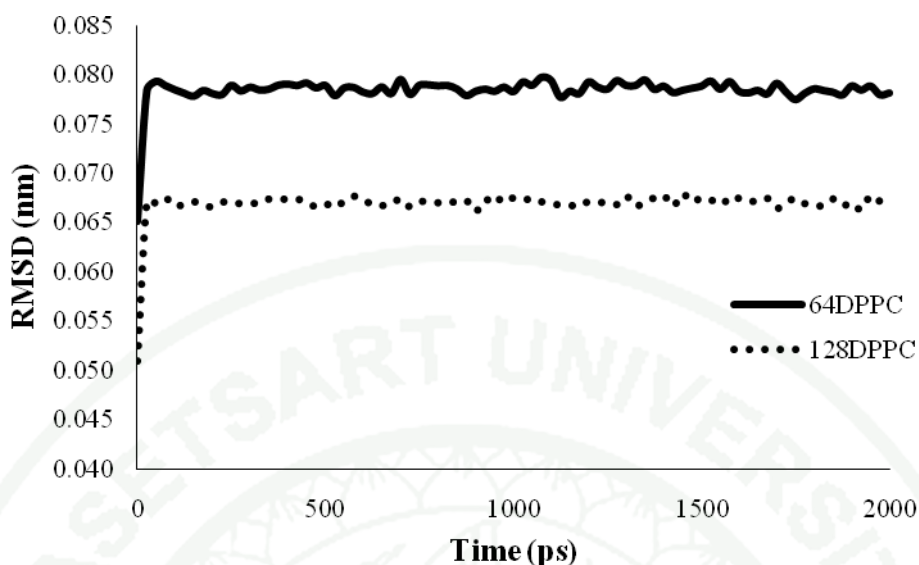


Figure 19 RMSD of 64 and 128 DPPC lipid bilayer for 2 ns.

Stability of the total energy (Figure 18), RMSD plot indicates good equilibrium. Some properties were averaging and reported in Table 3. Total energy of 64 and 128 DPPC lipid bilayer were -4.45×10^5 and -7.50×10^5 kJ/mol, respectively. Because structure of 64 DPPC lipid bilayer was smaller than 128 DPPC lipid bilayer so that internal energy (E^{bond}) of 64 DPPC lipid bilayer was less than 128 DPPC lipid bilayer. RMSD was calculated to compare with the starting structure that minimized. RMSD of 64 and 128 DPPC was 0.78 and 0.66 Å, respectively. Small RMSD value refers that structure of both DPPC lipid bilayer during molecular dynamic simulations were stable and not changed from starting structure that minimized. Density of DPPC bilayers along the z-dimension was calculated as show in Figure 20. Density different of 64 and 128 DPPC was averaging at 2-5 nm that it was 56.32 kg/m^3 . This was due to P-P distances between molecules of DPPC in 64 and 128 DPPC lipid bilayer. P-P distance was 9.63 Å and 6.82 Å in 64 and 128 DPPC lipid bilayer, respectively. Structure of DPPC lipid bilayer in z-dimesion 5 Å found that 2 peaks had similar pattern but level of density was different because density of Khandelia and coworker had complex in DPPC lipid bilayer (Khandelia *et al.*, 2008). The investigation by molecular dynamic simulations of 64 and 128 DPPC lipid bilayer found that the mainly different properties were the density along z-dimension of DPPC lipid bilayer. The results showed that the density of 64 DPPC lipid bilayer were lower than that of

128 DPPC lipid bilayer. P-P distance between DPPC molecules in 64 DPPC lipid bilayer was longer than in 128 DPPC lipid bilayer. Therefore, 64 DPPC lipid bilayer maybe lost the membrane property. The 128 DPPC lipid bilayer can be a representative of lipid membrane for studying by molecular dynamics simulations in next step.

Table 3 Averaging properties between 64 and 128 DPPC/water lipid bilayer.

Properties	64DPPC	128DPPC
Surface Area (\AA^2)	36.2	69.5
RMSD (nm)	0.078	0.066
Energy (kJ/mol)	-4.45×10^5	-7.50×10^5
Temperature (K)	326	326
Pressure (bar)	1.0	1.0

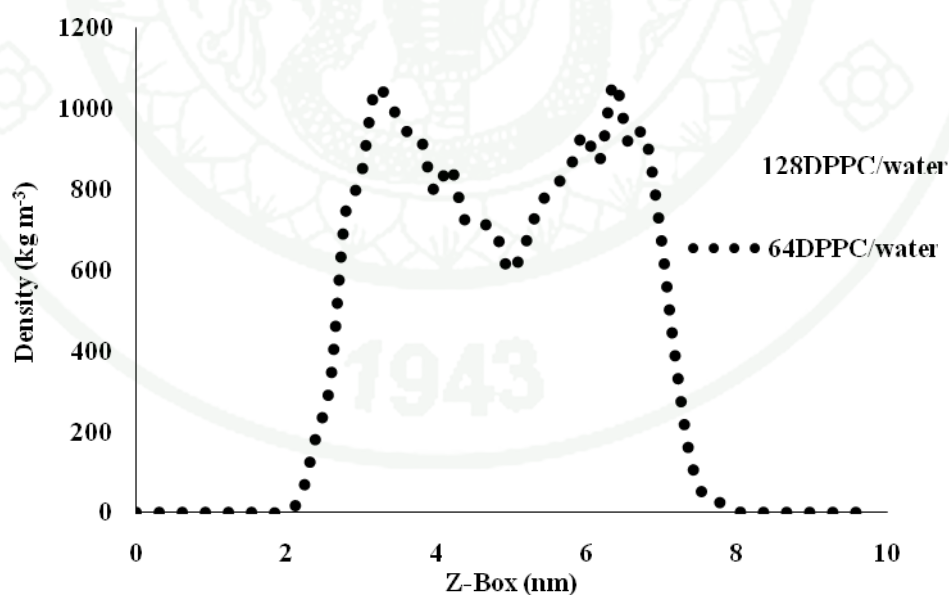


Figure 20 Mass Density along z-dimension of 64 and 128 DPPC lipid bilayer in water.

3. Three times of 128DPPC lipid bilayer

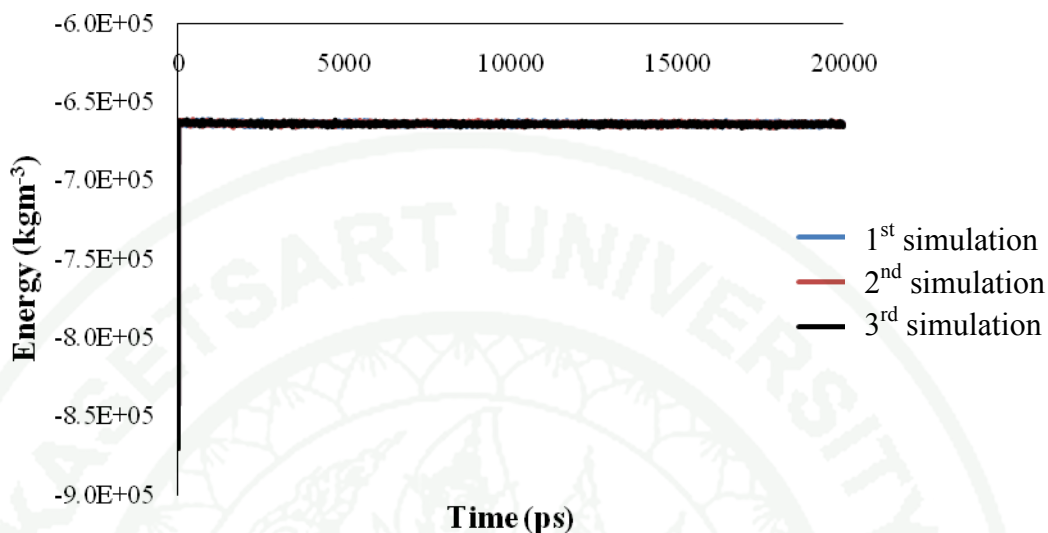


Figure 21 Energy comparison of three 128DPPC/water simulations at 20 ns.

Stability of energy three 128DPPC/water simulations at 20 ns that they were about -6.64×10^5 kJ/mol. Temperature and pressure properties were similar in three DPPC structures systems (Figures 22 and 23). All-atom RMSD has been calculated using GROMACS `g_rms` functions, which used independent similarity parameter. The result at 20 ns simulations of three domains of 128DPPC structures were shown in Figure 24. For the first 25 ps, RMSD values steadily increases and reached a plateau. After 25 ps of MD simulations, RMSD values fluctuated around an average value of 0.066 Å.

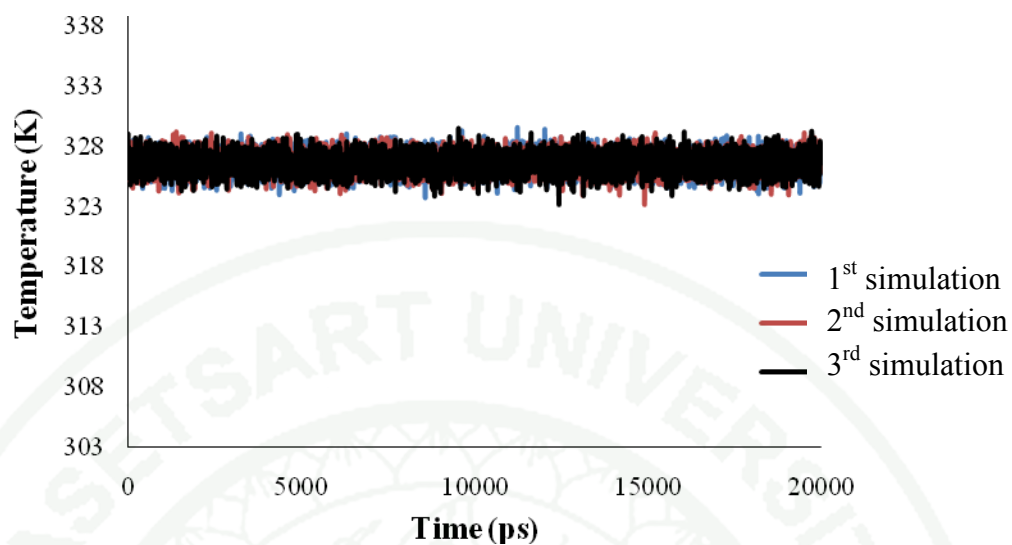


Figure 22 Temperature comparison of three 128DPPC/water simulations for 20 ns.

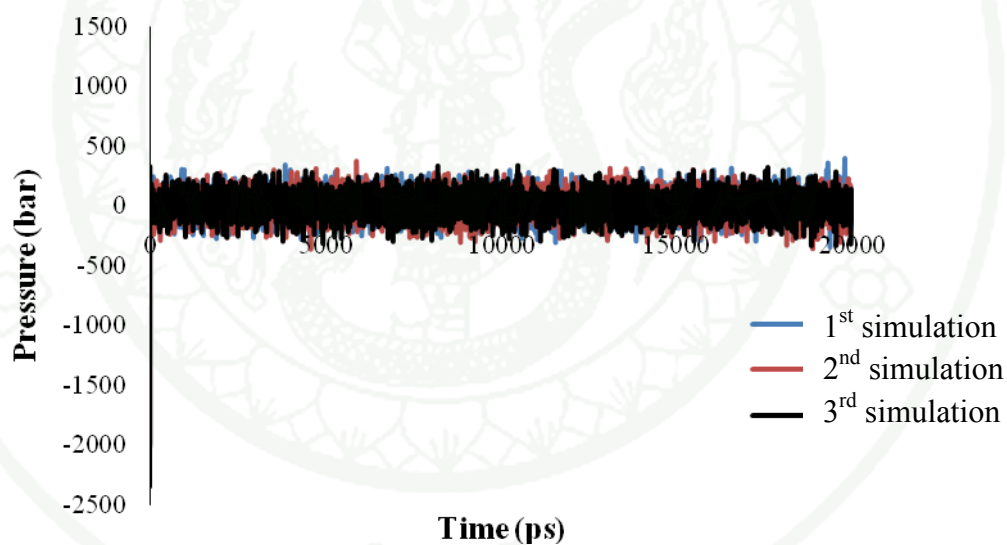


Figure 23 Pressure comparison of three 128DPPC/water simulations for 20 ns.

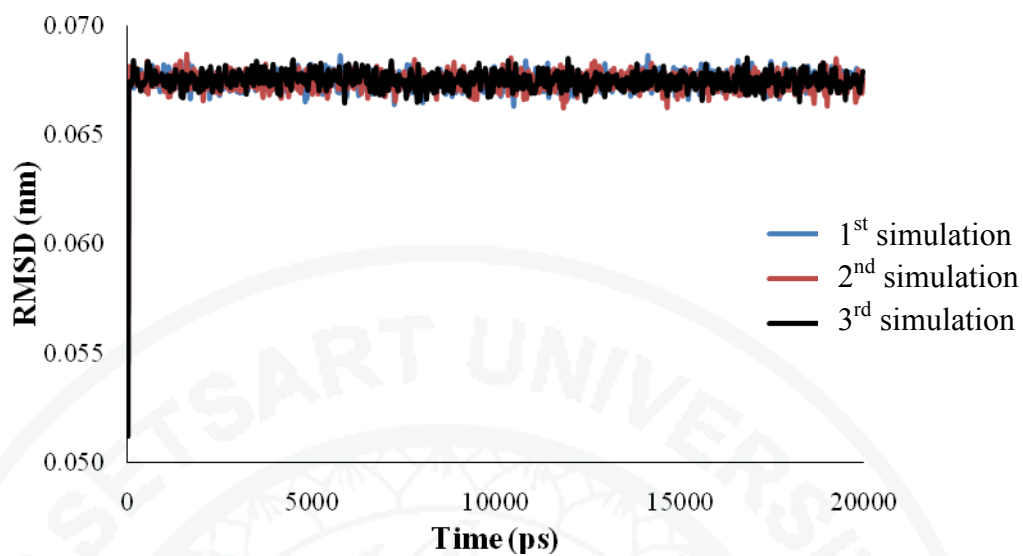


Figure 24 RMSD comparison of three 128DPPC/water simulations for 20 ns.

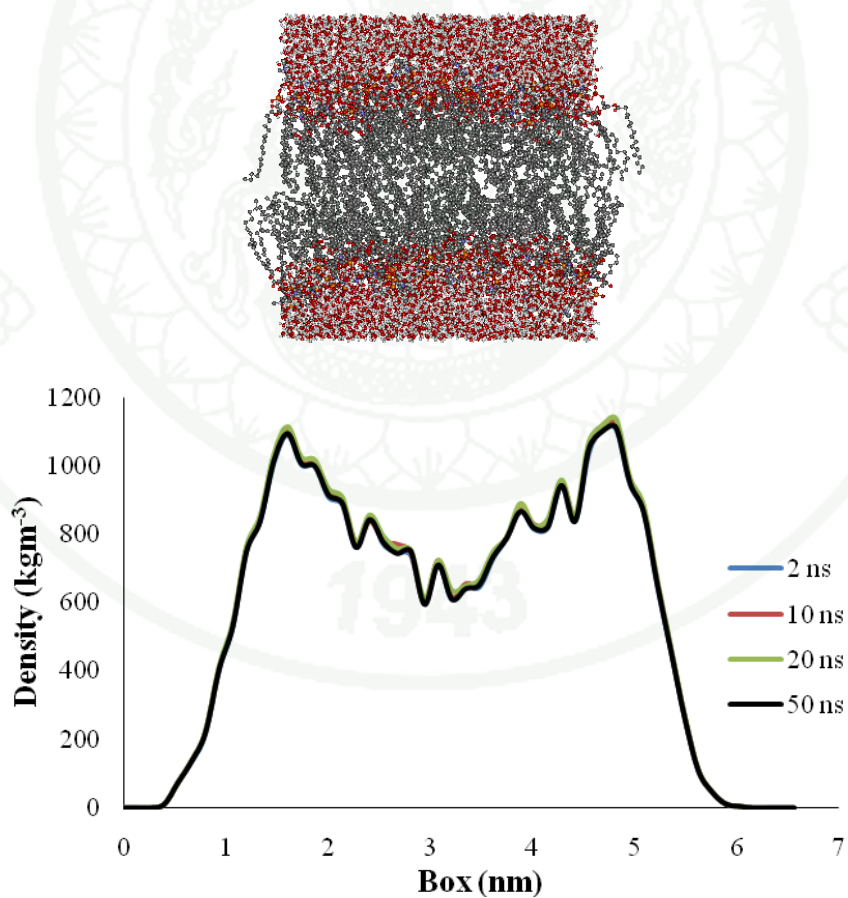


Figure 25 Mass density of 128DPPC/water at 2, 10, 20 and 50 ns.

The mass density of 128DPPC/water was shown in Figure 25. The mass density of 128DPPC was compared at 2, 10, 20 and 50 ns. They were similar position of individual of 128DPPC bilayer, therefore 128DPPC and 3655 water molecules at 10 ns was selected for further studied. The time average the density distributions of the individual functional groups of the bilayer, such as choline, phosphate and carbonyl group, as well as a glycerol backbone and acyl chains of phospholipids, were found to be fully consistent with previous MD simulations for the same bilayer (Figure 26).

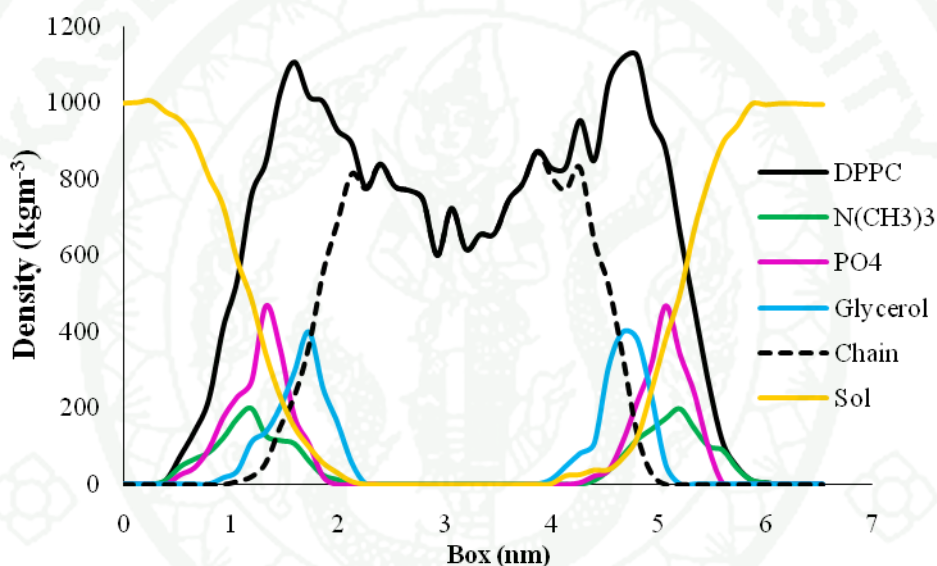


Figure 26 Mass density of 128DPPC/water lipid bilayer at 10 ns.

4. Vitamin E/128DPPC simulations

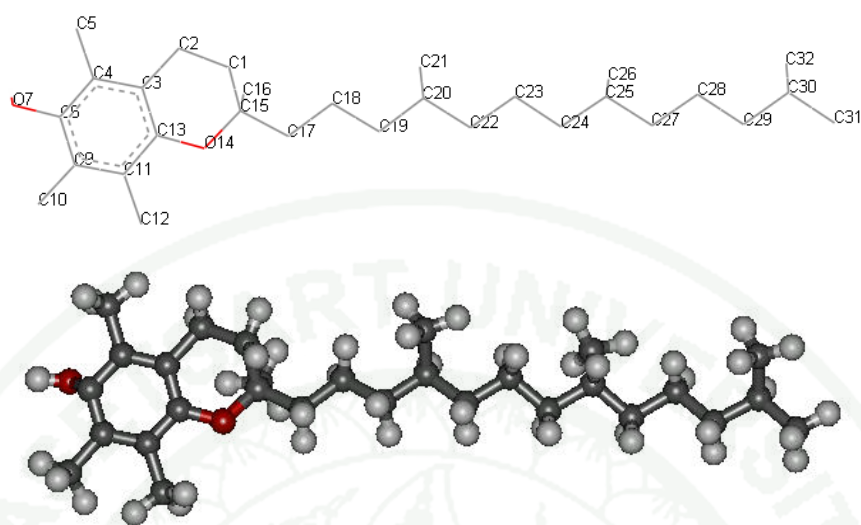


Figure 27 Starting structure of vitamin E (tocopherol).

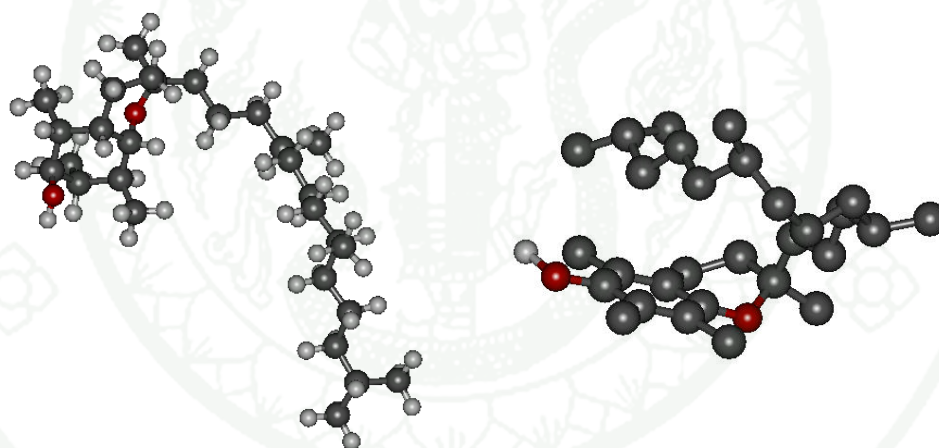


Figure 28 Optimized structure of vitamin E using by B3LYP/6-31G (d, p) (a) and molecular dynamics simulations in water (b).

Table 4 Optimized bond length, angle and torsion of vitamin E by B3LYP/6-31G (d,p) and molecular dynamics simulations in water at 2 ns

Bond length (Å)	B3LYP/6-31G(d,p)	MD	Angle (°)	B3LYP/6-31G(d,p)	MD	Torsion angle (°)	B3LYP/6-31G(d,p)	MD
C6-O7	1.42	1.53	C15-C17-C18	114.60	115.07	C15-C17-C18-C19	-179.78	177.65
C17-C18	1.51	1.53	C17-C18-C19	110.53	107.43	C17-C18-C19-C20	-172.54	-137.57
C18-C19	1.51	1.52	C18-C19-C20	112.79	114.65	C18-C19-C20-C22	-64.71	69.37
C19-C20	1.52	1.53	C19-C20-C22	110.85	111.82	C19-C20-C22-C23	175.71	-160.49
C20-C22	1.52	1.52	C20-C22-C23	112.60	111.41	C20-C22-C23-C24	-172.90	52.69
C23-C24	1.51	1.53	C22-C23-C24	110.90	113.48	C22-C23-C24-C25	-172.59	71.00
C24-C25	1.51	1.53	C23-C24-C25	113.00	112.00	C23-C24-C25-C27	-64.41	58.16
C26-C27	1.52	1.52	C24-C25-C27	111.07	115.13	C24-C25-C27-C28	175.55	-154.80
C27-C28	1.51	1.53	C25-C27-C28	112.39	106.26	C25-C27-C28-C29	-173.07	-177.22
C28-C29	1.51	1.52	C27-C28-C29	111.09	109.62	C27-C28-C29-C30	-173.90	165.90
C29-C30	1.52	1.53	C28-C29-C30	112.45	112.41			

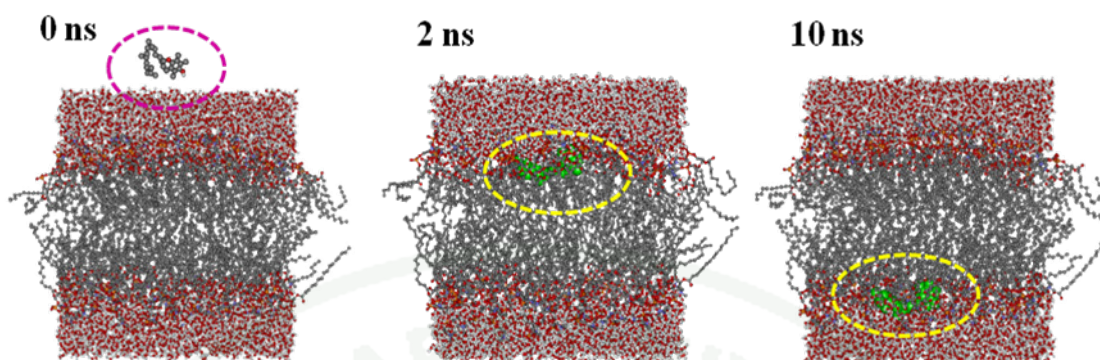


Figure 29 Snapshots of the MD boxes taken from the simulations of vitamin E molecules in the DPPC bilayer at 0 ns, 2 ns and 10 ns.

The initial configuration of vitamin E/DPPC system containing vitamin E molecule was shown in Figure 29. The MD simulations demonstrate that at 2 ns, a significant fraction of vitamin E tends to diffuse from aqueous solution into the polar interfacial region of DPPC bilayer. The distribution of vitamin E molecule at the end of 10 ns simulations was presented at the opposite of the entrance.

One of the most important structural parameter which describes packing of phospholipid molecules within a bilayer was the surface area per one lipid molecule. In the case of molecular dynamics simulations of a fully hydrated DPPC bilayer in pure water at $T = 323$ K. The average value of the surface area per lipid was equal to 63.3 \AA^2 . The calculated area agrees well with the experimental value of 62.9 \AA^2 . And the average value of surface area per lipid in the presence of vitamin E equal to 63.1 \AA^2 . (Figure 30)

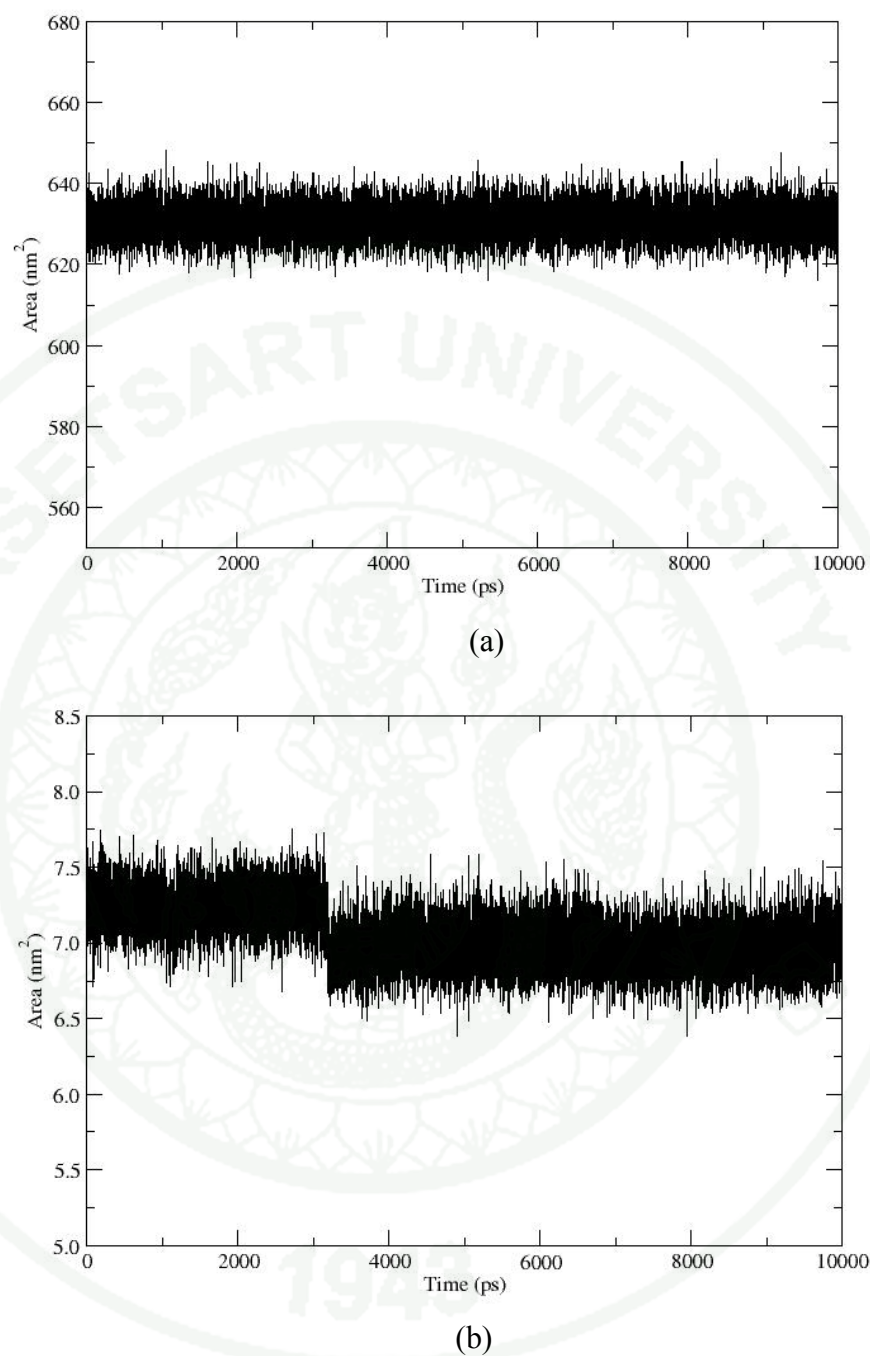


Figure 30 Surface area of 128DPPC bilayer (a) and vitamin E (b) for 10 ns.

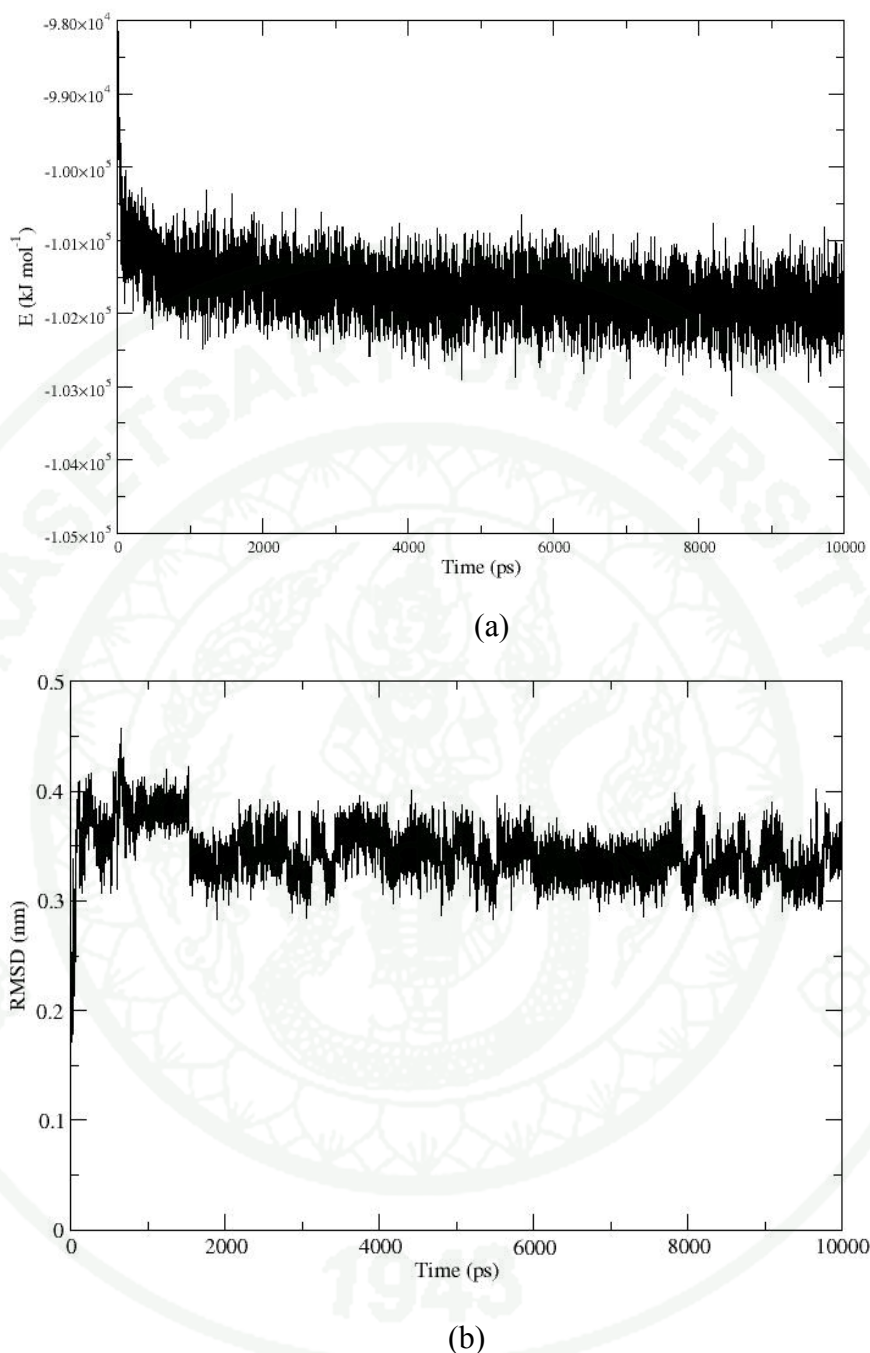
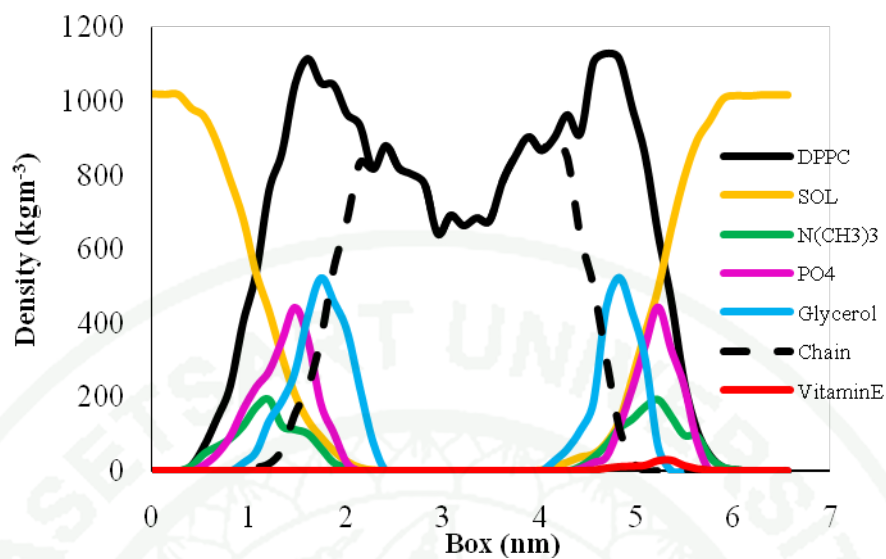
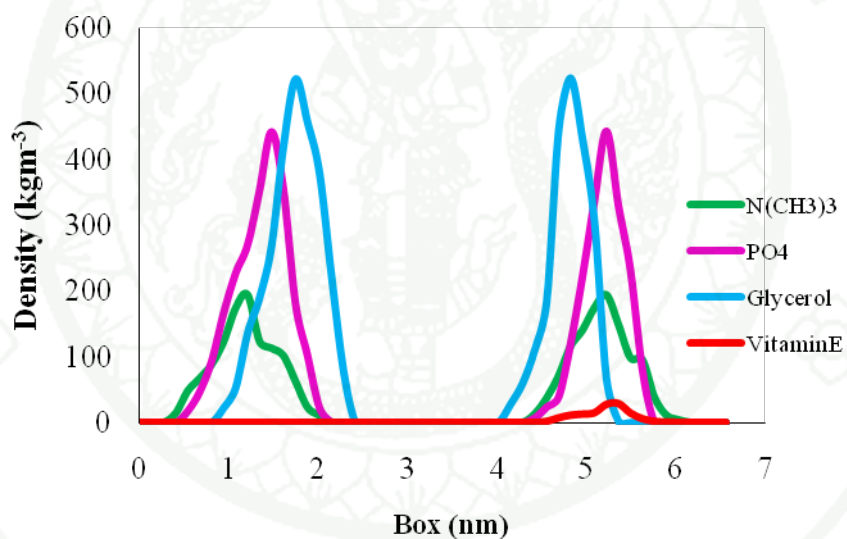


Figure 31 Total energy of DPPC/vitamin E system (a) and RMSD of vitamin E (b) for 10 ns.

From the vitamin E/DPPC system, total energy and RMSD were studied. The stability in the plot between total energy and RMSD indicated good equilibrium after 2 ns (Figure 31). The total energy of vitamin E/DPPC was $-1.02 \times 10^5 \text{ kJ/mol}$ and RMSD of vitamin E was 3.5 \AA as compared with the starting structure.



(a)



(b)

Figure 32 Mass density distribution profiles for individual components of the DPPC bilayer and for the total density distribution of molecules of vitamin E (a), (b).

To evaluate the distribution of vitamin E within DPPC bilayer quantitatively, mass density profiles of different molecular components across the bilayer were considered. The position of all atoms in the system were calculated and averaged with respect to the z axis. In Figure 32, the yellow line was the mass density of water molecules. It shown that mass density distribution of water molecules was gradually reduced until the middle of the membrane bilayer, of the DPPC molecules in the black line the highest value of DPPC was about 1.5 and 5.0 nm. Then, DPPC was separated to choline, phosphate, glycerol and acyl chain. The green, pink, blue and dash line represented the mass density of choline, phosphate, glycerol and acyl chain, respectively. The red color represents the mass density distribution of vitamin E. The position of vitamin E was located near the head group of DPPC bilayer.

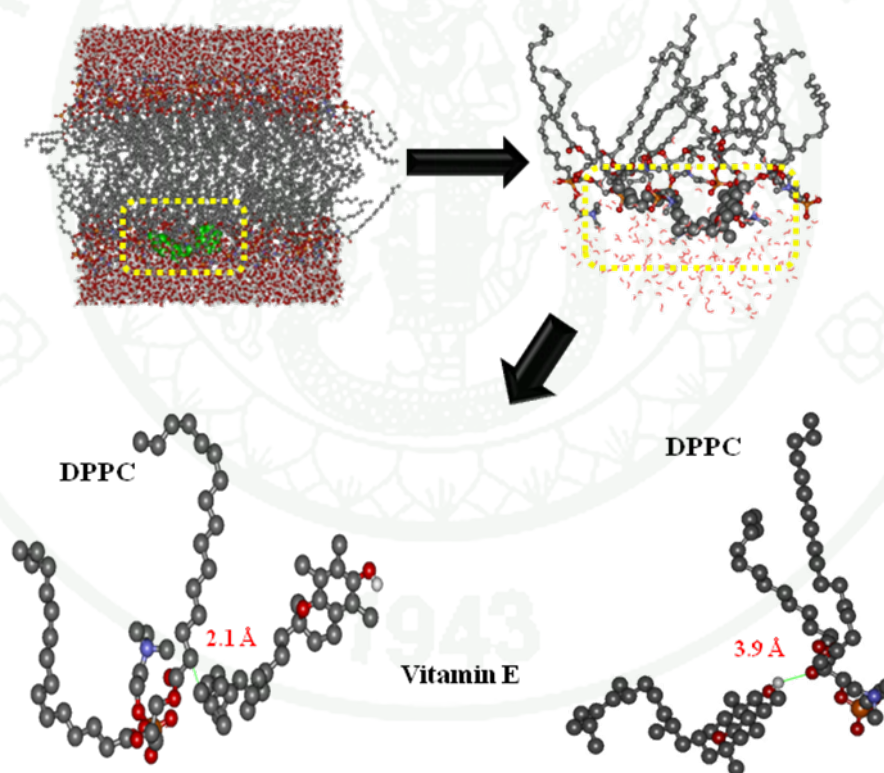
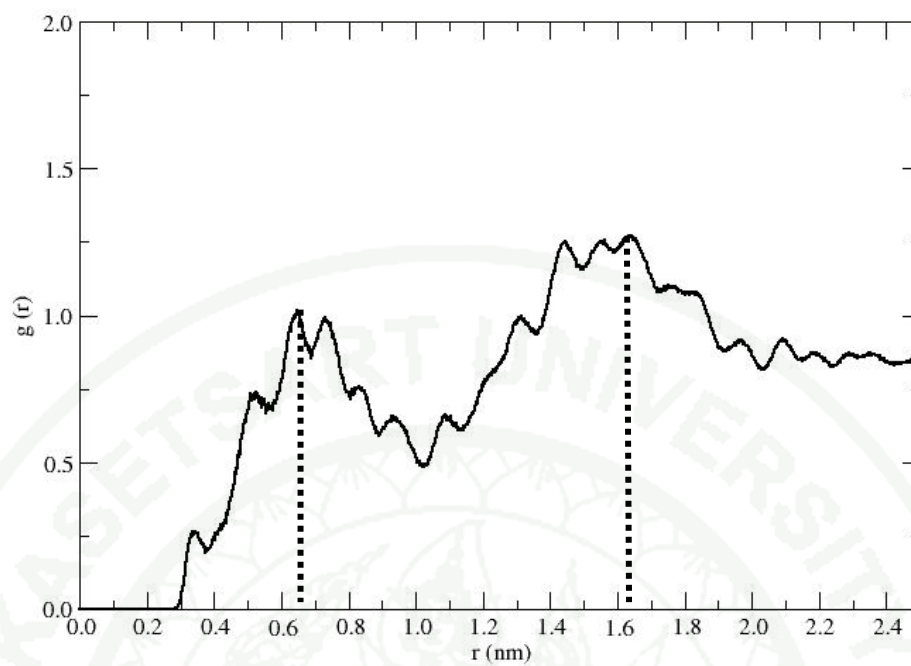
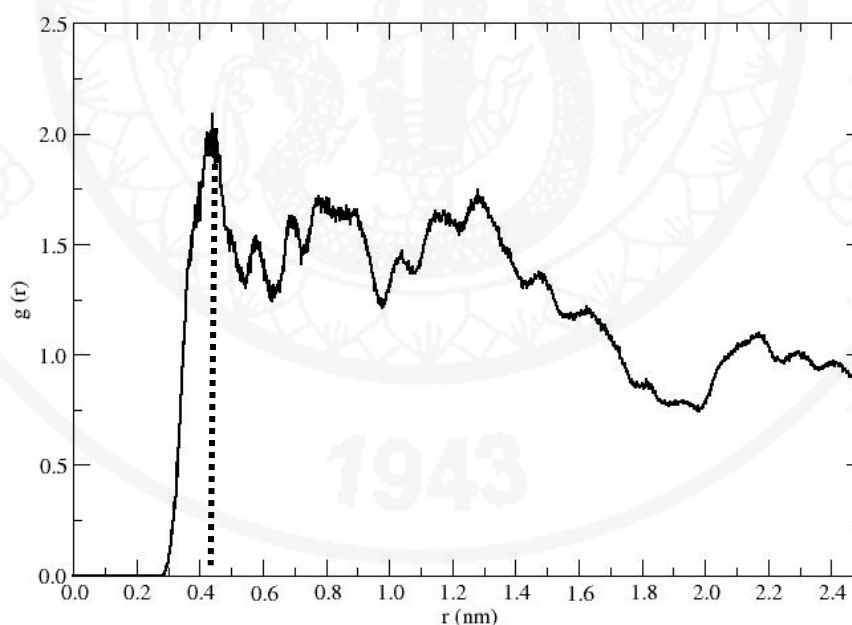


Figure 33 Snapshots of vitamin E molecule in the DPPC bilayer at 10 ns.

The vitamin E was preferably accommodated at the head of the bilayer about the glycerol moiety, shown in Figure 33. The weak hydrogen bond was found between hydroxyl group (OH) of vitamin E and oxygen atom of glycerol by average distance of 3.9 Å and van der Waals interaction was found with average distance of 2.1 Å. Radial distribution functions of hydroxyl group of vitamin E and oxygen atom of phosphate was at distance 6.0 and 15.0 Å. Radial distribution functions of hydroxyl group of vitamin E and oxygen atom of glycerol was at distance 4.0 Å. This distance corresponded to weak hydrogen bond between vitamin E and glycerol of DPPC bilayer. The radial distribution functions of hydroxyl atom of vitamin E and oxygen atom of phosphate was at distance 6.0 and 16.0 Å. The hydroxyl group of vitamin E and oxygen atom of glycerol was at distance 4.0 Å. This distance corresponded to weak hydrogen bond.



(a)



(b)

Figure 34 Radial pair distribution functions $g(R)$ between the O-H hydrogen atom of vitamin E and the oxygen atoms of the phosphate (a) and glycerol (b) groups of the DPPC lipids.

5. Inulin

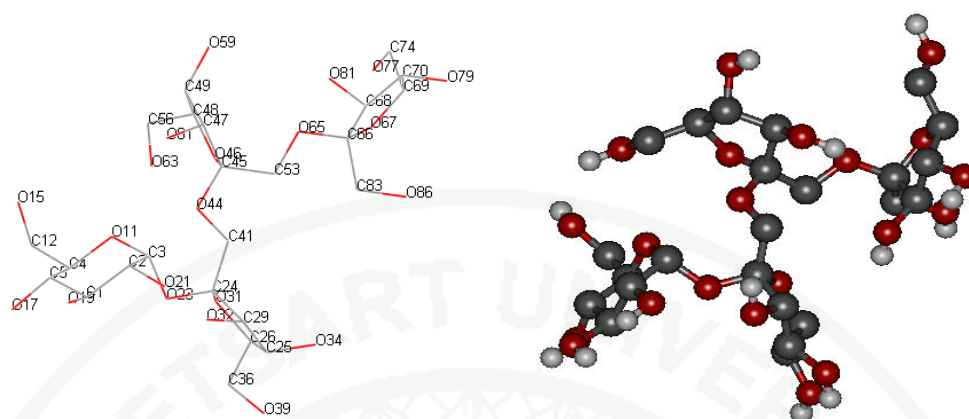


Figure 35 Starting structure of inulin.

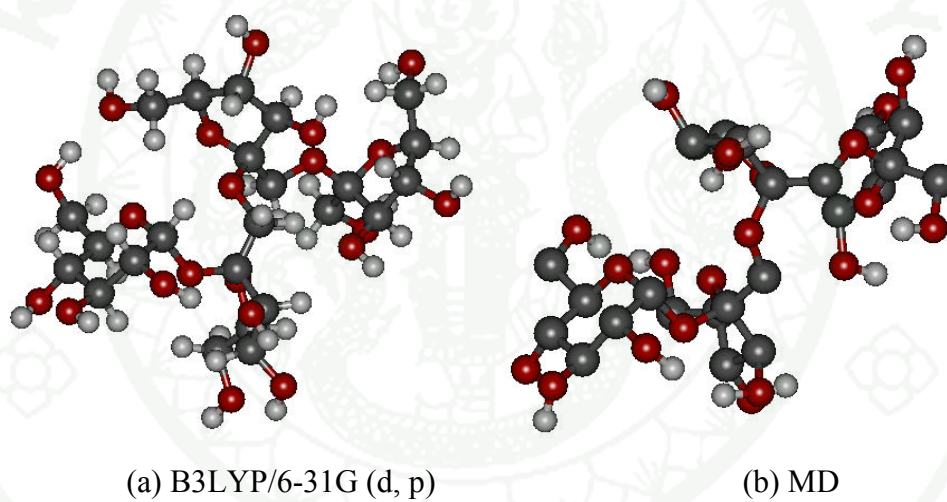


Figure 36 Optimized structure of inulin using by B3LYP/6-31G (d, p) (a) and molecular dynamics simulations in water (b).

Table 5 Optimized bond length, angle and torsion of inulin by B3LYP/6-31G (d,p) and molecular dynamics simulations in water at 2 ns.

Bond length (Å)	B3LYP/6- 31G(d,p)	MD	Angle (°)	B3LYP/6- 31G(d,p)	MD	Torsion angle (°)	B3LYP/6-31G(d,p)	MD
C1-O19	1.46	1.42	C4-C12-O15	109.45	112.46	C4-C12-O15-16	-179.27	162.71
C2-C21	1.46	1.44	C3-O23-C24	124.76	115.08	C3-O23-C24-C41	10.74	50.68
C4-C12	1.51	1.54	C26-C36-O39	105.90	111.26	C26-C36-O39- H40	-159.11	-48.56
C12-O15	1.47	1.48	C24-C41-O44	109.09	114.72	C24-C41-O44-C45	-164.42	-177.11
C36-O39	1.46	1.45	C41-O44-C45	127.95	115.65	C41-O44-C45-C53	28.75	-84.99
C25-C34	1.47	1.44	C48-C56-O63	111.43	114.19	C48-C56-O63-H64	-121.64	145.33
C56-O63	1.46	1.43	C45-C53-O65	101.90	119.58	C45-C53-O65-C66	-171.20	-154.32
C47-O61	1.46	1.43	C53-O65-C66	125.21	113.07	O65-C66-C83-O86	-177.12	-75.74
C68-O81	1.46	1.43	O65-C66-C83	112.64	111.72	C66-C83-O86-H87	173.68	108.63
C70-O79	1.46	1.43	C66-C83-O86	106.91	114.42	C69-C74-O77-H78	-131.58	108.02
C74-O77	1.46	1.43	C69-C74-O77	110.27	107.66			

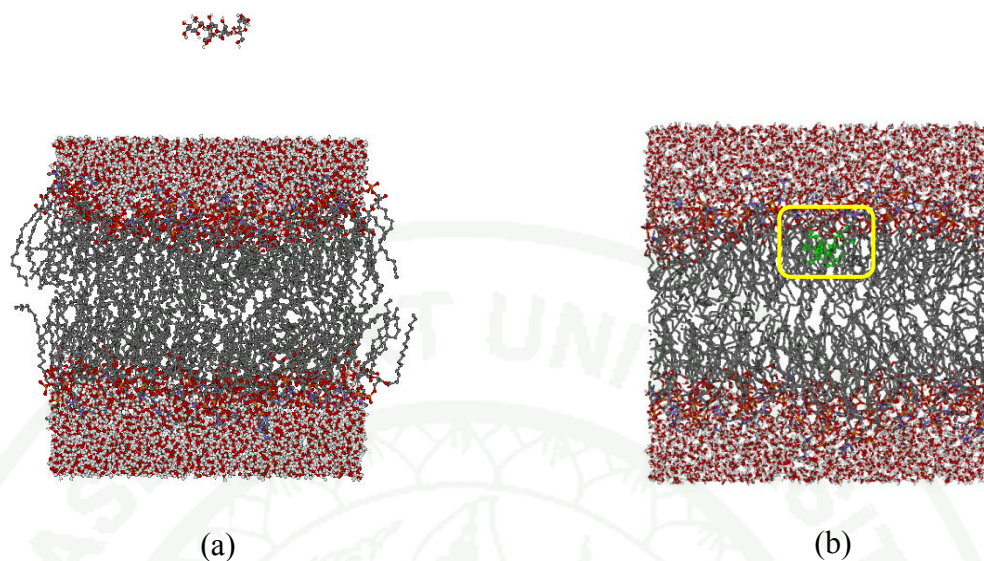


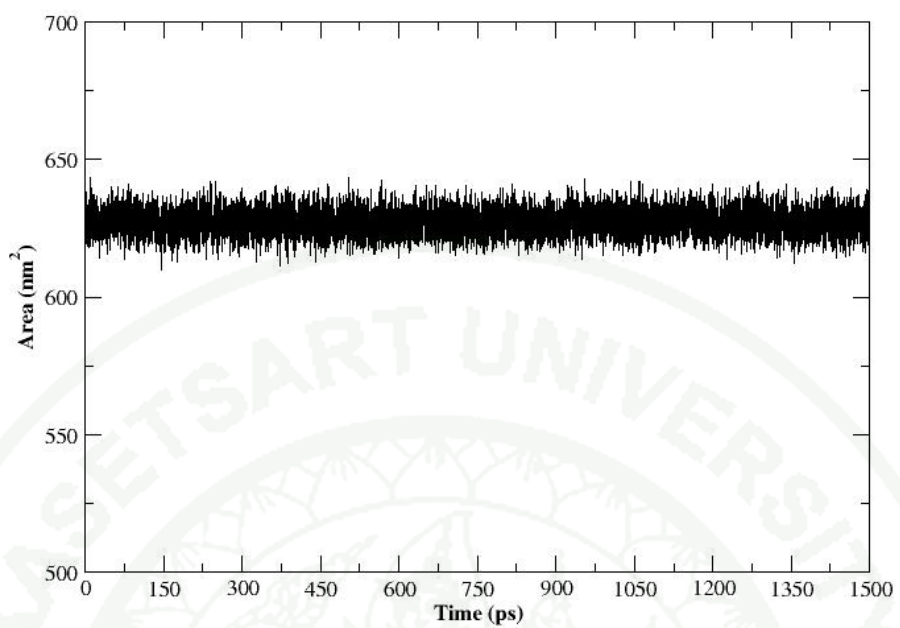
Figure 37 Snapshots of inulin molecule in the DPPC bilayer at 1.5 ns.

To gain insight into the partitioning behavior and distribution of inulin across the DPPC bilayer, inulin molecule was initially on the surface of aqueous solution at the vicinity of the bilayer interface. Series of MD equilibration runs of the studied inulin/DPPC systems were performed. After that, the process of the inulin distribution between aqueous solution at neutral pH and the lipid membrane was studied by the MD simulations. This type of simulations reproduced the passive driven diffusion of the inulin in the periodic simulation box. The initial configuration of inulin/DPPC system containing inulin molecule was shown in Figure 37. In addition, the MD results for all major structural and dynamics properties of a pure DPPC membrane were also found to be fully consistent with previous MD studies for the same bilayer in the liquid crystalline phase (de Vries *et al.*, 2005). Due to a low concentration, the influence of the inulin on the overall structure of the membrane was found to be small. This conclusion was confirmed by the analysis of regular bilayer properties evaluated for a pure DPPC bilayer and for the bilayer in the presence of the inulin. In the presence of the inulin, the surface area per lipid was found to be only slightly increased to 62.5 \AA^2 (Figure 38). In Figure 39, the total energy of inulin/DPPC system and RMSD of inulin were shown. So the stability in the plot

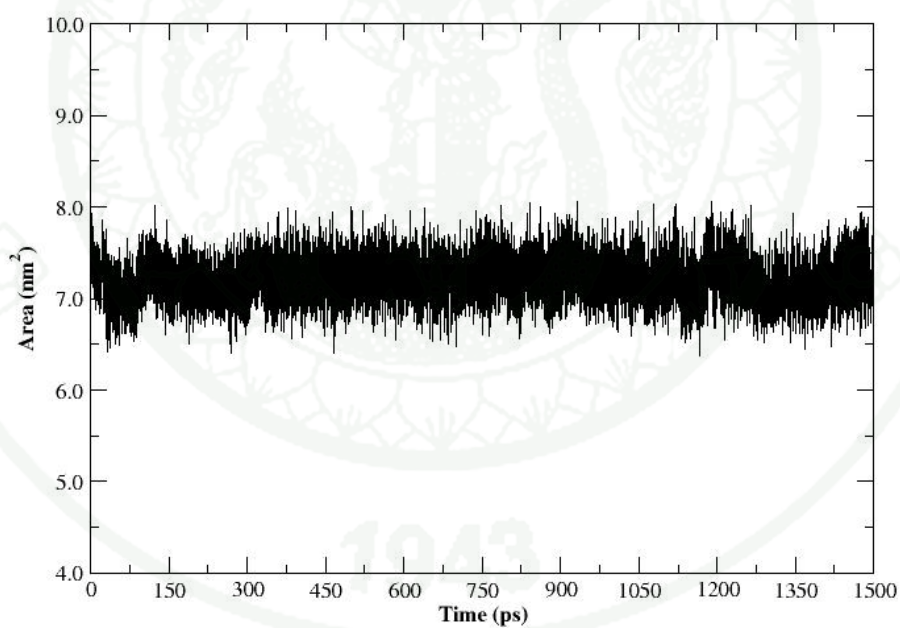
between total energy and RMSD indicated equilibrium after 1.0 ns. The total energy of vitamin E/DPPC was -1.02×10^5 kJ/mol and RMSD of vitamin E was about 2.0 Å.

To gain insight into the location of inulin inside a membrane, the mass density profiles of different molecular components across the bilayer was firstly considered. Using the symmetry of the bilayer, the final mass density profiles were obtained by averaging over the two leaflets of a bilayer. The mass density profiles for several different components across a bilayer were shown in Figure 40. The results for the pure DPPC bilayer were fully consistent with previous simulation studies and could be summarized as follows. First of all, water did not penetrate deeply into the membrane but rather stayed in the vicinity of the headgroup. As for the headgroup, its key components were located such that the choline group was slightly closer to water than phosphate, an idea consistent with the view that the P-N vector was almost in parallel to the membrane plane. The acyl chains, in turn, were well below the phosphate and choline groups. Based on these results, it seemed that molecular shape of the inulin played an important role for the inulin localization. The depth of the inulin (the dark blue line) localization in this sequence was gradually shifted deeper inside between the phosphate and glycerol core of the bilayer. In addition, we analyzed the possibility of the penetration of the inulin through the bilayer. During our MD analysis, we found inulin can not cross the bilayer from one leaflet to the other. The strong hydrogen bond was found between hydroxyl group (OH) of inulin and oxygen atom of phosphate and glycerol by average distance of 2.25 Å.

1943

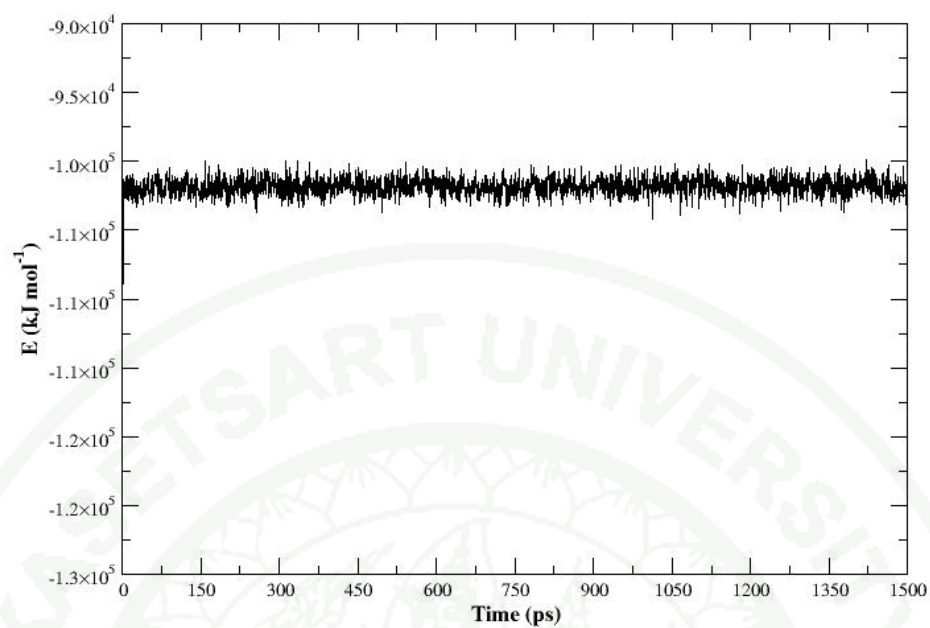


(a)

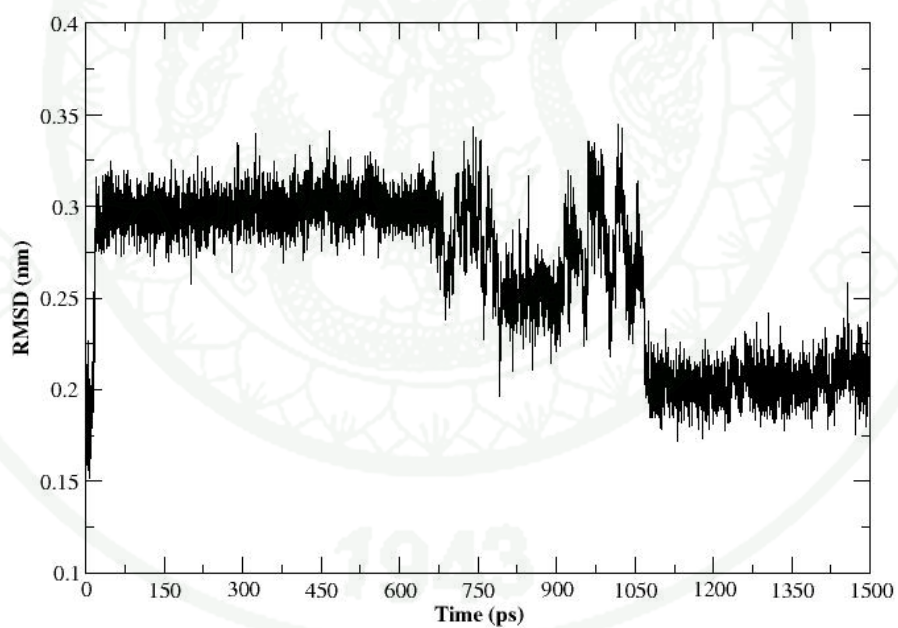


(b)

Figure 38 Surface area of 128DPPC bilayer (a) and inulin (b) at 1.5 ns.



(a)



(b)

Figure 39 Total energy of inulin/DPPC system (a) and RMSD of inulin (b) at 1.5 ns.

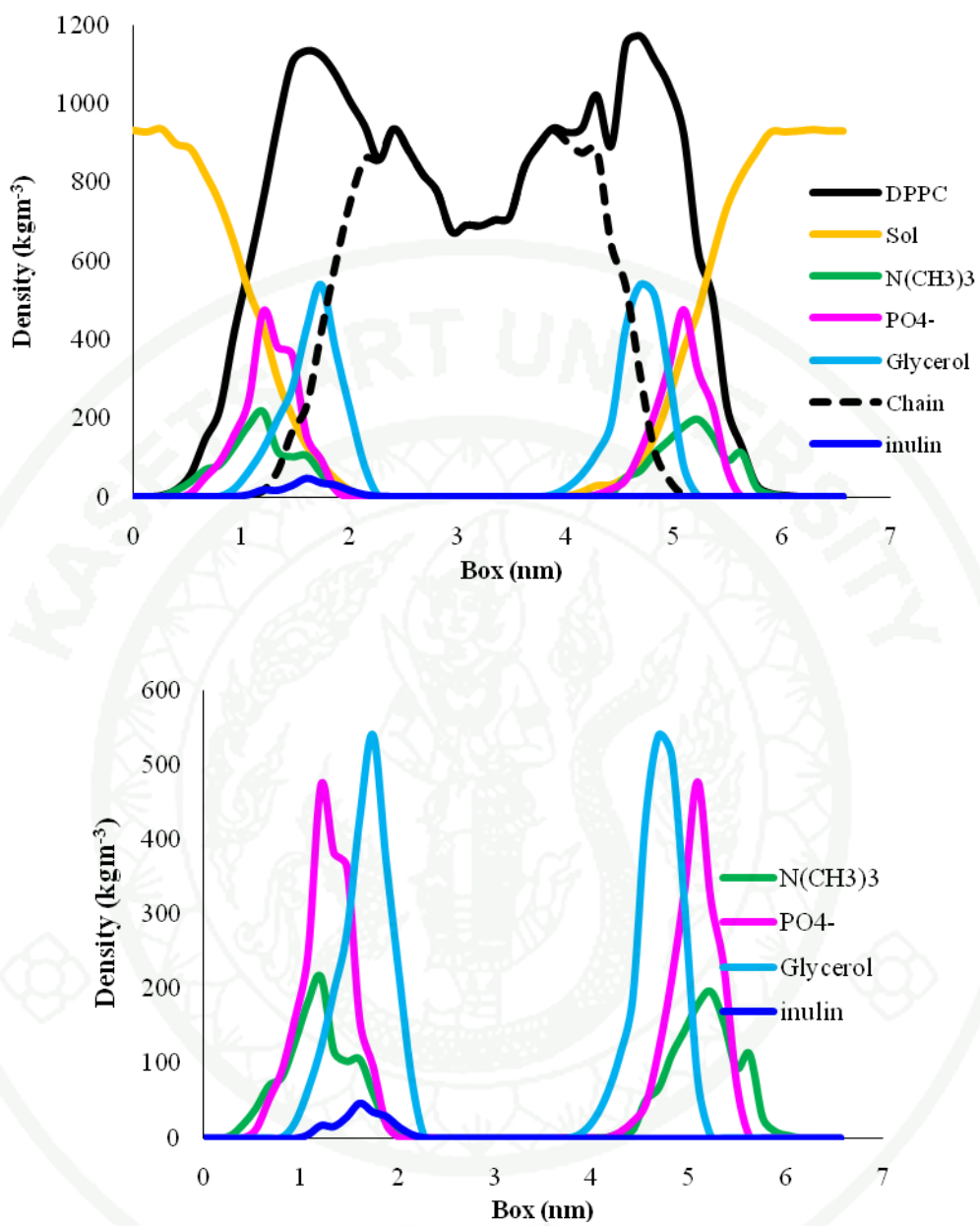


Figure 40 Mass density distribution profiles for individual components of the DPPC bilayer and for the total density distribution of molecules of inulin.

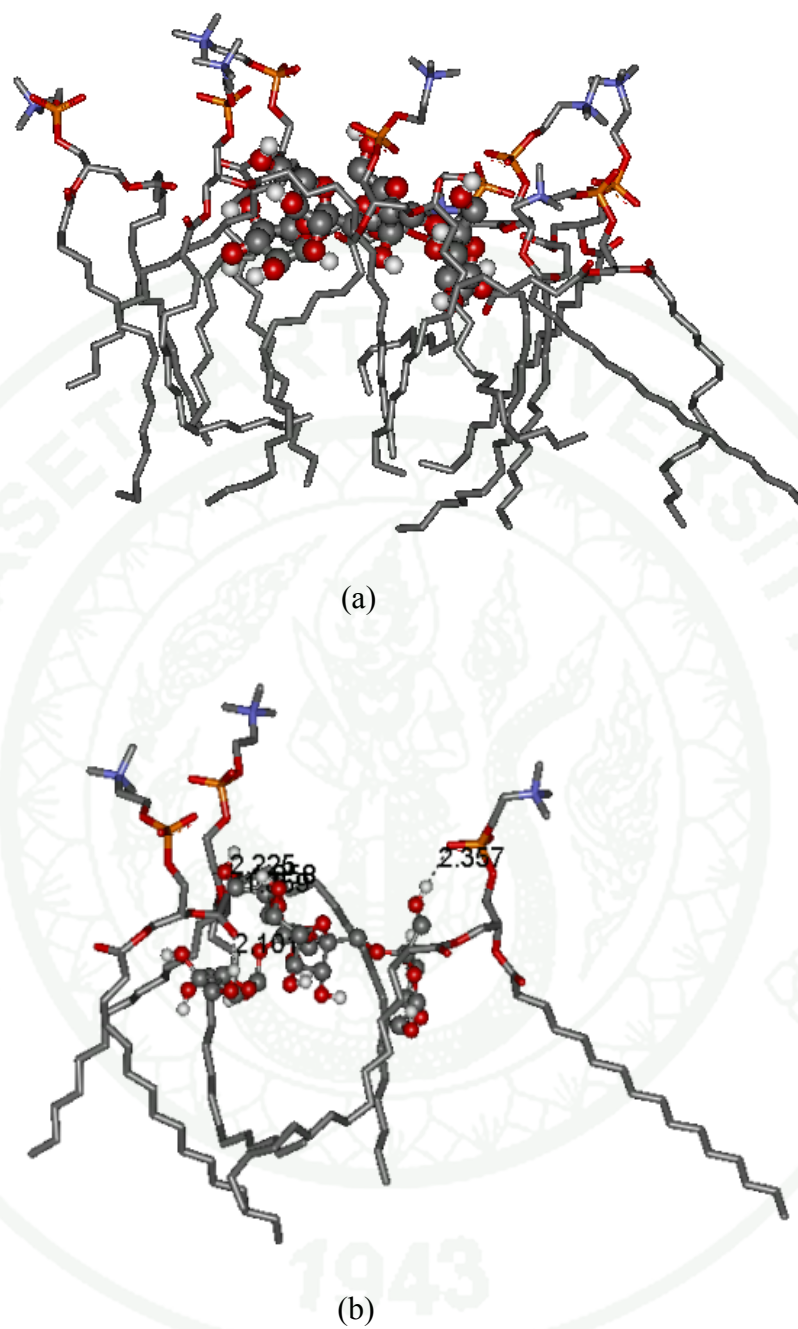


Figure 41 Interaction (a) and hydrogen bonding (b) between inulin and DPPC.

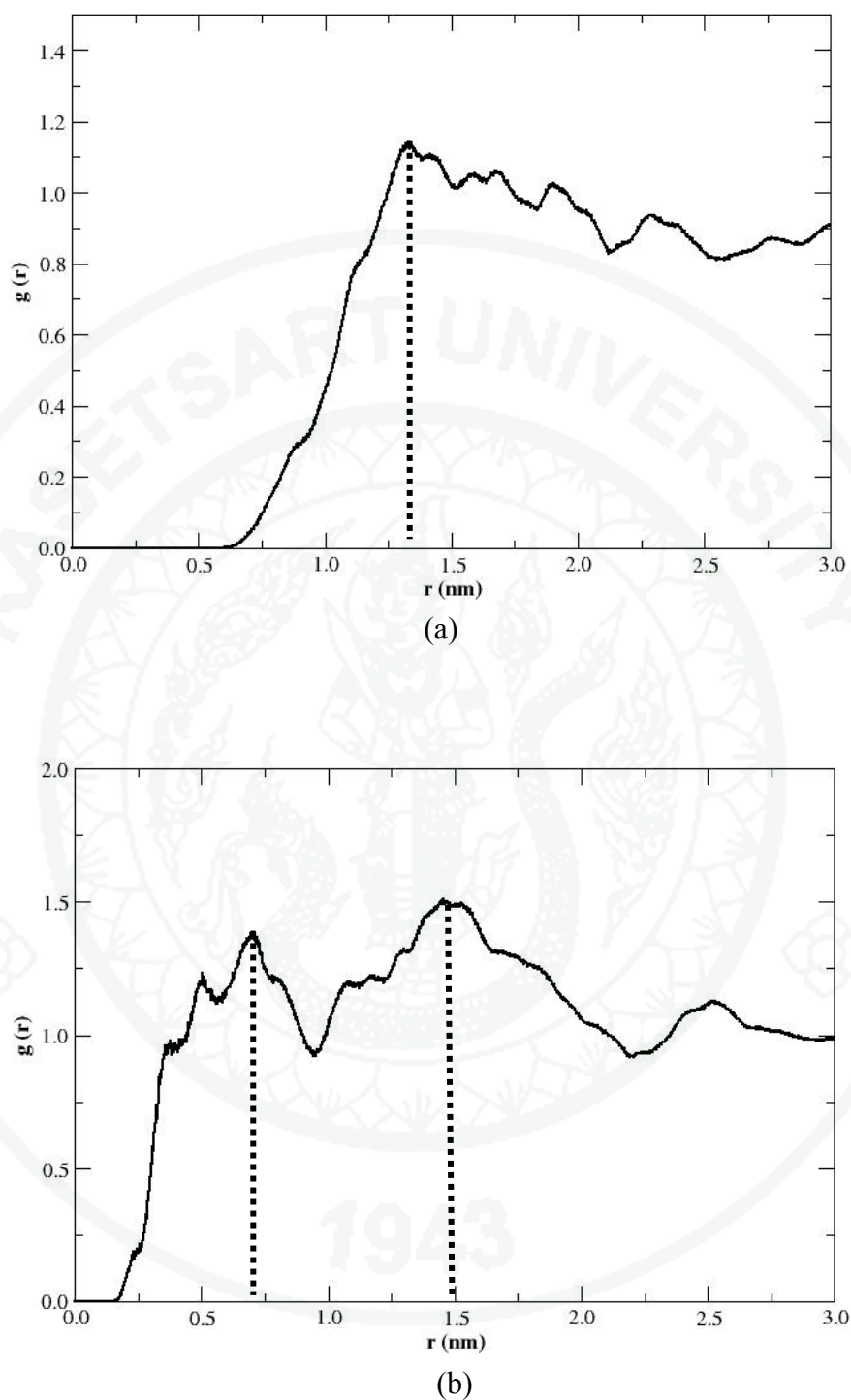


Figure 42 Radial pair distribution functions $g(r)$ between the O–H hydrogen atom of inulin and the oxygen atoms of the phosphate (a) and glycerol (b) groups of the DPPC lipids.

The partial radial distribution functions, $g(r)$, were calculated to study details of interactions of the inulin and the lipids. The $g(r)$ was therefore used as a complementary tool for the hydrogen bonding analysis. The $g(r)$ functions were useful to evaluate whether the inulin molecules interact with particular functional groups of the lipids to form hydrogen bonds or whether the overlapping distributions between the bilayer and inulin observed in Figure 41 were due to non-specific van der Waals interactions. Figure 42 shows the $g(r)$ functions calculated between the OH hydrogen atom of inulin and the oxygen atoms of the lipid molecules. Our analysis indicated that the structured features of $g(r)$ were observed between the OH hydrogen atoms and the phosphate or glycerol groups of the lipids. The first peak of $g(r)$ was seen for the inulin at distances 13.0 Å and the second peak was seen at distance 6.0 - 15.0 Å, Figure 42a–b. These distances corresponded to hydrogen-bonding between the OH hydrogen and the oxygen atoms of the functional groups of the lipids.

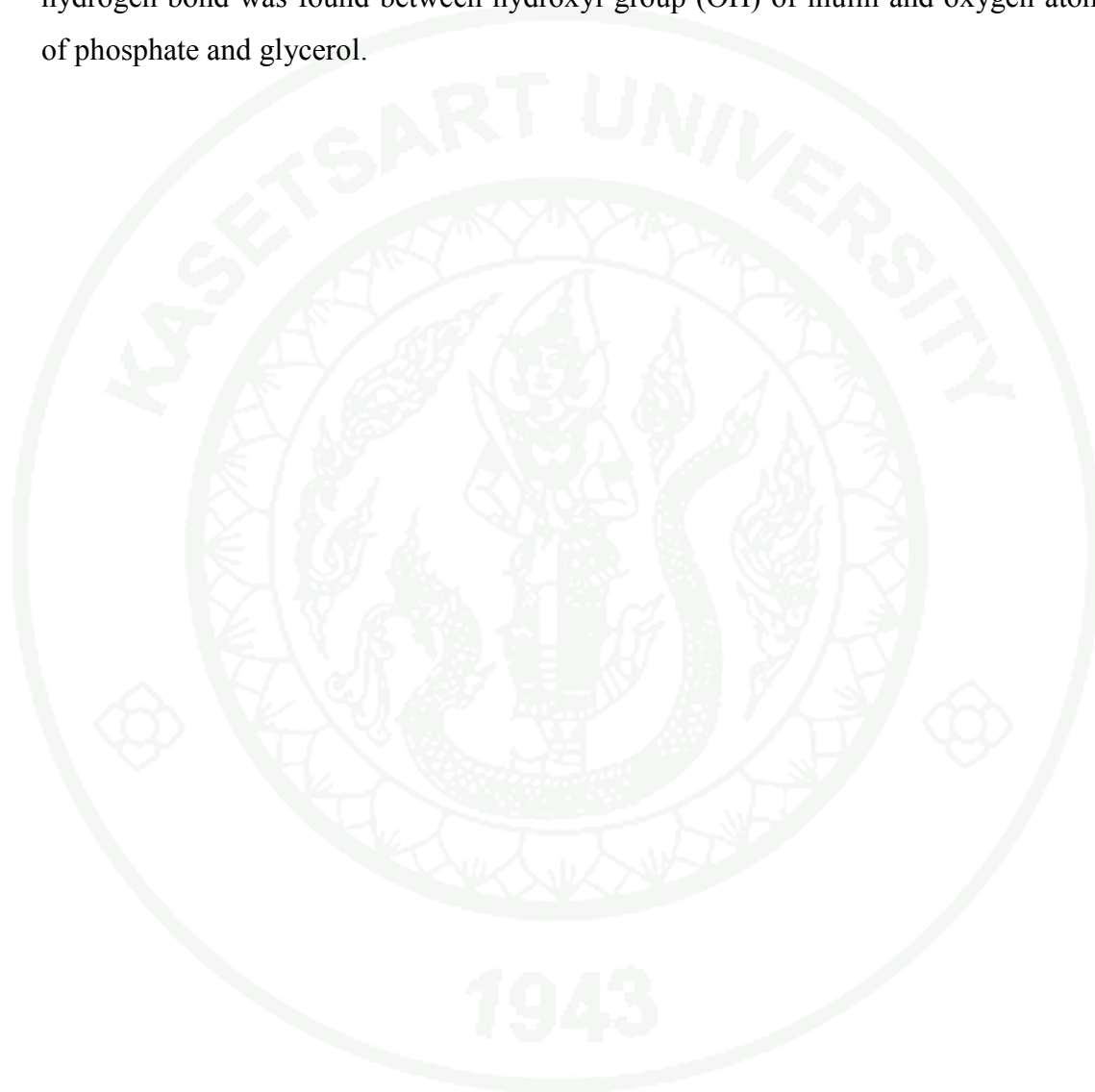
CONCLUSION

Molecular dynamics simulations of 64 and 128 DPPC lipid bilayer found that the mainly different properties were the density along z-dimension of DPPC lipid bilayer. The results showed that the density of 64 DPPC lipid bilayer were lower than that of 128 DPPC lipid bilayer. P-P distance between DPPC molecules in 64 DPPC lipid bilayer was longer than in 128 DPPC lipid bilayer. Therefore, 64 DPPC lipid bilayer maybe lost the membrane property. The 128 DPPC lipid bilayer can be a representative of lipid membrane for studying by molecular dynamics simulations.

The MD simulation study has been carried out to investigate the distribution of vitamin E and inulin at a water/membrane interface, so our interest has been focused on the favorable binding sites of the vitamin E and inulin within 128DPPC bilayer. Vitamin E and inulin molecules were used to sample a process of distribution between aqueous solution and the lipid membrane. The vitamin E and inulin distribution was simulated by reproducing the passive diffusion. The MD simulations showed that a significant fraction of vitamin E and inulin molecules tend to diffuse from aqueous solution into the polar interfacial region of the bilayer.

The MD simulations study focused on favorable binding sites of vitamin E embedded into DPPC bilayer. The simulations showed that vitamin E was preferably accommodated at the head of the bilayer upper the glycerol moiety. In addition, it was found that the hydrophobic aromatic part of the vitamin E was located inside more ordered region of DPPC from the hydrophobic character of vitamin E, the depth of the vitamin E localization was gradually shifted deeper inside the hydrocarbon core of the bilayer. We found that the vitamin E showed weak hydrogen bonding to DPPC bilayer and the distribution of vitamin E molecule simulations was presented at the opposite of the entrance.

The depth of the inulin localization was shifted deeper inside between the phosphate and glycerol core of the bilayer. In addition, the possibility of the penetration of the inulin through the bilayer was analyzed. During MD analysis, we found that the inulin can not cross the bilayer from one leaflet to the other. The strong hydrogen bond was found between hydroxyl group (OH) of inulin and oxygen atom of phosphate and glycerol.



LITERATURE CITED

- Abrams, S.A., I.J. Griffin, K.M. Hawthorne, L. Liang, S.K. Gunn, G. Darlington and K.J. Ellis. 2005. A combination of prebiotic short- and long-chain inulin-type fructans enhances calcium absorption and bone mineralization in young adolescents. **The American Journal of Clinical Nutrition** 82(2): 471-476.
- Anezo, C., A.H. de Vries, H.-D. Holtje, D.P. Tieleman and S.-J. Marrink. 2003. Methodological Issues in Lipid Bilayer Simulations. **The Journal of Physical Chemistry B** 107(35): 9424-9433.
- Anwar, K., J. Iqbal and M.M. Hussain. 2007. Mechanisms involved in vitamin E transport by primary enterocytes and in vivo absorption. **Journal of Lipid Research** 48(9): 2028-2038.
- Berendsen, H. 1995. GROMACS: A message-passing parallel molecular dynamics implementation. **Computer Physics Communications** 91(1-3): 43-56.
- _____, J. Postma, W. van Gunsteren, A. Dinola and J. Haak. 1984. Molecular dynamics with coupling to an external bath. **Journal of Chemical Physics** 81: 3684-3690.
- Coudray, C., C. Demigne and Y. Rayssiguier. 2003. Effects of Dietary Fibers on Magnesium Absorption in Animals and Humans. **The Journal of Nutrition** 133(1): 1-4.
- de Vries, A.H., I. Chandrasekhar, W.F. van Gunsteren and P.H. Hunenberger. 2005. Molecular Dynamics Simulations of Phospholipid Bilayers: Influence of Artificial Periodicity, System Size, and Simulation Time. **The Journal of Physical Chemistry B** 109(23): 11643-11652.

- Egberts, E., S.-J. Marrink and H.J.C. Berendsen. 1994. Molecular dynamics simulation of a phospholipid membrane. **European Biophysics Journal** 22(6): 423-436.
- Guarner, F. 2007. Studies with Inulin-Type Fructans on Intestinal Infections, Permeability, and Inflammation. **The Journal of Nutrition** 137(11): 2568-2571.
- Guvench, O., A.D. MacKerell. 2008. Comparison of Protein Force Fields for Molecular Dynamics Simulations. **Methods in Molecular Biology** 443: 63-88.
- Hess, B., H. Bekker, H.J.C. Berendsen and J.G.E.M. Fraaije. 1997. LINCS: A linear constraint solver for molecular simulations. **Journal of Computational Chemistry** 18(12): 1463-1472.
- Khandelia, H., J.H. Ipsen and O.G. Mouritsen. 2008. The impact of peptides on lipid membranes. **Biochimica et Biophysica Acta (BBA) - Biomembranes** 1778(7-8): 1528-1536.
- Kyrychenko, A., Y. Stepanenko and J. Waluk. 2000. Molecular Dynamics and DFT Studies of Intermolecular Hydrogen Bonds between Bifunctional Heteroazaaromatic Molecules and Hydroxylic Solvents. **The Journal of Physical Chemistry A** 104(42): 9542-9555.
- _____, and J. Waluk. 2008. Distribution and favorable binding sites of pyrroloquinoline and its analogues in a lipid bilayer studied by molecular dynamics simulations. **Biophysical Chemistry** 136(2-3): 128-135.
- Leekumjorn, S. and A.K. Sum. 2006. Molecular Simulation Study of Structural and Dynamic Properties of Mixed DPPC/DPPE Bilayers. **Biophysical Journal** 90(11): 3951-3965.

- Leontiadou, H., A. Mark and S. Marrink. 2004. Molecular dynamics simulations of hydrophilic pores in lipid bilayers. **Biophysical Journal** 86: 2156-2164.
- Levtsova, O.V., M.Y. Antonov, D.Y. Mordvintsev, Y.N. Utkin, K.V. Shaitan and M.P. Kirpichnikov. 2009. Steered molecular dynamics simulations of cobra cytotoxin interaction with zwitterionic lipid bilayer: No penetration of loop tips into membranes. **Computational Biology and Chemistry** 33(1): 29-32.
- Lindahl, E. and O. Edholm. 2000. Mesoscopic undulations and thickness fluctuations in lipid bilayers from molecular dynamics simulations. **Biophysical Journal** 79: 426-433.
- _____, B. Hess and D. van der Spoel. 2001. GROMACS 3.0: a package for molecular simulation and trajectory analysis. **Journal of Molecular Modeling** 7: 306-317.
- Lopez Cascales, J.J., M.L. Huertas and J.G. de la Torre. 1997. Molecular dynamics simulation of a dye molecule in the interior of a bilayer: 1,6-diphenyl-1,3,5-hexatriene in dipalmitoylphosphatidylcholine. **Biophysical Chemistry** 69: 1-8.
- Loura, L.M.S., F. Fernandes, A.C. Fernandes and J.P.P. Ramalho. 2008. Effects of fluorescent probe NBD-PC on the structure, dynamics and phase transition of DPPC. A molecular dynamics and differential scanning calorimetry study. **Biochimica et Biophysica Acta (BBA) - Biomembranes** 1778(2): 491-501.
- MacCallum, J.L., W.F.D. Bennett and D.P. Tieleman. 2008. Distribution of Amino Acids in a Lipid Bilayer from Computer Simulations. **Biophysical Journal** 94(9): 3393-3404.

- _____, and D.P. Tieleman. 2006. Computer Simulation of the Distribution of Hexane in a Lipid Bilayer: Spatially Resolved Free Energy, Entropy, and Enthalpy Profiles. **Journal of the American Chemical Society** 128(1): 125-130.
- Norman, K.E. and H. Nymeyer. 2006. Indole Localization in Lipid Membranes Revealed by Molecular Simulation. **Biophysical Journal** 91(6): 2046-2054.
- Orioni, B., G. Bocchini, J.Y. Kim, A. Palleschi, G. Grande, S. Bobone, Y. Park, J.I. Kim, K.-s. Hahn and L. Stella. 2009. Membrane perturbation by the antimicrobial peptide PMAP-23: A fluorescence and molecular dynamics study. **Biochimica et Biophysica Acta (BBA) - Biomembranes** 1788(7): 1523-1533.
- Poghosyan, A.H. and A.A. Shahinyan. 2009. A new parameter for validation molecular dynamics simulation (MD) data. **Computer Physics Communications** 180(2): 238-240.
- Prausnitz, M., V. Bose, R. Langer and J. Weaver. 1993. Electroporation of mammalian skin - a mechanism to enhance transdermal drug-delivery. **Proc Natl Acad Sci U S A** 90: 10504 - 10508.
- Qin, S.-S., Z.-W. Yu and Y.-X. Yu. 2009. Structural and Kinetic Properties of α -Tocopherol in Phospholipid Bilayers, a Molecular Dynamics Simulation Study. **The Journal of Physical Chemistry B** 113(52): 16537-16546.
- Repakova, J., P. Capkova, J.M. Holopainen and I. Vattulainen. 2004. Distribution, Orientation, and Dynamics of DPH Probes in DPPC Bilayer. **The Journal of Physical Chemistry B** 108(35): 13438-13448.

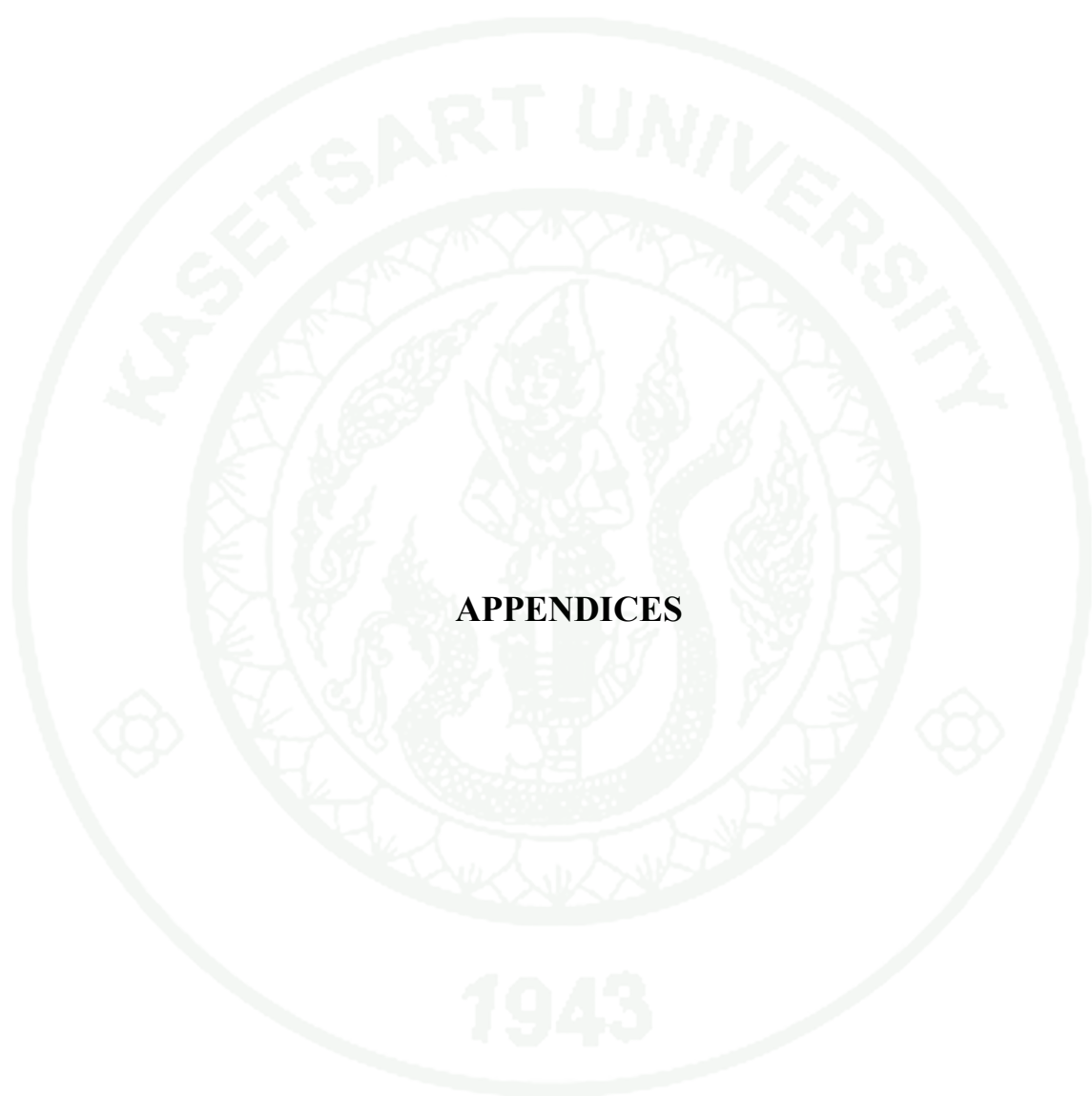
- _____, J.M. Holopainen, M.R. Morrow, M.C. McDonald, P. apkovu and I. Vattulainen. 2005. Influence of DPH on the Structure and Dynamics of a DPPC Bilayer. **Biophysical Journal** 88(5): 3398-3410.
- Roberfroid, M.B. 2007. Inulin-Type Fructans: Functional Food Ingredients. **The Journal of Nutrition** 137(11): 2493-2502.
- Saito, H., W. Shinoda and M. Mikami. 2009. Fluorination effects on structure and dynamics of phospholipid bilayer: A molecular dynamics study. **Chemical Physics Letters** 468(4-6): 260-263.
- T., D. and L. 1993. Particle mesh Ewald: An $N \cdot \log(N)$ method for Ewald sums in large systems. **The Journal of Chemical Physics** 98(12): 10089-10092.
- Tieleman, D.P. and H.J.C. Berendsen. 1996. Molecular dynamics simulations of a fully hydrated dipalmitoylphosphatidylcholine bilayer with different macroscopic boundary conditions and parameters. **The Journal of Chemical Physics** 105(11): 4871-4880.
- _____, S.J. Marrink and H.J.C. Berendsen. 1997. A computer perspective of membranes: molecular dynamics studies of lipid bilayer systems. **Biochimica et Biophysica Acta (BBA) Reviews on Biomembranes** 1331(3): 235-270.
- _____, Leontiadou, A. Mark and S. Marrink. 2003. Molecular dynamics simulation of pore formation in phospholipid bilayers by mechanical force and electric fields. **Journal of the American Chemical Society** 124: 6382-6383.
- _____, 2004. The molecular basis of electroporation. **BMC Biochemistry** 5(1): 10.

_____, 2006. Computer Simulations of Transport Through Membranes: Passive Diffusion, Pores, Channels and Transporters. **Clinical and Experimental Pharmacology and Physiology** 33(10): 893-903.

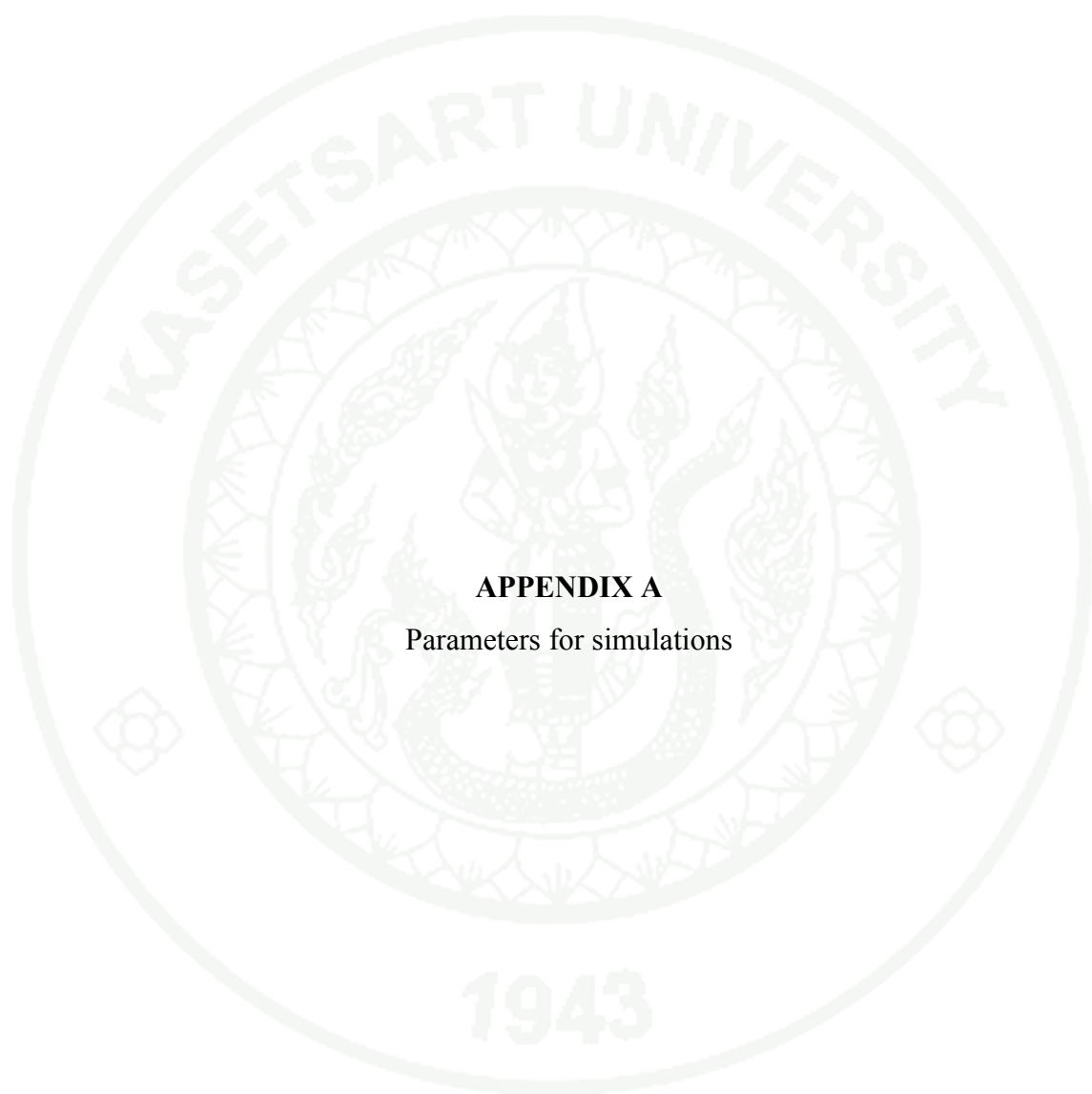
Verlet, L. 1967. Computer "Experiments" on Classical Fluids. I. Thermodynamical Properties of Lennard-Jones Molecules. **Physical Review** 159(1): 98.

_____, 1968. Computer "Experiments" on Classical Fluids. II. Equilibrium Correlation Functions. **Physical Review** 165(1): 201.

Zhang, Z., L. Lu and M.L. Berkowitz. 2008. Energetics of Cholesterol Transfer between Lipid Bilayers. **The Journal of Physical Chemistry B** 112(12): 3807-3811.



APPENDICES



APPENDIX A
Parameters for simulations

Parameters for molecular dynamics simulations using Gromacs 4.0.2

1. Contents in em,mdp parameter file for energy minimization of vitamin E/DPPC system

```

; VARIOUS PREPROCESSING OPTIONS =
title           = Vitamin E/DPPC
cpp             = /usr/bin/cpp
define         = -DFLEX_SPC
; BONDS PARAMETER
constraints     = none
; RUN CONTROL PARAMETER
Integrator     = steep
dt             = 0.002 ; ps !
nsteps        = 10000
; ENERGY MINIMIZATION PARAMETER
emtol         = 100.0
emstep        = 0.01
; NEIGHBORSEARCHING PARAMETER
; ns algorithm (simple or grid)
ns_type       = grid
; nblast cut-off
rlist         = 0.9
; OPTIONS FOR ELECTROSTATICS AND VDM
; Method for doing electrostatics
rcoulomb      = 0.9
; cut-off lengths
rvdw         = 1.0
; BERENDSEN TEMPERATURE COUPLING IS ON ONE GROUP
; Temperature coupling
Tcoupl       = no
; ISOTROPIC PRESSURE COUPLING
Pcoupl      = no

```

```
; GENERATE VELOCITIES FOR STARTUP RUN
```

```
gen-vel          = no
```

2. Contents in pr,mdp parameter file for restrained molecular dynamics simulations of vitamin E/DPPC system

```
; VARIOUS PREPROCESSING OPTIONS =
```

```
title            = Vitamin E/DPPC
```

```
cpp              = /usr/bin/cpp
```

```
define          = -DFLEX_SPC
```

```
; BONDS PARAMETER
```

```
constraints      = all-bonds
```

```
; RUN CONTROL PARAMETER
```

```
Integrator      = md
```

```
dt              = 0.001 ; ps !
```

```
nsteps          = 10000000 ;total 10000 ps
```

```
; number of steps for center of mass motion removal
```

```
Mstcomm         = 1
```

```
; OUTPUT CONTROL OPTIONS
```

```
; output frequency for coords (x), velocities (v) and forces (f)
```

```
nstxout         = 1000
```

```
nstvout         = 1000
```

```
nstfout         = 0
```

```
; Output frequency for energies to log file and enrgy file
```

```
nstlog          = 500
```

```
nstenrgy        = 500
```

```
; Output to write energy file
```

```
energrgps       = DPP SOL VIV
```

```
; NEIGHBORSEARCHING PARAMETER
```

```
; nblast update frequency
```

```
nblast          = 500
```

```
; ns algorithm (simple or grid)
```

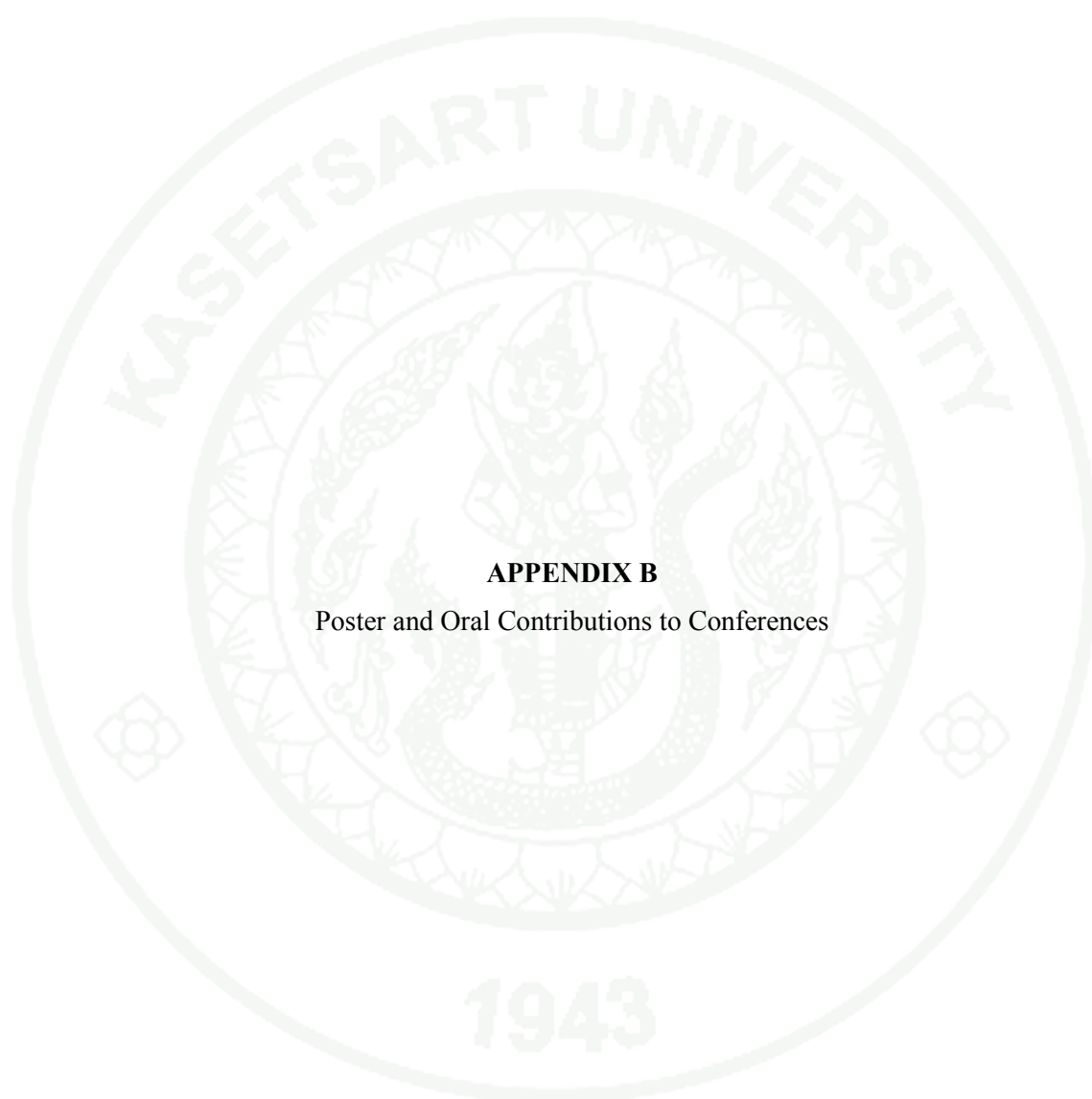
```
ns_type         = grid
```

```
; nblast cut-off
```

```

rlist                = 0.9
; OPTIONS FOR ELECTROSTATICS AND VDM
; Method for doing electrostatics
rcoulomb             = 0.9
; cut-off lengths
rvdw                 = 1.0
; BERENDSEN TEMPERATURE COUPLING IS ON ONE GROUP
; Temperature coupling
Tcoupl               = berendsen
; Groups to couple separately
tc-grps              = DPP SOL   VIV
; Time constant (ps) and reference temperature (K)
tau_t                = 0.1   0.1   0.1
ref_t                = 323   323   323
; ISOTROPIC PRESSURE COUPLING
Pcoupl               = berendsen
; Time constant (ps), compressibility (1/bar) and reference P (bar)
Tau-p                = 1.0
compressibility       = 4.5e-5
ref_p                 = 1.0
; GENERATE VELOCITIES FOR STARTUP RUN
gen_vel               = yes
gen_temp              = 323.0
gen_seed              = 173529

```

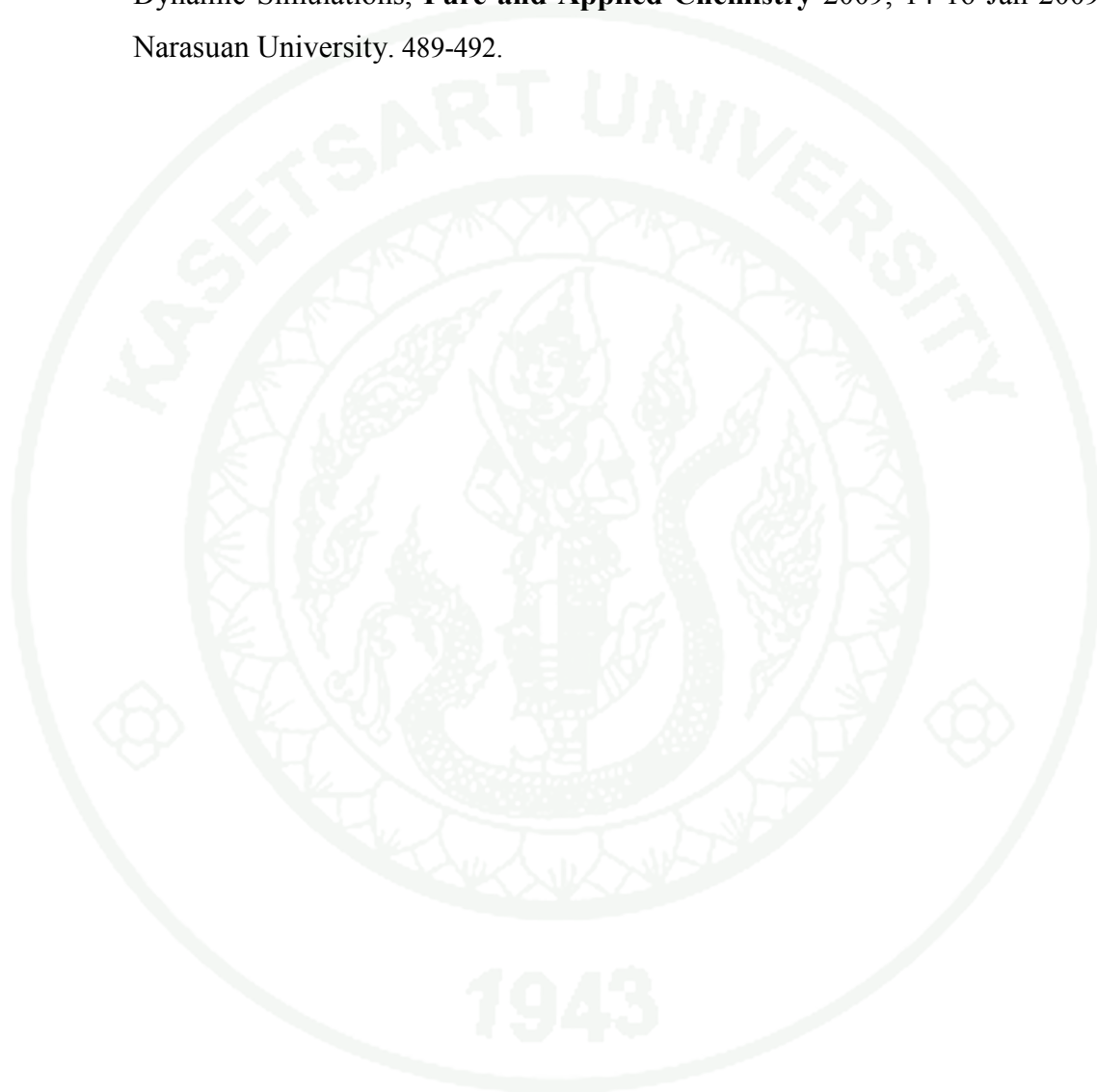


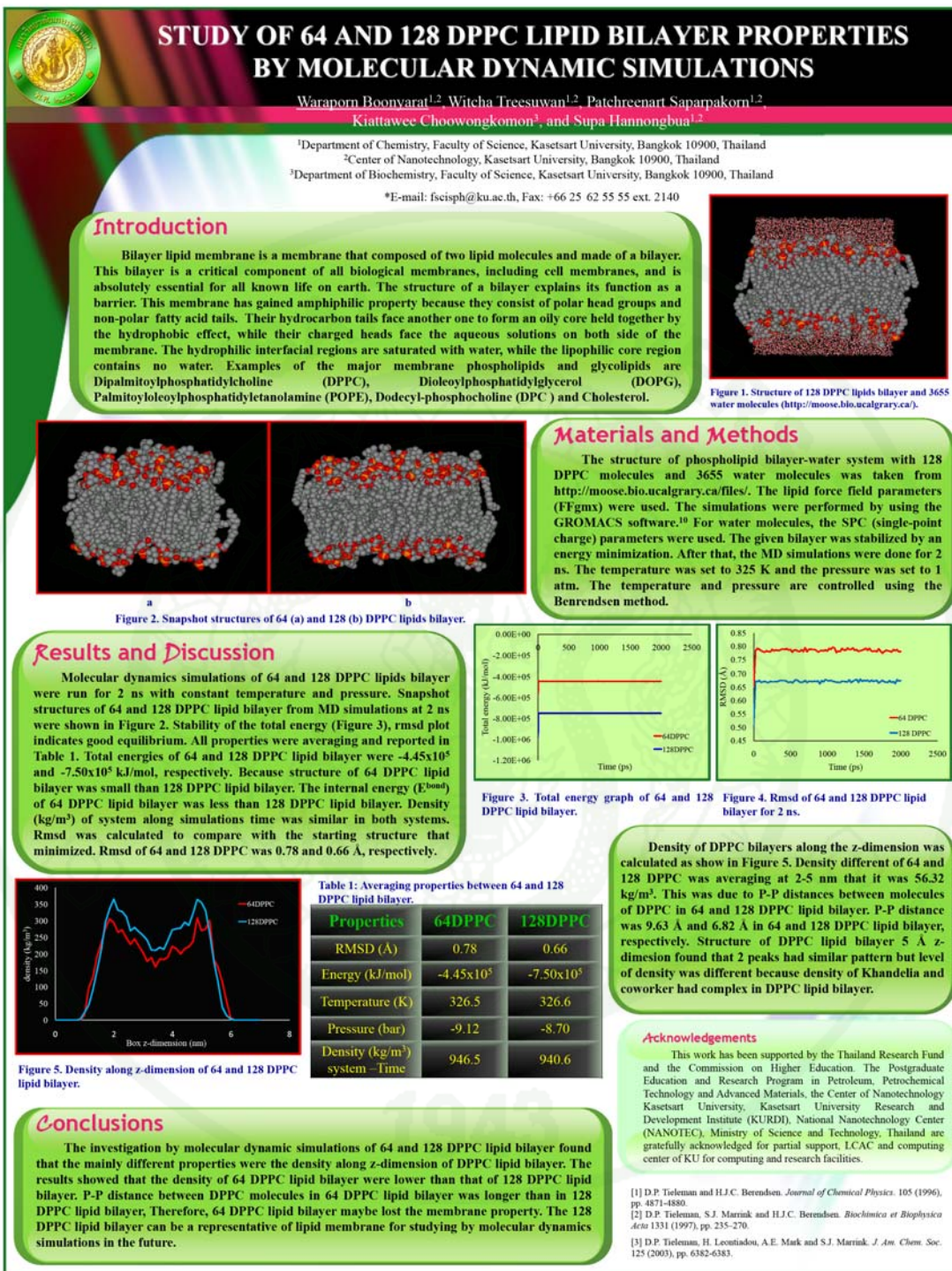
APPENDIX B

Poster and Oral Contributions to Conferences

1. Poster Presentation and Proceeding

Boonyarat W., W. Treesuwan, P. Saparpakorn, K. Choowongkomon, and S. Hannongbua, Study of 64 and 128 DPPC Bilayer Properties by Molecular Dynamic Simulations, **Pure and Applied Chemistry** 2009, 14-16 Jan 2009, Narasuan University. 489-492.





STUDY OF 64 AND 128 DPPC LIPID BILAYER PROPERTIES BY MOLECULAR DYNAMIC SIMULATIONS

Waraporn Boonyarat^{1,2}, Witcha Treesuwan^{1,2}, Patchreenart Saparpakorn^{1,2},
Kiattawee Choowongkomon³, and Supa Hannongbua^{1,2*}

¹Department of Chemistry, Faculty of Science, Kasetsart University, Bangkok 10900, Thailand,

²Center of Nanotechnology, Kasetsart University, Bangkok 10900, Thailand,

³Department of Biochemistry, Faculty of Science, Kasetsart University, Bangkok 10900, Thailand,

*E-mail: fscisph@ku.ac.th, Fax: +66 25 62 55 55 ext. 2140

Abstract: Dipalmitoylphosphatidylcholine (DPPC) is the type of phospholipids and also mainly constituted of pulmonary surfactant. Due to the saturated fatty acid chains, the DPPC can be formed as the lipid bilayer. Therefore, the DPPC were exclusively applied as a membrane model for investigating of the membrane properties generally by molecular dynamic (MD) simulations. Along with the parameters setting in MD simulations, the DPPC bilayer size can influence to the system of interest. Therefore, the aim of this work is to study the DPPC bilayer properties to the physical properties. The MD simulation was performed on 64 and 128 molecules of DPPC bilayer systems. The structures of 64 and 128 DPPC were obtained from <http://moose.bio.ucalgary.ca/>. Two simulations running on the time of 2 ns were carried out in the same conditions by using GROMACS software. The lipid force field parameters (ffgmx) and the SPC water parameters were applied following Tieleman and Berendsen works (1996). The DPPC bilayer was stabilized by the energy minimization at 325 K and 1 bar as constant. The results illustrated that the slightly difference in RMSD of 64 and 128 DPPC were 0.78 and 0.66 Å, respectively. Temperature and pressure properties are similar in both systems. The density of both DPPC bilayers along the z dimension was 146.28 and 165.96 kg/m³, respectively, due to P-P distances between molecules of DPPC in 64 DPPC are longer than in 128 DPPC bilayer. This knowledge gains the basis properties of DPPC bilayer which are important in the membrane-ligand study in future.

Introduction

Bilayer lipid membrane is a membrane that composed of two lipid molecules and made of a bilayer. This bilayer is a critical component of all biological membranes, including cell membranes, and so is absolutely essential for all known life on earth. The structure of a bilayer explains its function as a barrier. This membrane has gained amphiphilic property since they consist of polar head groups and non-polar fatty acid tails.¹ On top of that, the bilayer is composed of two layers of lipids arranged. Their hydrocarbon tails face another one to form an oily core held together by the hydrophobic effect, while their charged heads face the aqueous solutions on

both side of the membrane.² The hydrophilic interfacial regions are saturated with water, while the lipophilic core region contains no water. Examples of the major membrane phospholipids and glycolipids are phosphatidylcholine (PtdCho), phosphatidylethanolamine (PtdEtn), phosphatidylinositol (PtdIns) and phosphatidylserine (PtdSer).

Dipalmitoylphosphatidylcholine (DPPC) is the type of phospholipids and also mainly constituted of pulmonary surfactant. The DPPC can form as the lipid bilayer.¹ Therefore, the DPPC were exclusively applied as a membrane model for investigating of the membrane properties by molecular dynamic (MD) simulations.³ Along with the parameters setting in MD simulations, the DPPC bilayer size can influence to the system of interest.³ Therefore, the aim of this work is to study the DPPC bilayer properties. The MD simulation was performed on 64 and 128 molecules of DPPC bilayer systems. Computer simulations now offer the details of structure and dynamics of membrane Figure 1 shows a snapshot of DPPC lipid bilayer with solvent water from molecular dynamics (MD) simulations.⁴

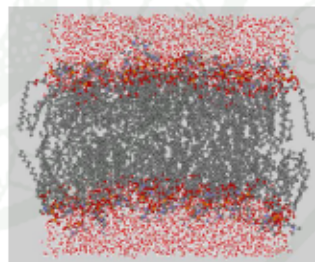


Figure 1. Structure of 128 DPPC lipids bilayer and 3655 water molecules (<http://moose.bio.ucalgary.ca/>).

Materials and Methods

The structure of phospholipid bilayer-water system with 128 DPPC molecules and 3655 water molecules was taken from <http://moose.bio.ucalgary.ca/files/>. The lipid force field parameters (FFgmx) were used.³ The simulation is performed by using the GROMACS software.¹⁰ For water molecules, the SPC (single-point charge) parameters are used. The given bilayer is stabilized by an energy minimization. After that, the MD simulation was done for 2 ns in the NPT ensemble. In order to reach L_d state, the temperature was set to 325 K and the pressure was set to 1 atm. The temperature and pressure are controlled using the Berendsen method.³ The integration time step was 5 fs.

Results and Discussion

DPPC was one of the most studied lipids. Molecular dynamics simulations of 64 and 128 DPPC lipids bilayer was run for 2 ns with constant temperature and pressure. In all the simulations, parameters were investigated including energy components and phosphate density profiles. Snapshot structures of 64 and 128 DPPC lipid bilayer from MD simulations at 2 ns were show in Figure 2.

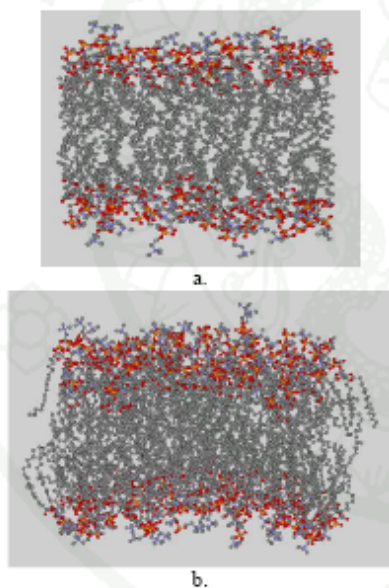


Figure 2. Snapshot structures of 64 (a) and 128 (b) DPPC lipids bilayer.

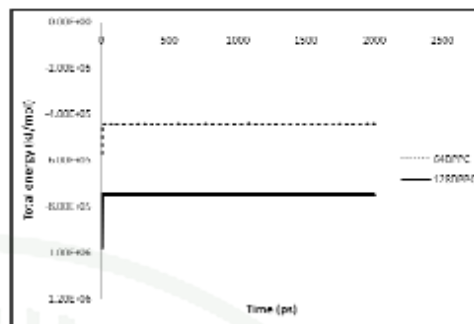


Figure 3. Total energy graph of 64 and 128 DPPC lipid bilayer.

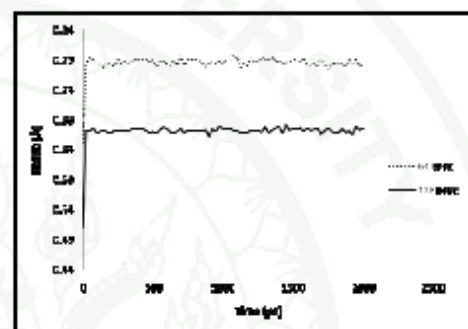


Figure 4. RMSD of 64 and 128 DPPC lipid bilayer for 2 ns.

Stability of the total energy (Figure 3), RMSD plot indicates good equilibrium. All properties were averaging and reported in Table 1. Temperature and pressure properties were similar in both systems. Total energy of 64 and 128 DPPC lipid bilayer were -4.45×10^5 and -7.50×10^5 kJ/mol, respectively. Because structure of 64 DPPC lipid bilayer was small than 128 DPPC lipid bilayer so that internal energy (E^{total}) of 64 DPPC lipid bilayer was less than 128 DPPC lipid bilayer. Density (kg/m^3) of system along simulations time was similar in both systems. RMSD was calculated to compare with the starting structure that minimized. RMSD of 64 and 128 DPPC was 0.78 and 0.66 Å, respectively. Small RMSD value refers that structure of both DPPC lipid bilayer during molecular dynamic simulations were stable and not changed from starting structure that minimized. Density of DPPC bilayers along the z-dimension was calculated as show in Figure 5. Density different of 64 and 128 DPPC was averaging at 2-5 nm that it was 56.32 kg/m^3 . This was due to P-P distances between molecules of DPPC in 64 and

128 DPPC lipid bilayer. P-P distance was 9.63 Å and 6.82 Å in 64 and 128 DPPC lipid bilayer, respectively. Structure of DPPC lipid bilayer in z-dimension 5 Å found that 2 peaks had similar pattern.

Table 1: Averaging properties between 64 and 128 DPPC lipid bilayer.

Properties	64DPPC	128DPPC
RMSD (Å)	0.78	0.66
Energy (kJ/mol)	-4.45x10 ⁵	-7.50x10 ⁵
Temperature (K)	326.5	326.6
Pressure (bar)	-9.12	-8.70
Density (kg/m ³) system -Time	946.5	940.6

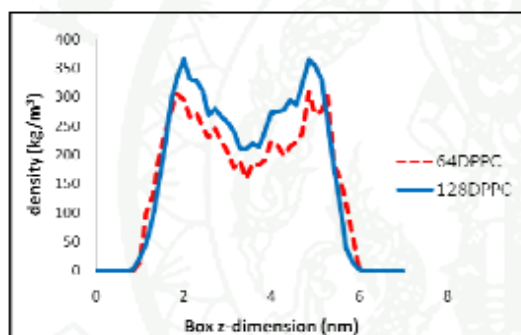


Figure 5. Density along z-dimension of 64 and 128 DPPC lipid bilayer.

Conclusions

The investigation by molecular dynamic simulations of 64 and 128 DPPC lipid bilayer found that the mainly different properties were the density along z-dimension of DPPC lipid bilayer. The results showed that the density of 64 DPPC lipid bilayer were lower than that of 128 DPPC lipid bilayer. P-P distance between DPPC molecules in 64 DPPC lipid bilayer was longer than in 128 DPPC lipid bilayer. Therefore, 64 DPPC lipid bilayer maybe lost the membrane property. The 128 DPPC lipid bilayer can be a representative of lipid membrane for studying by molecular dynamics simulations in the future.

Acknowledgements

This work has been supported by the Thailand Research Fund and the Commission on Higher Education. The Postgraduate Education and Research Program in Petroleum, Petrochemical Technology and Advanced Materials, the Center of Nanotechnology Kasetsart University, Kasetsart University Research and Development Institute (KURDI), National Nanotechnology Center (NANOTEC), Ministry of Science and Technology, Thailand are gratefully acknowledged for partial support, LCAC and computing center of KU for computing and research facilities.

References

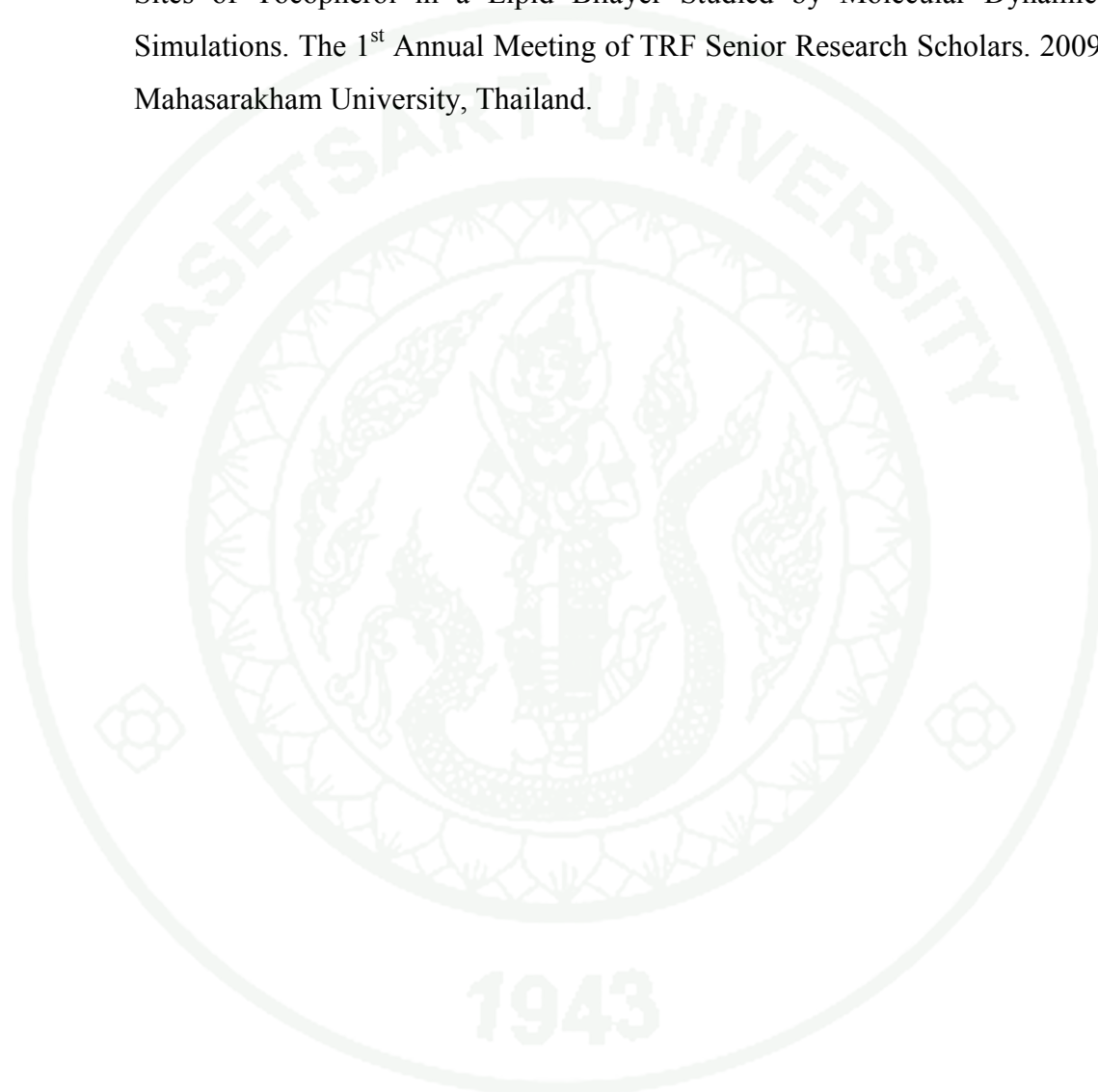
- [1] L. Sukit and K. S. Amadeu. *Biophysical Journal*. 90 (2006), pp. 3951-3965.
- [2] M. Patra, M. Karttunen, M.T. Hyvönen, E. Falck, P. Lindqvist and I. Vattulainen. *Biophysical Journal*. 84 (2003), pp. 3636-3645.
- [3] D.P. Tieleman and H.J.C. Berendsen. *Journal of Chemical Physics*. 105 (1996), pp. 4871-4880.
- [4] D.P. Tieleman, S.J. Marrink and H.J.C. Berendsen. *Biochimica et Biophysica Acta* 1331 (1997), pp. 235-270.
- [5] Y. Takaoka, M.P. Gierula, H. Miyagawa, K. Kitamura, Y. Tamura and A. Kusumi. *Biophysical Journal*. 79 (2000), pp. 118-3138.
- [7] A. Kyrtychenko and J. Waluk. *Biophysical Chemistry*. 136 (2008), pp. 128-135.
- [8] B.W. Lee, R. Faller, K.S. Amadeu, I. Vattulainen, M. Patra and M. Karttunen. *Fluid Phase Equilibria*. 228-229 (2005), pp. 135-140.
- [9] H. Khandelia, J.H. Ipsen and O.G. Mouritsen. *Biochimica et Biophysica Acta*. 1778 (2008), pp. 1528-1536.
- [10] D. Spoel, E. Lindahl, B. Hess, A.R. Buuren, E. Apol, P. J. Meulenhoff, D. P. Tieleman, A. L.T.M. Sijbers, K. A. Feenstra, R. Drunen, H.J.C. Berendsen. *GROMACS USER MANUAL Version*. 2005, pp. 1-300.
- [11] L.M.S. Lora, F. Fernandes, A.C. Fernandes and J.P.P. Ramalho. *Biochimica et Biophysica Acta*. 1778 (2008), pp. 491-50.
- [12] A. Glättli, C. Oostenbrink, X. Daura, D.P. Geerke, H. Yu, and W.F. Gunsteren. *Brazilian Journal of Physics*. 34 (2004), pp. 116-125.
- [13] D.P. Tieleman, H. Leontiadou, A.E. Mark and S.J. Marrink. *J. Am. Chem. Soc.* 125 (2003), pp. 6382-6383.
- [14] R. Jarmila, M.H. Juha, R.M. Michael, C.M. Mark, C. Pavla, and V. Ilpo. *Biophysical J.* 88 (2005), pp. 3398-3404.
- [15] M. Patra, M. T. H. Karttunen, E. Falck and I. Vattulainen. *J. Phys. Chem. B.* 108 (2004), pp. 485-492.

- [16] M.M. Sperotto, S. May, A Baumgaertner. *Chemistry and Physics of Lipids*. 141 (2006), pp. 2–29.



2. Poster Presentations

Waraporn Boonyarat, Witcha Treesuwan, Patchreenart Saparpakorn, Kiattawee Choowongkomon and Supa Hannongbua. Distribution and Favorable Binding Sites of Tocopherol in a Lipid Bilayer Studied by Molecular Dynamics Simulations. The 1st Annual Meeting of TRF Senior Research Scholars. 2009, Maharakham University, Thailand.





Distribution and Favorable Binding Sites of Tocopherol in a Lipid Bilayer Studied by Molecular Dynamics Simulations

Waraporn Boonyarat^{1,2}, Wicha Treesuwan^{1,2}, Patchreenart Saparpakorn^{1,2},
Kiattawee Choowongkorn³, and Supa Hannongbua^{1,2*}

¹Department of Chemistry, Faculty of Science, Kasetsart University, Bangkok 10900, Thailand

²Center of Nanotechnology, Kasetsart University, Bangkok 10900, Thailand

³Department of Biochemistry, Faculty of Science, Kasetsart University, Bangkok 10900, Thailand

*E-mail: fscisph@ku.ac.th, Fax: +66 25 62 55 55 ext. 2140



Introduction

Vitamin E (tocopherol) is one of four fat-soluble vitamins. It is synthesized by plants and found in plant oils. Moreover it is hydrophobic and absorbed similarly to other dietary lipids. After solubilization by bile acid, it is absorbed into small intestinal epithelial cells. Vitamin E is stored with the fat droplets of adipose tissue cells. The general structure of vitamin E is shown in Figure 1. The binding of vitamin E in a biomembrane and its subsequent influence on membrane properties are an important problem. This is particularly so as the presence of vitamin E can severely influence various physiological processes in the body. A microscopic understanding of the location of vitamin E within the membrane is crucial as it will provide direct information regarding its interaction with membrane components. Such information will have an impact on the mechanism of the effect of vitamin on regular membrane properties. However, despite significant efforts, understanding of the mechanism of action of vitamin E is not clear.

Materials and Methods

The structure of vitamin E /phospholipid bilayer-water system with 128 DPPC molecules, 3655 water and vitamin E molecules were taken from <http://moose.bio.ucalgary.ca/files/>. The lipid force field parameters (FFGms) were used. The simulations were performed by using the GROMACS software. For water molecules, the SPC (single-point charge) parameters were used. The given bilayer was stabilized by an energy minimization. After that, the MD simulations were done for 10 ns. The temperature was set to 323 K and the pressure was set to 1 atm. The temperature and pressure are controlled using the Berendsen method. The vitamin E/DPPC system was using the same as 3 times.

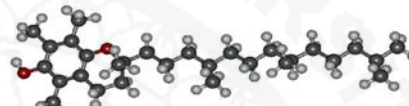


Figure 1. A general structure of vitamin E (tocopherol).

Results and Discussion

The simulations show that vitamin E was preferably accommodated at the head of the bilayer upper the glycerol moiety. In addition, it was found that the hydrophobic aromatic part of the vitamin E was located inside more ordered region of DPPC from the hydrophobic character of vitamin E, the depth of the vitamin E localization was gradually shifted deeper inside the hydrocarbon core of the bilayer at the opposite of the entrance (Figure 2). Stability of the total energy and RMSD plotted indicate good equilibrium (Figure 3). Total energy of vitamin E/DPPC was -1.02×10^8 kJ/mol. RMSD was calculated to compare with the starting structure that minimized. RMSD of vitamin E was 0.35 nm. Small RMSD value referred that structure of both vitamin E during molecular dynamic simulations were stable and not changed from starting structure that minimized. Density of vitamin E/DPPC bilayer along the z-dimension was calculated as show in Figure 4. The position of vitamin E in density peaks was about head group of DPPC because vitamin E-DPPC bilayer shown weakly hydrogen-bonding to the binding.

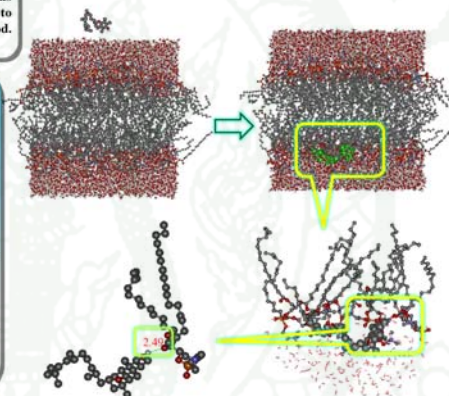


Figure 2. A snapshot of the MD boxes taken from the simulations of vitamin E molecule in the DPPC bilayer of the NPT simulation. Vitamin E molecule is rendered with hydrogen bonding.

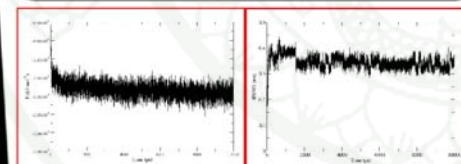


Figure 3. Total energy of DPPC/vitamin E system and RMSD of vitamin E at 10 ns.

Conclusions

The MD simulation study has been carried out to investigate the distribution of vitamin E at a water/membrane interface. Our interest has been focused on the favorable binding sites of vitamin E within DPPC bilayer. The MD simulations of vitamin E/DPPC show that a significant fraction of vitamin E molecules tends to diffuse from aqueous solution into the polar interfacial region of the bilayer. The depth of the vitamin E localization in this sequence was gradually shifted deeper inside the head group core of the bilayer. The MD simulations reveal that the favorable localizations of the studied vitamin E within the DPPC bilayer were not driven by vitamin E-lipid hydrogen-bonding.

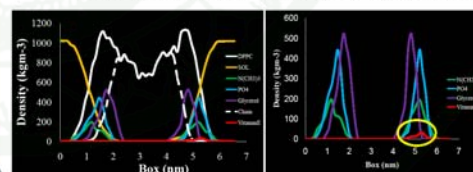


Figure 4. Mass density distribution profiles for individual components of the DPPC bilayer and for the total density distribution of molecules of vitamin E.

Acknowledgements

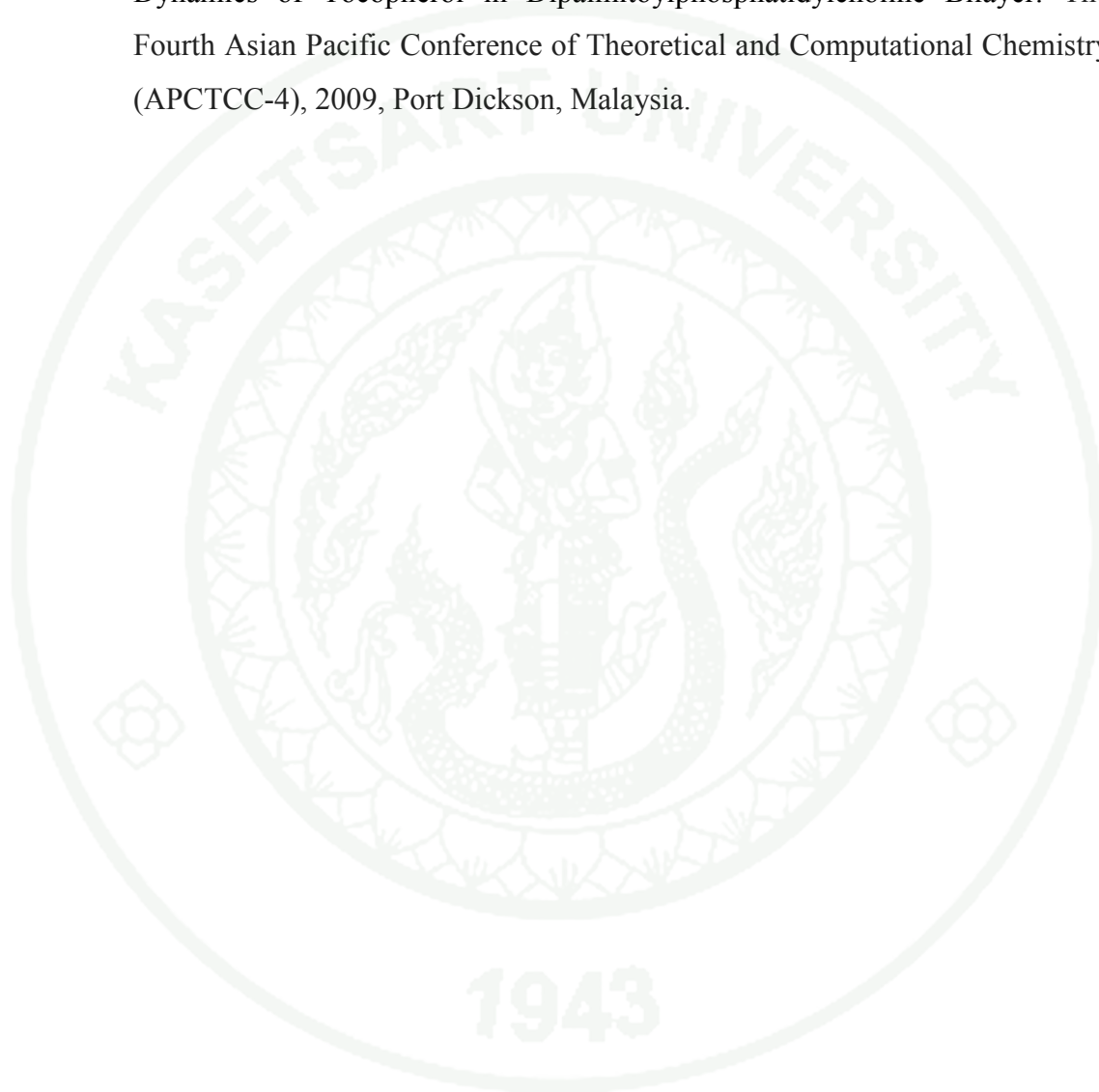
This work has been supported by the Thailand Research Fund and the Commission on Higher Education, The Postgraduate Education and Research Program in Petroleum, Petrochemical Technology and Advanced Materials, the Center of Nanotechnology Kasetsart University, Kasetsart University Research and Development Institute (KURDI), National Nanotechnology Center (NANOTEC), Ministry of Science and Technology, Thailand are gratefully acknowledged for partial support. L.C.A.C. and computing center of KU for computing and research facilities and The 6th Thai Summer School of Computational Chemistry Workshop.

References

- [1] D. P. Tieleman, S. J. Marrink, *Journal of Chemical Physics*, 105 (1996), pp. 4871-4880.
- [2] D. P. Tieleman, S. J. Marrink and H. J. C. Berendsen, *Biochimica et Biophysica Acta* 1331 (1997), pp. 235-270.
- [3] D. P. Tieleman, H. Leontiadou, A. E. Mark and S. J. Marrink, *J. Am. Chem. Soc.* 125 (2003), pp. 6382-6383.

3. Oral Presentation

Waraporn Boonyarat, Witcha Treesuwan, Patchreenart Saparpakorn, Kiattawee Choowongkomon, and Supa Hannongbua. Distribution, Orientation, and Dynamics of Tocopherol in Dipalmitoylphosphatidylcholine Bilayer. The Fourth Asian Pacific Conference of Theoretical and Computational Chemistry (APCTCC-4), 2009, Port Dickson, Malaysia.



S004

Distribution, Orientation, and Dynamics of Tocopherol in Dipalmitoylphosphatidylcholine Bilayer

Waraporn Boonyarat^{1,2}, Witcha Treesuwan^{1,2}, Patchreenart Saparpakorn^{1,2},
Kiattawee Choowongkorn³, and Supa Hannongbua^{1,2*}

¹Department of Chemistry, Faculty of Science, Kasetsart University, Bangkok 10900, Thailand,

²Center of Nanotechnology, Kasetsart University, Bangkok 10900, Thailand,

³Department of Biochemistry, Faculty of Science, Kasetsart University, Bangkok 10900, Thailand,

*E-mail: fscisph@ku.ac.th, Fax: +66 25 62 55 55 ext. 2140

Vitamin E is a probiotic and highly accumulated in the chloroplast containing in leaves of most plants. Vitamin E is hydrophobic and is absorbed similarly to other dietary lipids. After solubilization by bile acid, it is absorbed into small intestinal epithelial cells. The binding of vitamin E in a biomembrane and its subsequent influence on membrane properties are an important problem. This is particularly as the presence of vitamin E can severely influence various physiological processes in the body. The understanding of the location of vitamin E within the membrane is crucial as it will provide direct information regarding its interaction with membrane components. In this study the distribution of Vitamin E at water/membrane interface has been investigated by molecular dynamics (MD) simulations. The MD simulations running on the time of 10 ns were carried out in the same conditions by using GROMACS software and the SPC (single-point charge) parameters were used. The dipalmitoylphosphatidylcholine (DPPC) bilayer was stabilized by the energy minimization at 323 K and 1 bar as constant. The MD study focused on favorable binding sites of Vitamin E embedded into DPPC bilayer. We show the binding of Vitamin E absorption in DPPC bilayer. The simulations show that Vitamin E is preferably accommodated at the head of the bilayer upper the glycerol moiety. In addition, it is found that the hydrophobic aromatic part of the Vitamin E is located inside more ordered region of DPPC from the hydrophobic character of Vitamin E, the depth of the Vitamin E localization is gradually shifted deeper inside the hydrocarbon core of the bilayer. We found that the Vitamin E shows weak hydrogen-bonding to DPPC bilayer.

References:

1. A. Kyrychenko, J. Waluk *Biophysical Chemistry*. 2008, 136, 128-135.
2. K. Hac-Wydro, P. Wydro, A. Jagoda, J. Kapusta *Chemistry and Physics of Lipids*. 2007, 150, 22-34.
3. C. Anezo, A. de Vries, H.-D. Holtje, D. Tieleman, S. Marrink *J Phys Chem B*. 2003, 107, 9424 - 9433.
4. D. Tieleman, H. Leontiadou, A. Mark, S. Marrink *J Am Chem Soc*. 2003, 124, 6382 - 6383.

CURRICULUM VITAE

NAME : Miss Waraporn Boonyarat

BIRTH DATE : January 11, 1984

BIRTH PLACE : Phatthalung, Thailand

EDUCATION : **YEAR** **INSTITUTION** **DEGREE/DIPLOMA**
2003-2006 Prince of Songkla University B.Sc.
(Chemistry-Biology)

SCHOLARSHIPS : Thailand Research Fund (RTA5080005)

Commission on Higher Education (CHE)

National Nanotechnology Center (NANOTEC)

The National Center of Excellence for Petroleum,
Petrochemicals, and Advanced Materials
(NCE-PPAM)

Kasetsart University Research and Development
Institute (KURDI)

Faculty of Science, Kasetsart University

SHORT TERM VISIT : University of Vienna, Austria (March – April 2010)